Analysis of light-dependent leaf development in *Arabidopsis* and cotyledon development in *Flaveria* species

Inaugural-Dissertation

zur

Erlangung des Doktorgrades

der Mathematisch-Naturwissenschaftlichen Fakultät

der Universität zu Köln

vorgelegt von

Eva Willée

aus Bonn

Köln 2018

Berichterstatter:	Prof. Dr. Ute Höcker
	Prof. Dr. Martin Hülskamp
Prüfungsvorsitzende:	Prof. Dr. Karin Schnetz
Tag der mündlichen Prüfung:	10. September 2018

Table of Contents

Table of Contents

Table of Contents

List of Figures

List of Tables

List of Abbreviations

°C	degree Celsius
2-PG	2-phosphoglycolate
3-PGA	3-phosphoglycerate
ABA	abscisic acid
AMPRIL	*Arabidopsis* multiparent recombinant inbred lines
ApE	A plasmid editor
ATP	adenosine triphosphate
Bp, Kb, MBp	base pair(s), kilo base pair(s), Mega base pair(s)
BSC(s)	bundle sheath cell(s)
CAPS	cleaved amplified polymorphic sequences
CDS	coding sequence
cm, mm, µm, nm	centimetre(s), millimetre(s), micrometre(s), nanometre(s)
d	day(s)
Dc	continuous darkness
ddH_2O	double distilled water
DNA	deoxyribonucleic acid
et al.	*et alii* (and others)
g	gravity
g, mg, µg	gram(s), milligram(s), microgram(s)
GA	gibberellic acid
GDC	glycine decarboxylase
GFP	green fluorescen protein
GO	gene ontology
GWAS	genome-wide association study
h	hour(s)
H^2	Broad sense heritability
HIF	heterogenous inbred family
HSP	heat shock protein
IAA	indole-3-acetic-acid
JA	jasmonic acid
Lc	continuous light
MAGIC	multiparent advanced generation intercross
min	minute(s)
mL, µL	millilitre(s), microlitre(s)
mol, µmol	mole(s), micromole(s)
mRNA	messenger RNA
MS	Murashige & Skoog
NIL	near isogenic line
OAA	oxaloacetate
OPDA	oxophytodienoic acid
PCR	Polymerase chain reaction
PEP	phospho*enol* pyruvate
PEPC	PEP carboxylase
PI	propidium iodide

List of Abbreviations

QTL	Quantitative trait locus
R^2	coefficient of determination / % phenotypic variation explained by marker variation
RIL	recombinant inbred line
RNA	ribonucleic acid
ROS	reactive oxygen species
RT	room temperature
RT-PCR	reverse transcriptase PCR
RuBisCO	Ribulose 1,5-bisphosphate carboxylase / oxygenase
s	second(s)
SA	salicylic acid
SAM	shoot apical meristem
SDS	sodium dodecyl sulphate
SNP	single nucleotide polymorphism
T-DNA	transfer-DNA
Taq	*Thermus aquaticus*
TF	transcription factor
Tris	tris (hydroxymethyl) aminomethane
v/v	volume per volume
V_E	environmental variance
V_G	Genetic variance
V_P	phenotypic variance
w/v	weight per volume
YFP	yellow fluorescent protein

Abstract

Light not only provides the electromagnetic radiation plants need to perform photosynthesis, it is also an important environmental factor for plant development. Internal leaf architecture is one of the most essential features of plant development. Leaf architecture adaptations such as cell elongation and leaf vein density increase towards light intensities and enable the plant to optimize the photosynthesis rates and water use efficiency. This thesis comprises two different approaches to analyse light-dependent regulators of leaf development. The first one involves the analysis of light-dependent C_4 photosynthesis-specific Kranz anatomy in *Flaveria* species. The second approach utilizes the genetic variation of *Arabidopsis* accessions and next generation sequencing.

Kranz anatomy is a very specific leaf architecture composed of bundle sheath cells (BSC) that surround the veins and furthermore features reduced vein spacing. In this thesis, I investigated the light-dependent formation of the Kranz anatomy by analysing the BSC area increase in *Flaveria* species. In all species analysed comprising C_3, C_3-C_4 and C_4 species, the increase of BSC area was light-dependent. Since several genes of the C_4 photosynthetic pathway are expressed in a light-dependent matter, another research question of this experiment was, whether the promoters of *GLDPA* and *PPCA* deriving from *Flaveria trinervia* show light-dependent activation. Here, light-dependent expression of two reporter genes was not verified in dark-and light-grown cotyledons of *Flaveria bidentis* and *Arabidopsis*.

In a second approach in order to understand leaf development, quantitative trait loci (QTL) analysis was performed to identify regulators of estimated leaf thickness and leaf vein density in *Arabidopsis*. A QTL on chromosome 4 for leaf vein density was identified using the *Arabidopsis* multiparent recombinant inbred lines (AMPRIL) and SNP-based polymorphism analysis in the parental accessions of the RILs lead to the identification of *AXR6* as the putative QTL for leaf vein density.

The last part of this thesis comprises the transcriptome analysis of high-light- and low-light-grown *Arabidopsis* leaves. Using 3 leaf-developmental stages this experiment gives insight into the transcriptome of developing high-light stressed *Arabidopsis* leaves.

In summary, I confirmed light-dependent BSC area increase in different *Flaveria* species. In the used model systems, the expression of GLDPA- and PPCA-reporter constructs was found to be light-independent. QTL analysis using AMPRIL lead to the identification of *AXR6* as putative QTL for leaf vein density. Transcriptome analysis of high-light- and low-light-grown *Arabidopsis* leaves gave first insights into differentially expressed genes in developing leaves and requires further investigations.

Zusammenfassung

Licht liefert nicht nur die elektromagnetische Strahlung, die Pflanzen für die Photosynthese benötigen, es ist auch ein wichtiger Umweltfaktor für die Pflanzenentwicklung. Die interne Blattarchitektur ist eines der wichtigsten Merkmale der Pflanzenentwicklung. Anpassung der Blattarchitektur, wie zum Beispiel Zellstreckung und Zunahme der Blattaderdichte bei wachsender Lichtintensität, ermöglichen der Pflanze, die Photosyntheseraten und die Wassernutzungseffizienz zu optimieren. Diese Arbeit umfasst zwei verschiedene Ansätze zur Untersuchung lichtabhängiger Blattentwicklungsregulatoren. Die erste beinhaltet die Untersuchung der lichtabhängigen Ausbildung der C_4-spezifischen Kranz-Anatomie in *Flaveria*-Arten. Der zweite Ansatz nutzt die genetische Vielfalt von *Arabidopsis*-Akzessionen und Transkriptomsanalysen.

Die Kranz-Anatomie ist eine spezifische Blattarchitektur, die aus Bündelscheiden-Zellen und Mesophyll-Zellen besteht, die kranzförmig die Venen umgeben. Ein weiteres Merkmal der Kranz-Anatomie ist ein verringerter Venenabstand. In dieser Arbeit wurde die lichtabhängige Ausbildung der Kranz-Anatomie durch Messung der Bündescheidenzellen-Flächen in verschiedenen *Flaveria*-Arten untersucht. Hier war bei allen analysierten Arten, die sowohl C_3, als auch C_3-C_4- und C_4-Arten umfassten, der Anstieg der Bündelscheidenzellen-Fläche lichtabhängig. Da mehrere Gene des C_4-Photosynthesewegs lichtabhängig exprimiert werden, war eine weitere Fragestellung dieses Experiments, ob die Promotoren von *GLDPA* und *PPCA* von *Flaveria trinervia* lichtabhängig aktiviert werden. Hier konnte die lichtabhängige Expression von Reportergenen beider Promotoren in Dunkel- und Helligkeit angezogenen Keimblättern von *Flaveria bidentis* und *Arabidopsis* nicht bestätigt werden.

In einem zweiten Ansatz wurde eine QTL Analyse durchgeführt, um Regulatoren der Blattdicke und der Blattaderdichte in *Arabidopsis* zu identifizieren. Ein QTL verantwortlich für die Blattaderdichte wurde in den Linien auf Chromosom 4 identifiziert. Die SNP-basierte Polymorphismus-Analyse in den Gründerakzessionen führte zur Identifizierung von *AXR6* als putativen QTL für die Blattvenendichte.

Der letzte Teil dieser Arbeit umfasst die Transkriptom-Analyse von unter Hochlicht und Schwachlicht angezogenen *Arabidopsis*-Blättern. Anhand von 3 Entwicklungsstadien gab dieses Experiment einen Einblick in das Transkriptom von hochlicht-behandelten *Arabidopsis*-Blättern.

Zusammenfassend bestätigte ich die lichtabhängige Flächenzunahme der Bündelscheidenzellen bei verschiedenen *Flaveria*-Arten. In den verwendeten Modellsystemen erwies sich die Expression von GLDPA- und *PPCA*-Promoter-Reportergenkonstrukten als lichtunabhängig. Die QTL-Analyse unter Verwendung von AMPRIL führte zur Identifizierung von *AXR6* als mutmaßlichen QTL für die Blattaderdichte. Die Transkriptom-Analyse von *Arabidopsis*-Blättern unter 2 verschiedenen Lichtquantitäten lieferte erste Einblicke in differentiell exprimierte Gene in sich entwickelnden Blättern.

1 Introduction

Plants as sessile organisms have to constantly adapt to their changing environment. Besides biotic factors such as herbivores, pathogenic fungi and competition with neighbouring plants, they have demand for nutrients, water and sunlight to perform photosynthesis and grow. Light, besides being the primary source of energy for plants, is also an environmental factor which regulates many developmental processes such as seed germination, de-etiolation of seedlings, shade avoidance, phototropism, circadian rhythm, chloroplast movement, leaf development and induction of flowering. Leaves are the primary site of photosynthesis in most plants and plants need to adapt their leaf morphology to the environment to assure their capability to thrive. Leaf morphogenesis is an important process for the plant to adjust the cellular arrangement of photosynthetic tissue in an optimized way to improve photosynthetic activity.

1.1 The *Arabidopsis* leaf

Arabidopsis thaliana is native to Western Eurasia and can grow in a multitude of climatic amplitudes (Hoffmann, 2002). *Arabidopsis* leaves are simple leaves with an undivided leaf blade and the petiole that attaches the blade to the stem (Bar & Ori, 2014; Tsukaya *et al*., 2002). Leaves are the main functional unit for photosynthesis, with only a few exceptions in the plant kingdom (Kalve *et al*., 2014; Terashima *et al*., 2011). The internal structure of the *Arabidopsis* leaf is as follows: The leaves are composed of an adaxial (upper) layer of epidermis with trichomes. Below the epidermis lie one or more adaxial layers of palisade mesophyll, several layers of spongy mesophyll with loosely packed cells surrounded by air space to facilitate photosynthetic gas exchange including the veins. An abaxial layer of epidermis and stomata form the lower border of the leaf (Figure 1; Bolhàr-Nordenkampf & Draxler, 1993).

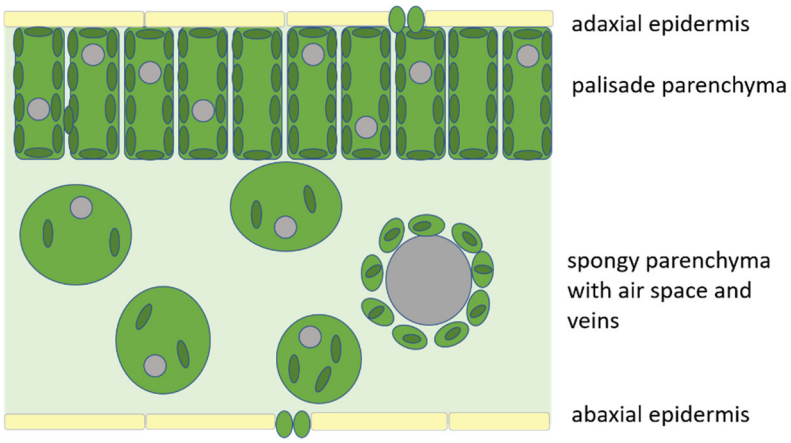

Figure 1 Schematic cross-section of an *Arabidopsis* leaf
Displayed are adaxial epidermis with stomata, palisade parenchyma, spongy parenchyma with air space and a vein, surrounded by bundle sheath cells. Also, abaxial epidermis with stomata is shown.

1.1.1 *Arabidopsis* leaf development

Leaves derive post-embryonically from the shoot apical meristem (SAM), which contains a pluripotent cell population, and which is located at the tip of the plant (Steeves & Sussex 1989). Flowering shoots are derivatives of leaves and develop from the SAM (Kim *et al*., 1999). Leaf growth can be divided into three main stages: the primordium initiation, primary morphogenesis and secondary morphogenesis (Donnelly *et al*., 1999). Leaf initiation involves the formation of leaf polarity and axes of symmetry (reviewed in Bar & Ori, 2014). In the primary morphogenesis, the leaf blade expands and structures such as veins and stomata are formed. In secondary morphogenesis, leaf growth is continued, and cells undergo differentiation and cell-fate determination (Bar & Ori, 2014). The process of growth needs to be strictly coordinated by an interplay of plant hormones and transcription factors (TFs) and is highly dependent on the coordination of cell proliferation and cell differentiation.

Leaves are initiated at the flanks of the SAM at a site of high auxin and low cytokinin concentration, which is most distant from existing primordia (Reinhardt *et al*., 2000; Traas & Monéger, 2010). Leaves are thus arranged in a spiral pattern that approaches the Fibonacci angle of 137.5° (Steeves & Sussex, 1989). Leaf initiation is a process highly regulated by hormone concentration and hormone interplay. For example, auxin concentrations play a major role in the regulation of the leaf initiation. High levels of auxin transported towards the SAM inhibit cytokinin biosynthesis by the repression of KNOTTED-LIKE HOMEOBOX TF family proteins (KNOX; Reinhardt *et al*., 2003). KNOX-TFs are required for cytokinin biosynthesis and the maintenance of the SAM (Jackson *et al.,* 1994; Long *et al.,* 1996). The distribution of auxin is regulated by auxin-influx carriers AUXIN RESISTANT1 (AUX) and LIKE-AUXIN RESISTANT (LAX) and efflux carriers PIN-FORMED1 (PIN1) and P-GLYCOPROTEIN (PGP) family members (Geisler *et al.,* 2003; Gälweiler *et al.,* 1998; Yang *et al.,* 2006). The efflux carriers orient the transport of auxin towards adjacent cells with higher auxin concentration leading to an enhancement of auxin concentration at the tip of the leaf primordium (Reinhardt *et al.,* 2000). ASYMMETRIC LEAF1/ROUGH SHEATH2/PHANTASTICA (ARP) proteins are expressed specifically in the developing primordium and initiate differentiation of the leaf primordium (Bryne *et al.,* 2002). The growing leaf primordium then establishes its leaf polarity by feedback communication of PHABULOSA (PHB), PHAVOLUTA (PHV), and REVOLUTA (REV) that confer adaxial domain identity, while the abaxial domain is specified by KANADI (KAN), YABBY and AUXIN RESPONSE FACTOR (ARF) gene family members (Eshed *et al.,* 2004; Kerstetter *et al.,* 2001; Siegfried *et al.,* 1999).

During primary morphogenesis, leaf growth is sustained by cell division. Also, the pattern formation of structures such as vein, stomata and trichomes begins (Bar & Ori, 2014). The period of cell proliferation is crucial for reaching the final leaf size and is highly regulated. Cytokinin is not only involved in the maintenance of the SAM, but it also is, together with auxin, a regulatory signal for cell proliferation (Harrar *et al*., 2003). AUXIN-RELATED GENE INVOLVED IN ORGAN SIZE (ARGOS) acts downstream of auxin signalling (Hu *et al.,* 2003).

ARGOS enhances the expression of *AINTEGUMENTA* (*ANT*), which is a member of the APETALA (AP2)-like TF-family. Despite its role in floral organ initiation, ANT has also been shown to be involved in general organ size regulation by controlling the cell number in proliferating tissues through activation of cell cycle driver *CYCLIN D3;1* (*CYCD3*) and extending duration of cell proliferation (Mizukami & Fisher, 2000; Nole-Wilson *et al*., 2005). Cytokinin is also known to regulate the expression of CYCD3 (Dewitte *et al.,* 2007). Cytokinin and auxin induce the expression of *CYCLIN-DEPENDENT KINASE A-1* (*CDKA;1*), which regulates the transition from interphase to synthesis or mitosis (Perrot-Rechenmann, 2010; Schaller *et al.,* 2014). Both hormones have antagonistic function, since the ratio of cytokinin to auxin is important for the regulation of the cell division (Schaller *et al.,* 2014). Cell proliferation is also controlled by protein degradation: the anaphase-promoting complex/cyclosome (APC/C) is one of the largest E3 ubiquitin-ligase complexes in plants. Its subunit APC10 regulates the proteolysis rate of mitotic cyclin CYCB1;1 and thereby enhances cell division rate (Eloy *et al*., 2011).

In secondary morphogenesis, cell division is replaced by cell expansion starting from the tip of the leaf to the leaf base (Donelly *et al*., 1999). Cell expansion requires the loosening of the cell walls. Auxin is involved in the process of cell expansion. When auxin is perceived by auxin receptor molecules, the proton pump ATPase is activated and leads to the acidification of the extracellular space (reviewed in Perrot-Rechenmann, 2010). This activates hydration and subsequent increase of turgor pressure leads to cell expansion. Also, cell wall-loosening enzymes are activated such as EXPANSINS, which are cell-wall associated proteins that are involved in cell wall loosening during cell expansion and play an important role in cell size regulation (Mason *et al*., 1992). Other enzymes involved in cell wall loosening are xyloglucanendotransglucosylase/hydrolases (XTHs), xyloglucan endohydrolases (XEH), and xyloglucan endotransglucosylases (XET; Rose *et al*., 2002; Eklöf & Brumer, 2010). Cell expansion is also associated with endoreduplication. Cells that enter the endoreduplication process are not able to resume mitotic activity (Roeder *et al*., 2010), which renders this process irreversible. The outgrowth of the leaf is regulated by ROTUNDIFOLIA 3 (ROT3) and ROT4 which regulate longitudinal expansion, while ANGUSTIFOLIA (AN) regulates lateral expansion (Tsuge *et al*., 1996).

1.1.2 Leaf vein formation

Vascular tissue is composed of xylem and phloem. The xylem is responsible for transporting water and salts, while the phloem transports signalling molecules and carbohydrates (Crawford & Zambryski, 1999). Vein formation starts early in leaf development and proceeds simultaneously with leaf expansion (Esau, 1977; reviewed in Nelson & Dengler, 1997). Auxin is a key player in vein formation and further differentiation. During leaf growth, auxin is distributed by PIN1 to the tip of the developing primordium (Reinhardt *et al*., 2003). After primordium initiation, the primordium starts to produce auxin itself and auxin is then transported to internal tissues of the primordium towards the centre, leading to the formation of the midvein from elongated procambial cells (Ljung *et al*., 2001; reviewed in Scarpella *et*

al., 2010). This process of auxin distribution is regulated by MONOPTEROS (MP), also known as AUXIN RESPONSE FACTOR 5 (ARF5), which controls the expression of PIN1 (Berleth & Jürgens, 1993). During primary morphogenesis, auxin maxima at the margins of the developing leaf correlate with the sites of lateral vein formations (Scarpella *et al.,* 2010). Many auxin biosynthesis and signalling mutants such as *axr6* exhibit defects in vein patterning and vein density (Esteve-Bruna *et al.,* 2013).

Veins function not only in the transport of solutes, they are also mechanical stabilizers of the plant leaves (reviewed in Roth-Nebelsick *et al*., 2001). Photosynthesis requires the uptake of CO_2 from the atmosphere. With each molecule CO_2 entering, up to 400 molecules H_2O exit the leaf by transpirational exchange with the atmosphere (McElrone *et al.,* 2013), which makes water loss a limiting factor for photosynthesis. As veins function in transport of water through the plant, they influence hydraulic conductance in the leaf and ultimately, they can influence photosynthetic performance (Sack & Scoffoni, 2013). While some studies indicate a positive correlation of leaf vein density with photosynthetic parameters across species (Brodribb *et al*., 2007; Sack & Scoffoni, 2013), a recent study focussing on whole *Arabidopsis* leaves could not verify a correlation (Rishmawi *et al*., 2017). This indicates, that there are species-specific differences regarding leaf vein density and photosynthesis. However, leaf vein density is thought to be an important prerequisite for elevated C_4 photosynthesis (Dengler & Nelson, 1999; McKown & Dengler, 2009). Here, high vein density is required for optimal photosynthesis due to the separation of CO_2 fixation in two different cell types, the bundle sheath cells (BSCs) surrounding the veins and the mesophyll cells (MCs). C_4 photosynthesis will be explained in further detail in chapter 1.2.

1.1.3 Leaf thickness

Leaf thickness is a trait positively correlated with photosynthetic capacity in some species (Niinemets, 2002), although it has recently been shown that this is not the case in *Arabidopsis* (Rishmawi *et al*., 2017). Leaves grown in the sun are thicker than leaves grown in shade. This is because in the sun light the plant adjusts the mesophyll size in the leaves according to the higher fluence rate. This leads to changes in ratio of the mesophyll area that is exposed to intercellular spaces and the rate of gas exchange for photosynthesis. (Lichtenthaler *et al*., 1981). An increase of leaf thickness is often positively correlated with the increase of palisade cell length and the development of more palisade cell layers (Coneva & Chitwood, 2018; John *et al*., 2013).

Several genes have been identified that regulate leaf thickness in *Arabidopsis*. The elongation of palisade cells is dependent on the photoreceptors PHOT1 and PHOT2 in a tissue-autonomous manner (Kozuka *et al*., 2011). Mutations in *AN* lead to narrow, thick leaves with highly cylindrical palisade cells and more MC layers than wild-type. Interestingly, *an* mutants have more chloroplasts and show higher CO_2 assimilation capacity than the wild-type (Gotoh *et al*., 2018). In C_4 plants, which exhibit a higher rate of photosynthesis in arid and warm climates, leaves are often thinner than those of closely related C_3 species (Raghavendra &

Sage, 2010). Understanding the regulation of leaf thickness can therefore be crucial in terms of modification of C_3 to C_4 plants.

1.1.4 Light stress

Light plays a crucial role in the development of plants. To sense the light intensity, quality and duration of light trigger and to react to it developmentally, plants have evolved a complex regulatory network consisting of photoreceptors, transcription factors and protein degradation. Under natural conditions in the sun light, plants are faced with high irradiation from the sun, contrasting to shading through neighbouring plants, clouds and changes in the sun angle (Vialet-Chabrand *et al.,* 2017).

Plants possess five classes of photoreceptors that act synergistically or antagonistically depending on the perceived light signal. Phytochromes (PHYA-PHYE) detect red (R) and far-red (FR) light (Sharrock & Quail, 1989), cryptochromes (CRY1-CRY3) and phototropins (PHOT1 and PHOT2) sense UV-A and blue light (Chaves *et al*., 2011; Takemiya *et al*., 2005). The F-box proteins ZEITLUPE (ZTL), FLAVIN-BINDING KELCH REPEAT, F-BOX1 (FKF1) and LOV-KELCH PROTEIN2 (LKP2) perceive blue light (Kim *et al*., 2007; Kong & Okajima, 2016). UV-B signals are perceived by the UV-B RESISTANCE 8 (UVR8) pathway (Favory *et al*., 2009; Heijde & Ulm, 2012), and might regulate leaf expansion and stomatal development (Wargent *et al*.,2009).

Plants grown under high irradiance show specific adjustment of their leaf architecture. These include the PHOT2-dependent anticlinal cell elongation of palisade cells that contribute to increased leaf thickness (Kozuka *et al*., 2011). Also, reorganization of chloroplast structure, reduction of antennae size, decrease of the ratio of PSII to PSI, enhanced energy dissipation from excited chloroplasts and decrease of size of chloroplasts are adaptations towards high-light (Kalve *et al*., 2014; Weston *et al*., 2000).

Excess of light creates an overflow of electrons from photosynthetic electron transport system, resulting in the generation of reactive oxygen species (ROS), that are toxic and can lead to inhibition of growth (Müller *et al*., 2001). Plants evolved several adaptation mechanisms to prevent and cope with photooxidative damage. Detoxification of ROS is achieved by synthesis of carotenoids, α-tocopherols, anthocyanins and flavonoids, as well as up-regulation of expression of superoxide dismutases, glutathione S-transferases/peroxidases and catalases (Niyogi, 1999). Also, enhanced transcription of *EARLY LIGHT INDUCIBLE PROTEINS* (*ELIPS*) and filament-forming temperature-sensitive (FtsH) proteases that are involved in turnover of photodamaged PSII was found in light-stressed plants (Bailey, 2002). Expression of *ELIP* is activated by UV-B-receptor UVR8 and CRY1 (Brown *et al*., 2005; Kleine *et al*., 2007).

To avoid excess sunlight, another mechanism is the phototropin-mediated chloroplast light-avoidance response. Under strong light, chloroplasts move to the anticlinal cell walls of the palisade cells to avoid the light, which is however not true for some climbing plant species (Kagawa *et al.,* 2001; Sztatelman *et al*., 2010). Furthermore, transcriptional regulation of light stress response can be observed by down-regulation of genes encoding antenna proteins and activation of genes encoding for enzymes responsible for flavonoid synthesis (Kimura *et al*.,

2003; Rossel *et al*., 2002). Long-term acclimatization towards high-light requires light harvest complex (LHC) protein regulation and changes in PSII/PSI ratio (Anderson *et al*., 1986).
Stress-enhanced proteins (SEPs) and one-helix proteins (OHPs) were identified by sequence comparisons using conserved domains of ELIPS and belong to the ELIP subfamily. Expression of *SEP* and *OHP* genes was found to be upregulated under high-light conditions, with a lower expression under low-light conditions (Adamska, 1997; Andersson *et al*., 2003). Another protein family found to be induced by high-light is the light stress regulated (LSR) *Lsr1-Lsr5*. These genes have been also found to be up-regulated by other environmental stresses (Dunaeva & Adamska, 2001). High-light also induces hormone signalling. Levels of abscisic acid (ABA), salicylic acid (SA), oxylipins, jasmonic acid (JA) and JA-intermediate oxophytodienoic acid (OPDA) rise under high-light conditions (Alsharafa *et al*., 2014; Galvez-Valdievieso *et al*., 2009).

1.1.5 Natural variation in *Arabidopsis*

A multitude of agricultural traits such as seed dormancy, fruit production, resistance to diseases and water demand can be quantified and the understanding of their genetic regulation and variation is of high economic and agronomic interest. The observable phenotypes are highly dependent on both environmental and genetic factors. *Arabidopsis* is a member of the *Brassicaceae* family, as are important crops e.g. rape seed, cabbage and ornamental flowers such as wallflowers. Therefore, the identification of genes responsible for quantitative traits in *Arabidopsis* may lead to the identification of homologous genes in crop species and can ultimately help to improve crop quality. *Arabidopsis* as a selfing plant is prone to inbreeding in the nature (Koornneef *et al*., 2004). Therefore, most plants collected in nature are inbred lines. These so-called accessions are products of natural selection under diverse ecological conditions (Alonso-Blanco & Koornneef, 2000; Weigel, 2012) and can be used as parental lines for quantitative trait loci (QTL)- analysis or in genome wide association studies (GWAS) since they show genetic and phenotypic variation. The genomic sequences of 1001 *Arabidopsis* accessions have been organized into the world's largest database for *Arabidopsis* sequences (1001 genome project), which can be used for GWAS by computational association of the data with phenotypic values. GWAS has been widely used in human disease research (Visscher *et al.,* 2017). GWAS is also applied in *Arabidopsis*, utilizing natural variation of *Arabidopsis* accessions. GWAS does not require the time-consuming creation and genotyping of recombinant inbred lines (RILs) as for QTL (Korte & Farlow, 2013). While GWAS analysis can be conducted very fast, it can suffer from population structure- induced errors (Korte & Farlow, 2013).
QTL analysis in *Arabidopsis* has been used in the past to unravel novel genes regulating mechanisms concerning *Arabidopsis* development. These genes comprise flowering time - controls such as *FRIGIDA* (Clarke & Dean 1994), *AERIAL ROSETTE* (*ART*) and *ENHANCER ROSETTE* (*EAR*) as a new allele for FRI (Grbić & Bleecker, 1996). The principle of QTL analysis is to identify associations between the phenotype of a mapping population and the genotype of markers. Markers such as simple sequence repeats (SSR) markers, which differ in the number

of repetitive nucleotides, or restriction fragment length polymorphisms (RFLPs) which differ in the absence or presence of a restriction site between individuals can be detected by PCR. Single nucleotide polymorphisms (SNPs) can be detected by sequencing.

For QTL analysis, the phenotypes of a segregating population with known markers is assessed. This is called a mapping population. A mapping population is the offspring of a cross of two or more parents, that have differences in the alleles affecting the trait of interest. In traditional two-parental mapping systems, two parental lines are used as providers for genetic material for QTL-analysis. Then, association analysis is performed between the phenotypic values and the genotypic information of F2 or RILs is performed. This step is performed using statistical software such as TASSEL (Bradbury *et al.,* 2007). In QTL analysis, only the allelic diversity that is segregating in the analysed population can be analysed. To reduce environmental effects and increase the power for QTL detection, it is more efficient to use recombinant inbred lines (RILs) or near isogenic lines (NILs), which have a high percentage of homozygosity and can be used in biological replicates. RILs are produced by an initial cross between two or more parental lines and subsequent selfing or sibling mating for several generations (Broman, 2005). NILs are produced by crossing a line showing phenotype to a reference line not showing the phenotype of interest. From the F1, individuals that show the phenotype of interest are back-crossed to the reference line and after several generations, the NILs will contain small genomic fragments from the phenotype-holding parent in an otherwise homozygous background of the reference line (Blanco *et al*., 2006). The amount of recombination events during the creation of the inbred lines has limiting effects on the mapping resolution (Korte & Farlow, 2013). For QTL analysis, the amount of RILs, representing independent recombination events, limits the accuracy of QTL detection (Keurentjes *et al*., 2007). The higher the recombination frequency, the better the resolution of QTL mapping. To increase allelic variation and improve recombination frequency, multiparent recombinant inbred lines, deriving from several parental lines have been produced. Lines such as "*Arabidopsis* multiparent recombinant inbred lines" (AMPRIL; Huang *et al*., 2011) and "multiparent advanced generation intercross" (MAGIC; Kover *et al*., 2009) are derived from 8-19 founder accessions. In this study, a set of AMPRIL has been used to identify QTL responsible for leaf vein density and leaf thickness (Figure 2).

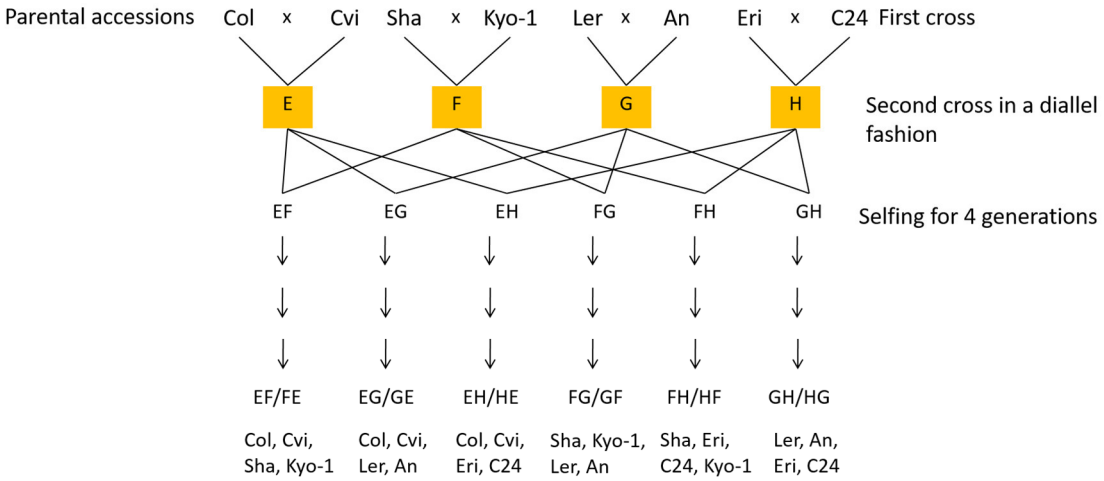

Figure 2 AMPRIL crossing scheme.
Figure was drawn according to Huang *et al.*, 2011. Pairwise cross of eight parental accessions lead to four two-way hybrids. The hybrids were crossed in a diallel fashion to produce six four-way hybrids. F5 was used in Huang *et al.*, 2011 for genotyping. In this study, the F7 was used.

For identifying the specific genetic region of the QTL, fine-mapping is performed. Useful populations for fine-mapping are heterogenous inbred families (HIF; Tuinstra *et al.,* 1997). These lines represent RILs with a heterozygous region at the locus of interest. Even after several rounds of selfing, RILS still contain a certain percentage of heterozygous regions in their genome. By taking advantage of segregation of the heterozygous region according to mendelian rules, the phenotypic and genotypic analysis of HIFs can help fine-mapping the trait of interest (Tuinstra *et al.,* 1997).

1.2 C_4 photosynthesis

Due to the increasing world population and the changing climate conditions, the demand for food increases, while arable areas decrease. Unfavourable environments such as heat and drought lead to a decrease in productivity of most plants used in agriculture. One cause for reduced productivity is the ability of ribulose 1,5-bisphosphate carboxylase/oxygenase (RuBisCO), to carboxylate or oxygenate its substrate ribulose-1,5 bisphosphate (RuBP). However, in the plant kingdom, evolution has brought several adaptations towards harsh climate conditions. Three different types of carbon fixation during photosynthesis are known, C_3, C_4 and the crassulacean acid metabolism (CAM) photosynthesis. The terms C_3 and C_4 derive from the first stable product deriving from carbon assimilation which is the 3 carbon atoms containing compound 3-phosphoglycerate (3-PGA) in C_3 plants and a 4 carbon-containing compound oxaloacetate (OAA) in C_4 plants. C_4 and CAM photosynthesis are thought to be derived from C_3 photosynthesis (Ehleringer *et al.*, 1997) and display advanced adaptations to specific habitats. CAM plants are highly adapted to arid climate, but their net CO_2 fixation is less efficient than in C_4 plants and they grow slower than C_3 plants (Nobel, 1991). Of all angiosperms, only about 3% utilize C_4 photosynthesis, however they contribute to about 23% to fixated carbon globally (Kellogg, 2013). C_4 plants have higher growth rates and better

nitrogen and water use efficiencies under high temperatures than C_3 plants (Oaks, 1994). Therefore, the analysis of the C_4 pathway and the introduction of the C_4 pathway into C_3 crops are of high interest regarding the anthropogenic climate change and the currently growing world population (Covshoff & Hibberd, 2012).

1.2.1 Photorespiration and C_2 pathway

RuBisCO is thought to be the most abundant protein on earth (Ellis, 1979). It is the key enzyme in carbon fixation of photoautotrophic plants. In plant chloroplasts, it catalyses the carboxylation of ribulose 1,5-bisphosphate (RuBP), which results in 2 molecules of 3-PGA. 3-PGA is incorporated into the Calvin-Benson cycle for sugar formation (Calvin & Benson, 1948). Besides its carboxylation function, RuBisCO also displays oxygenase function with RuBP in presence of cellular O_2 (Bowes *et al*., 1971). Instead of two C_3-compounds in reaction with CO_2, this reaction leads to the generation of one molecule 3-PGA and one molecule 2-phosphoglycolate (2-PG). This side-reaction is highly unfavourable for plants, since 2-PG cannot be further used in carbon metabolism and is toxic (Hagemann *et al*., 2010). 2-PG is metabolized in a highly costly pathway, the photorespiration. Photorespiration requires enzymatic reactions in chloroplasts, peroxisomes and mitochondria (Figure 3). 2-PG is hydrolysed to glycolate in the chloroplasts. Glycolate is transported to the peroxisome where it is oxidised to glyoxylate. Glyoxylate is further transaminated to α-ketoglutarate and glycine. In the mitochondrion, two molecules of glycine are converted to serine by glycine decarboxylase (GDC) and serine hydroxymethyl-transferase. Serine is converted into hydroxypyruvate and glycerate in the peroxisome. Hydroxypyruvate is finally converted to 3-PGA in the chloroplast to re-enter the Calvin-Benson cycle (Figure 3). RuBisCO has a higher affinity for CO_2 than for O_2, however the ratio shifts towards O_2 with increasing temperature (Ku & Edwards, 1977). In C_4 plants photorespiration is also found, albeit in smaller levels than in C_3 plants, due to the restriction of the respiratory pathway to the BSCs (Ohnishi & Kanai, 1983).

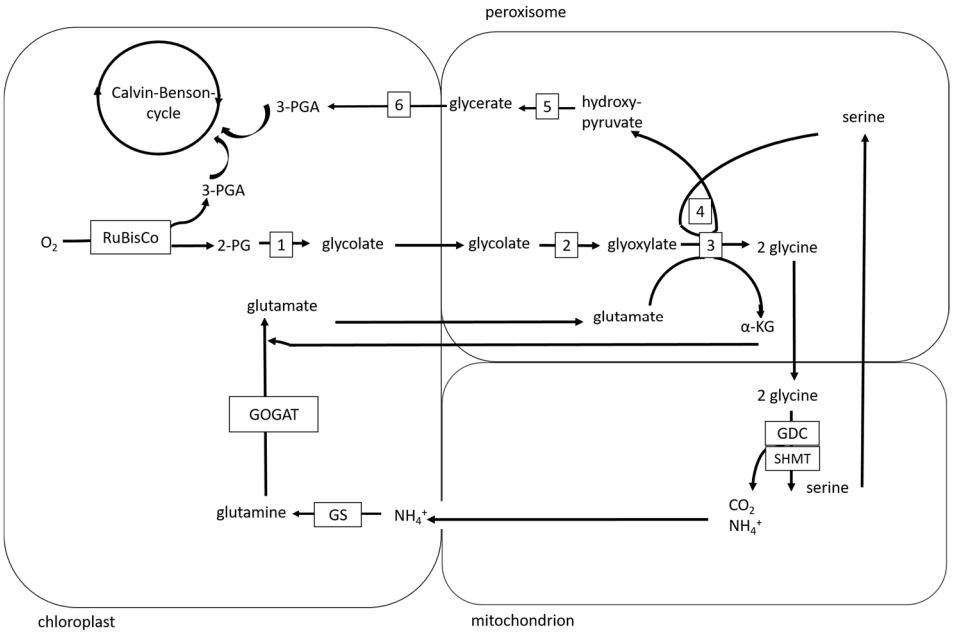

Figure 3 The photorespiratory pathway.
RuBisCO: ribulose 1;5 bisphosphate carboxylase/oxygenase; 2-PG: 2-phosphoglycolate; α-KG: α-ketoglutarate; GDC: glycine decarboxylase; SHMT: serine hydroxymethyltransferase; 3-PGA: 3-phosphoglycerate. 1: phosphoglycolate phosphatase; 2: glycolate oxidase; 3: glutamate glyoxylate aminotransferase; 4: serine-glyoxylate aminotransferase; 5: hydroxypyruvate reductase; 6: glycerate kinase; GS: glutamine synthetase; GOGAT: ferredoxin-dependent glutamate synthase.

The C_2 pathway (or glycine shuttling) is an alternate way to recapture photorespired CO_2 and with this to additionally enhance CO_2 concentration in BS cells. Computational modelling suggests C_2 photosynthesis as a prerequisite for C_4 photosynthesis (Mallmann *et al.,* 2014; Sage, 2003). In the C_2 pathway, the C_2 compound 2-PG is oxidised to glycine and transported into the BS cells. In the BS cells, the glycine decarboxylase (GDC) shows cell-specific expression and releases CO_2 where it can be refixed by RuBisCO and enter the Calvin cycle. The C_2 pathway leads to a refixation efficiency of 75–90 % for C_4 plants in comparison to the photorespiratory C_3 efficiency of 50–80 % at a given temperature (Sage *et al.,* 2012).

1.2.2 C_4 anatomy

The Kranz anatomy is the most apparent feature of C_4 photosynthesis and is defined by an inner layer of BSCs and an outer layer of MCs that surround the veins as a wreath-like structure (Figure 4; Brown, 1975). The Kranz anatomy in C_4 plants is accompanied by a functional specialisation of MC and BSCs regarding primary carbon assimilation in the MC and photosynthetic carbon reduction in the BSC (McKown & Dengler, 2007).
In between C_4 species, high variation in the Kranz anatomy can be found (Muhaidat *et al*., 2007). However, most C_4 species share certain features. C_4 plants also show higher vein density compared to their C_3 relatives and a low MC to BSC tissue volume ratio (Dengler *et al*., 1994; Dengler & Nelson, 1999; Dengler & Taylor, 2000; Hattersley,1984).
Kranz anatomy leads to short diffusion pathways for C_4 metabolites. Also, BSC and MC are connected via plasmodesmata to guarantee high flux of metabolites between the two cell types (Botha, 1992). Another feature of C_4 plants is the arrangement of MC close to

intercellular space and peripheral to BSC (McKown & Dengler, 2007). BSC often also show suberized cell walls, which putatively reduces apoplastic leakage of CO_2 (Dengler & Nelson 1999). Also, BSC are larger than BSC of their C_3 relatives and contain more chloroplasts, mitochondria and peroxisomes. MC in contrast are similar in C_4 species as in their C_3 relatives (Dengler &Taylor, 2000). An additional anatomical feature is often reduced leaf thickness in C_4 plants to obtain maximized contact of MC and BSC (Dengler & Nelson, 1999). BSC chloroplasts in C_4 plants often do not show grana formation in the thylakoids and have a high starch content (Majeran *et al*., 2010).

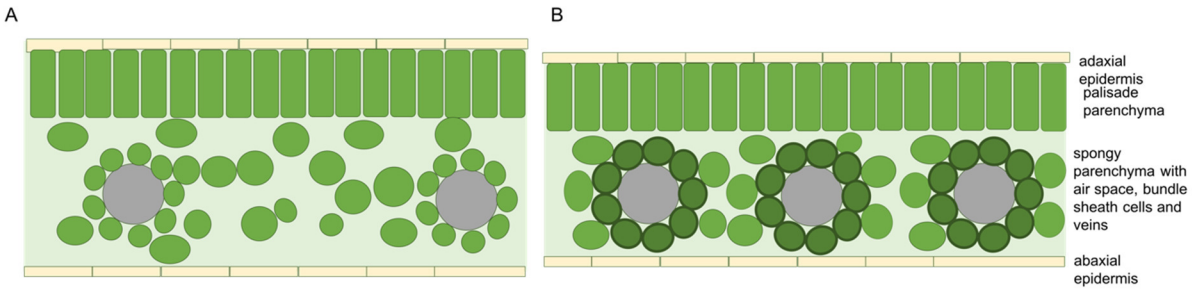

Figure 4 Schematic cross-section of C3 and C4 eudicotyledonous leaves.
A: schematic cross-section of a C3 leaf. B: Schematic cross-section of a C4 leaf. In comparison to the C3 leaf, the distance between the veins is reduced in the C4 leaf. Also, the BSCs appear in a darker green due to increased number of chloroplasts. Cell organelles are not shown. The cell walls of the BSC are thicker compared to the MCs and the BSCs are enlarged compared to the C3 BSCs. Grey circles represent veins.

1.2.3 The C_4 cycle

C_4 photosynthesis is defined by the spatial separation of a primary in MCs and a secondary CO_2 fixation in the BSC leading to a CO_2 concentration mechanism also called CO_2 pump (von Caemmerer & Furbank, 2003). The establishment of C_4 photosynthesis is dependent on several anatomical and biochemical adjustments. C_4 photosynthesis evolved independently over 68 times in the plant kingdom (Sage *et al*., 2012) and led to the formation of several C_4 types.

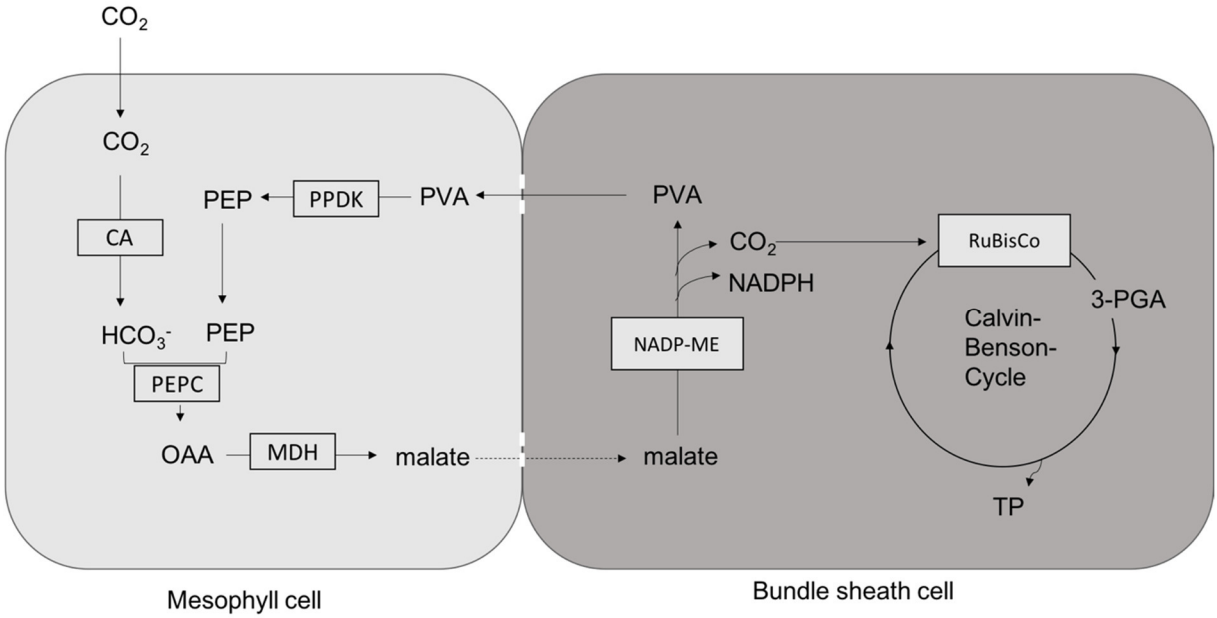

Figure 5 C_4 photosynthesis pathway NADP-ME type.
Schematic overview of C_4 NADP-ME subtype photosynthesis. CA: carbonic anhydrase, HCO_3^- : bicarbonate, PEPC: Phosphoenolpyruvate carboxylase, OAA: oxaloacetate, MDH: malate dehydrogenase, NADP-ME: NADP-dependent malic enzyme, PVA: pyruvate, PPDK: pyruvate, orthophosphate dikinase, PEP: phosphoenolpyruvate, RuBisCO: Ribulose 1,5 bisphosphate carboxygenase oxygenase, 3-PGA: 3-phosphoglycerate, TP: triose phosphate.

In most C_4 plants, CO_2 enters the MC from intercellular air spaces. Carbonic anhydrase converts CO_2 and H_2O to bicarbonate and protons. Phospho*enol* pyruvate carboxylase (PEPC) carboxylates phospho*enol* pyruvate (PEP) using bicarbonate as substrate leading to oxaloacetate (OAA), a C_4 compound (Hatch, 1988). The expression of *PEPC* is restricted to the MCs in C_4 plants. Oxaloacetate is reduced to malate or aspartate which can diffuse into the BSCs. CO_2 is released in the BSCs from the C_4 acid by specific decarboxylating enzymes, leading to an enhanced CO_2 concentration in the BSC compared to the surrounding MC. CO_2 is then re-fixated by RuBisCO in the Calvin-Benson cycle (reviewed in Kellogg, 2013; Figure 5). Expression of *RuBisCO* is restricted to the BSC in C_4 plants (Hatch, 1988; Patel & Berry, 2008; Schulze *et al*., 2016). These mechanisms ensure high affinity for CO_2 for RuBisCO and reduce the rate photorespiration in C_4 plants. Three types of C_4 photosynthesis are known, NADP-ME, NAD-ME and PEP-CK, which show differences in the C_4 acid transported to the BSCs after primary CO_2 fixation, and the enzyme used during decarboxylation in the BSC (Kanai & Edwards, 1999). Some C_4 species use combinations of decarboxylation reactions. *Gynandropsis gynandra* shows PEP-CK activity in older leaves, while otherwise classified as NAD-ME type (Sommer *et al*., 2012). Also, the existence of single-cell C_4 photosynthesis has been reported in the species *Borszczowia aralocaspica* that achieves functional C_4 photosynthesis without Kranz anatomy (Voznesenskaya *et al*., 2001). However, the majority of C_4 plants utilizes C_4 photosynthesis that requires two distinct cell types (Wang *et al*., 2010).

1.2.4 Understanding the C_4 syndrome

Several C_4 model systems are available such as *Amaranth*, *Cleome,* maize and *Flaveria* (Brown *et al*., 2005; Covshoff *et al*., 2014). *Flaveria* is an excellent model of choice to investigate the development of C_4 photosynthesis, as the genus *Flaveria* is comprised of several C_3, C_3-C_4 intermediate and C_4 species. The species of the genus *Flaveria* (*Asteraceae*) are mostly native to North America and are found in disturbed and arid regions (Powell *et al*., 1978). Due to the unique pattern of C_3, C_3-C_4 and C_4 distribution in this genus, it is possible to observe the C_4 syndrome differentiation from an evolutionary point of view (Sage *et al*., 2012; 2014).
Most genes active in C_4 photosynthesis are already established in C_3 photosynthesis (Aubry *et al*., 2011; Moore, 1982). The expression of genes central in C_4 photosynthesis has been shown to be cell-type specific for *PEPC*, *PPDK*, *RuBisCO* and *GDC*. Promoter-analysis revealed MC-specific expression of *PEPC* and *PPDK* in C_4 plants (Kausch, *et al*., 2001; Rosche *et al*., 1998). GDC is composed of four different subunits: P, H, T and L (Oliver *et al*., 1990). The P-subunit of GDC (GLDP) serves as the decarboxylating unit and mRNA was found to be exclusively accumulated in the BS-cells in C_4 plants, with the promoter sequence of the gene also showing BSC-specific activation in the C_3-species *Arabidopsis* (Engelmann *et al*., 2008). Besides the cis-acting elements conferring tissue-specificity, also environmental regulations of C_4 gene expression were found. Light was identified as a key regulator of the C_4 cell-type differentiation, the activation of C_4 photosynthetic genes at transcriptional level and the cell-type specificity of expression of C_4 genes (Langdale *et al*., 1988; Shu *et al*., 1999). While using grasses it is possible to analyse the development of true leaves also in the darkness, due to primordial foliage leaves present in the embryo (Shu *et al.,* 1999), in eudicotyledonous plants a direct approach analysing true leaves is not possible. It was shown in *Flaveria trinervia*, that light-dependent formation of the Kranz anatomy and expression of photosynthetic genes are already present in cotyledons (Shu *et al*., 1999). However, other *Flaveria* species were not yet analysed and whether the formation of Kranz anatomy is light-dependent in other *Flaveria* species, is yet not addressed. If the assessed *Flaveria* species show different behaviour in BSC area increase dependent on the light condition, comparisons of the transcriptomes of each species grown in darkness and in light can give valuable insights into the regulation of Kranz anatomy. The comparison of related C_3 and C_4 transcriptomes has already brought insights into regulation of the C_4 photosynthesis (Gowik *et al*., 2011). By comparing transcriptomes of C_3 and C_4 *Flaveria* cotyledons grown under darkness and light, specific elements for light-dependent pathways would be identified.

1.3 Aims of this thesis

Light as the external source of energy for plants is also a crucial signal for plant development. Plants grown under high-light show adaptations of their leaf anatomy for successful growth of the plants. This thesis aimed to investigate light-dependent anatomy and gene-expression changes in two model species, *Arabidopsis* and *Flaveria*. The first part focussed on C_4-specific light-dependent gene-expression and cotyledon development in *Flaveria* species. The second

part of this thesis focussed on the natural variation of leaf thickness and vein density in the C_3 plant *Arabidopsis* and analysis of the transcriptome of high-light grown *Arabidopsis*.

1) Investigation of the light-dependent C_4 cotyledon differentiation in *Flaveria* species
In *Flaveria trinervia*, light-dependent enlargement of BSC was found in cotyledons (Shu *et al.,* 1999). This thesis aimed to investigate, whether BSC area increase is light dependent in C_3, C_3-C_4 intermediate and C_4 *Flaveria* species. This served as a pre-experiment for future RNA-sequencing attempts, that will be performed if the development of BSCs is different in between the species. Furthermore, light-dependent expression of reporter gene fusion constructs was analysed in C_4 *Flaveria bidentis* and C_3 species *Arabidopsis thaliana*.

2.1) Analysis of leaf traits in *Arabidopsis* using QTL approach
To identify QTLs for estimated leaf thickness, petiole length and leaf vein density, a QTL approach was used. For leaf thickness, two different light and environmental conditions were analysed, high-light and greenhouse (ambient light) conditions, to investigate whether different QTLs could be detected.

2.2) Transcriptome analysis of high-light grown *Arabidopsis* leaves
High-light leads to adaptations in the plant, resulting in different gene-expression and leaf development. In this thesis, the transcriptomes of low-light-grown and high-light grown *Arabidopsis* leaves were compared. Three growth stages were chosen comprising developmental aspects for analysis. The experiments are aimed to understand which regulators are active in the adaptational leaf anatomical changes towards growth under high-light conditions.

2 Results

2.1 Investigation of the light-dependent C_4 cotyledon differentiation in *Flaveria* species

2.1.1 Analysis of BSC area in dark-and light-grown seedlings

Kranz anatomy is an important leaf anatomical feature of C_4 photosynthesis and is, with few exceptions, present in all C_4 species. It is required for successful C_4 photosynthesis, since it allows the spatial separation of primary and secondary CO_2-fixation in two different cell-types (reviewed in Sage *et al*., 2014; Voznesenskaya *et al*., 2001). Kranz anatomy is defined by close vein spacing and enlarged bundle sheath cells surrounding the veins. The specialisation of both MCs and BSCs to primary carbon assimilation and photosynthetic carbon reduction, respectively (McKown & Dengler, 2007) is the most important feature of Kranz anatomy. McKown & Dengler (2007) described the Kranz anatomy in *Flaveria* species in adult leaves. Here, BSCs are larger in the C_3 plant *F. cronquistii* as well as in the C_3-C_4 intermediate species *F. ramosissima* and *F. sonorensis* than in the C_4 plants *F. bidentis* and *F. trinervia* (C_4). The ratio of mesophyll : bundle sheath is high in the C_3 while low in the C_4 species. In *F. trinervia* (C_4) cotyledons, light-dependent formation of the Kranz anatomy was shown (Shu *et al*., 1999), however, light-dependent Kranz anatomy formation in growing cotyledons of other *Flaveria* species has not been analysed yet.

This experiment was performed to shed light onto the question, whether cotyledons of different *Flaveria* species show light-dependent BSC area increase in dependence of their photosynthetic type. To identify regulators of light-dependent BSC area increase in C_4, transcriptome analysis would be performed, if C_3 plants showed no light-dependent BSC area increase. In eudicotyledonous plants the only option to investigate whether leaf-development is light-dependent is to analyse cotyledon growth. True leaves would not grow in the darkness, as the emergence of true leaves is the last step of photomorphogenesis (Arsovski *et al.,* 2012). To this end, *F. pringlei* (C_3) and *F. robusta* (C_3), *F. ramosissima* (C_3-C_4-intermediate) as well as *F. trinervia (C4)* and *F. bidentis* (C_4) were grown under continuous darkness or light regimes. Two different time points were analysed. The first one 3 days after germination representing cotyledons freshly emerged from seed coats and 8 days after germination with cotyledons in their final size, at a stage of the emergence of the first true leaves. Since *Flaveria* species do not germinate equally, germination was monitored daily. Cotyledons were cross-sectioned, stained with propidium iodide and pictures of stacks were taken by confocal microscopy.

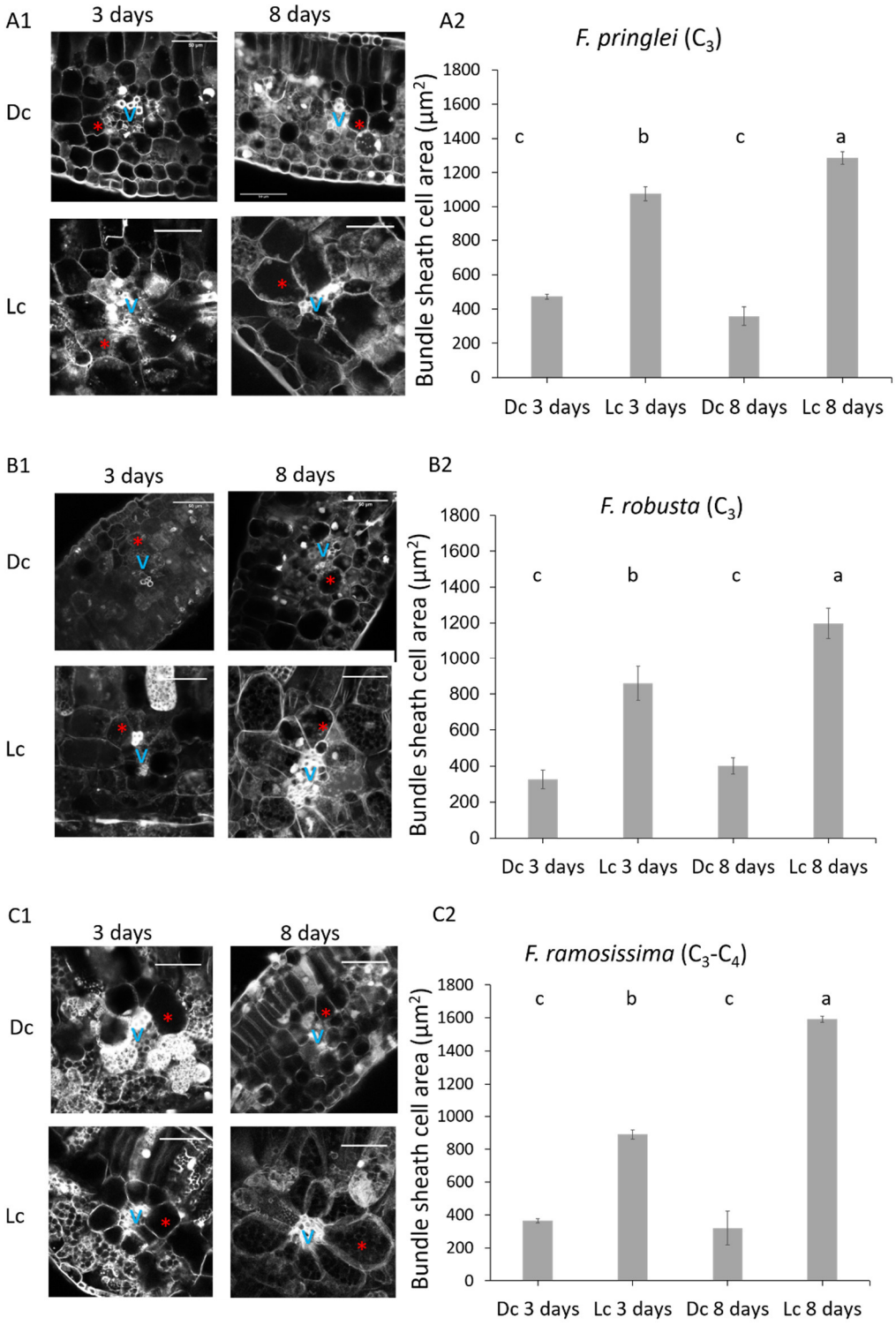
A1
3 days
8 days
Dc
Lc
A2
F. pringlei (C3)
Bundle sheath cell area (µm2)
c
b
c
a
Dc 3 days
Lc 3 days
Dc 8 days
Lc 8 days
B1
3 days
8 days
Dc
Lc
B2
F. robusta (C3)
Bundle sheath cell area (µm2)
c
b
c
a
Dc 3 days
Lc 3 days
Dc 8 days
Lc 8 days
C1
3 days
8 days
Dc
Lc
C2
F. ramosissima (C3-C4)
Bundle sheath cell area (µm2)
c
b
c
a
Dc 3 days
Lc 3 days
Dc 8 days
Lc 8 days

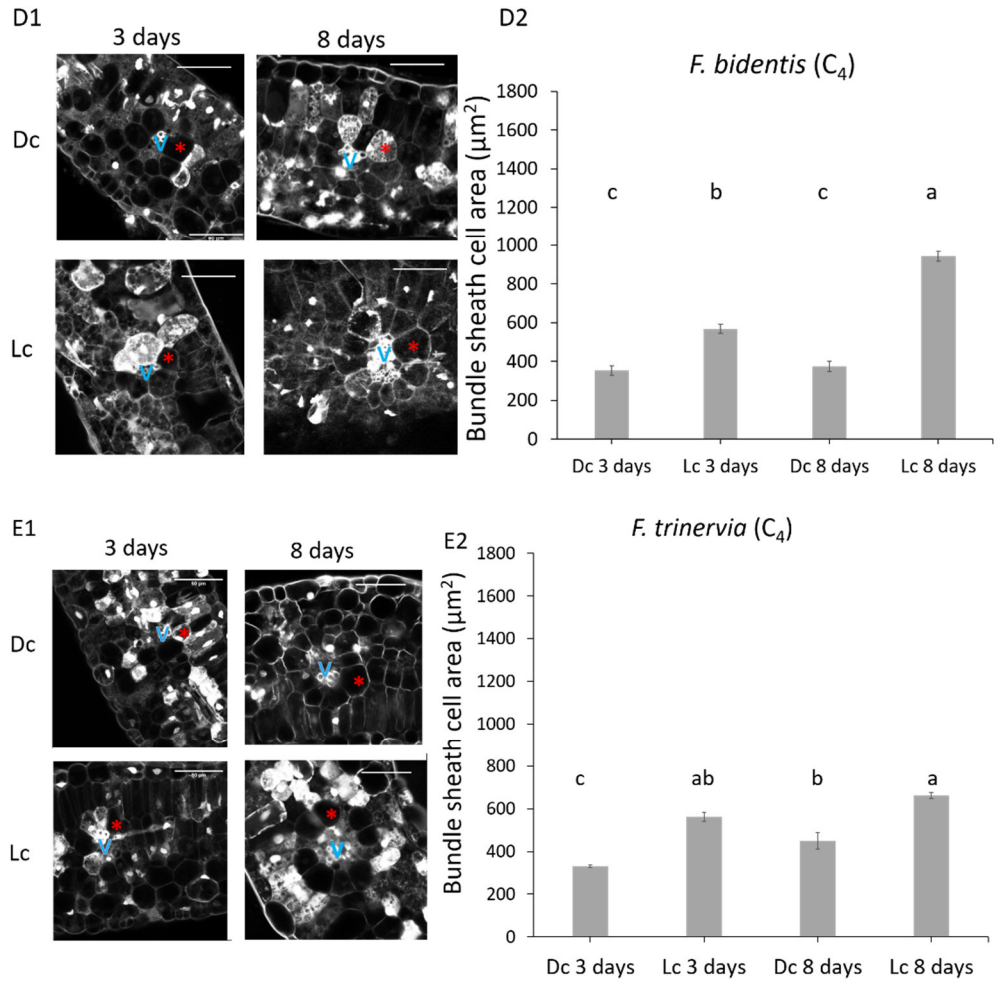

Figure 6 BSC areas of *Flaveria* species grown in darkness or in light.
BSC area of A: *F. pringlei* (C_3), B: *F. robusta* (C_3), C: intermediate *F. ramosissima* (C_3-C_4), D: *F. bidentis* (C_4) and E: *F. trinervia* (C_4)-*Flaveria* species. A1–E1: Cross-sections of 3 and 8 days- old cotyledons stained with propidium iodide. Red asterisks mark a BSC surrounding the vein. A2–E2: Depicted are means of BSC area in µm^2 and standard errors as error bars. Cross-sections of 8–10 individual cotyledons were analysed. Dc: darkness continuous, Lc: light continuous. Letters indicate statistical significance according to ANOVA analysis with Tukey HSD post hoc test. Same letters indicate no statistical significance. p≤0.05.

In all assessed *Flaveria* species, a light-dependent BSC area increase was observed (Figure 6). While BSC size of dark-grown cotyledons did not increase in *F. robusta* (C_3), *F. pringlei* (C_3), *F. ramosissima* (C_3-C_4) and *F. bidentis* (C_4), *F. trinervia* (C_4) cotyledons did also show a significant increase in BSC area over time in the dark.
Interestingly, the BSCs of the analysed C_3 *Flaveria* species*, F. robusta* and *F. pringlei*, as well as those of *F. ramosissima*, a C_3-C_4 species, were larger than the cells of the C_4 species *F. bidentis* and *F. trinervia*. *F. trinervia* shows even smaller bundle sheath cells than *F. bidentis* after 8 days of growth in the light.
To investigate whether the difference in bundle sheath cell size between the *Flaveria* species is due to larger embryonic cells in the C_3 species, also embryonic cotyledon BSCs were quantified (Figure 7).

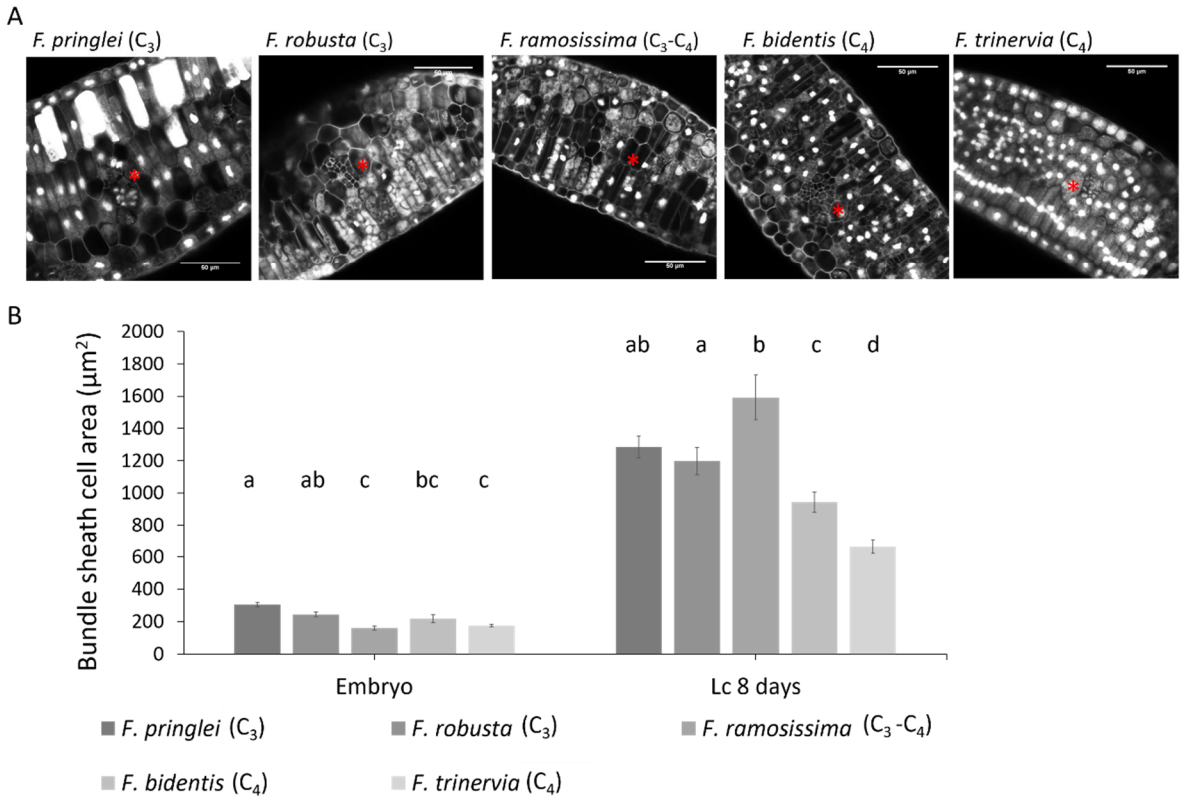

Figure 7 BSC area of embryonic *Flaveria* cotyledons.
A: Embryonic BSC area of five *Flaveria* species. Displayed are cross-sections of embryos acquired using confocal microscopy and propidium iodide staining. Red asterisks mark BSC. B: Bar plot displays BSC area mean values, error bars depict standard error of 8–10 analysed individual embryo and fully-grown light-grown cotyledons, Lc: light continuous. Letters indicate statistical significance according to ANOVA analysis with Tukey HSD post hoc test. Same letters indicate no statistical significance $p \leq 0.05$.

F. pringlei (C_3) embryos displayed significantly larger cells than the C_4-species as well as the C_3-C_4 intermediate *F. ramosissima*. The intermediate species and *F. trinervia* (C_4) displayed the smallest embryonic BSCs, while *F. robusta* (C_3) and *F. bidentis* (C_4) had medium-sized BSCs.
F. pringlei (C_3) and *F. ramosissima* (C_3-C_4) both exhibited large BSCs in mature light-grown cotyledons but differed in their embryonic BSC area. This could give a hint that in the embryo and developing cotyledons, *Flaveria* species follow different mechanisms to increase their cell volumes, since *F. ramosissima* (C_3-C_4) had about half the size of embryonic BSC than *F. pringlei* (C_3) but in fully-grown cotyledons both species had similar BSC areas.
Since for C_4 photosynthesis the ratio of mesophyll to bundle sheath is low to allow rapid diffusion of C_4 metabolites (reviewed in Sage, 2003), this ratio was analysed in cotyledons. In this study both BSC and MC areas are compared and for mature cotyledons compartment ratios are calculated.

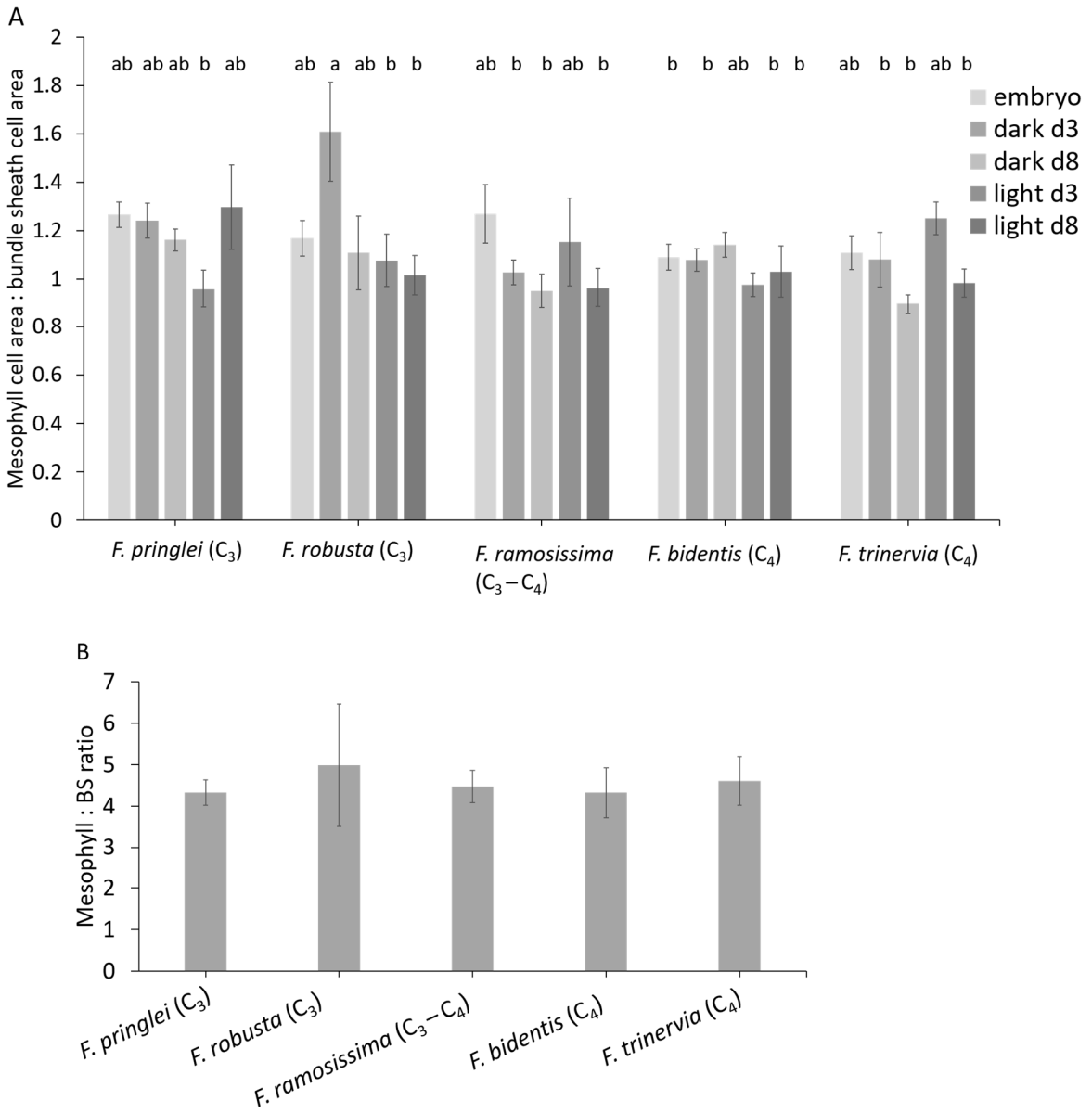

Figure 8 Mesophyll and BSC ratio of *Flaveria* species.
A: Ratio of MC area: BSC area in *Flaveria* embryos and seedlings grown under continuous light or darkness. Depicted are mean values of 9–10 cross-sections per treatment. B: Ratio of mesophyll and BSC compartment area from 8 days old light grown cotyledons. Compartments were measured inside a rectangular area comprising one vein and the distance to the next vein (altered from McKown & Dengler 2007). Depicted are mean values of 6–10 cross-sections. Error bars depict standard error. Letters indicate statistical significance according to Anova with Tukey HSD post hoc test $p \leq 0.05$.

A comparison of the ratio of MC area to BSC area over the developmental stages revealed, that it is not significantly changing in different developmental stages as well as among species (Figure 8A). Only *F. pringlei* (C_3), 3 days grown under light conditions, and *F. robusta* (C_3), 3 days grown under dark conditions, showed a lower and higher ratio, respectively. Comparison of MC and BSC compartments in 8 days old cotyledons grown in the light showed, that the ratio of mesophyll: BS was similar in all species, showing no significant difference (Figure 8B). Since the 8 days old stages grown in light represent the fully-grown status of cotyledons in the species, it is evident from the results that C_3 and C_3-C_4 *Flaveria* species exhibit larger BSCs compared to C_4 *Flaveria* species, when grown in the light (Figures 6; 7). These differences are already established in the embryos for *F. pringlei* (C_3). All analysed *Flaveria* species share a

similar mesophyll: BS compartment area ratio in cotyledons (Figure 8A), which contrasts with the adult leaves (McKown & Dengler 2007). The similar ratios of mesophyll: BSC area ratios in all species in contrast to the different BSC areas in the species indicate, that all cells are larger in the C_3 and C_3-C_4 intermediate *Flaveria* species compared to their C_4 relatives.

2.1.2 Expression of *GLDPA-Ft::YFP* and *PPCA-Ft::YFP* in *Flaveria* is not light-dependent

The expression of the C_4 genes phospho*enol*pyruvate-carboxylase (PEPC) and glycine decarboxylase (GDC) is mesophyll- and BSC-specific in C_4 plants (Andreo *et al.,* 1987; Ohnishi *et al.,* 1985). In C_3 plants, these enzymes show ubiquitous expression. Cell-type-specific expression of C_4 genes was shown to be light-dependent in *F. trinervia* (C_4) (Shu *et al.,* 1999). To analyse whether the expression of PEPC and GDC shows light-dependent cell-type-specific expression, the expression of YFP driven by the *F. trinervia* (C_4)-derived phosphoenolpyruvate carboxylase promoter::YFP (PPCA-L-Ft::H2B-YFP) and of the glycine decarboxylase subunit P promoter::YFP (GLDPA-Ft-::H2B-YFP) was analysed in seedlings of C_4 *F. bidentis*. This experiment was designed to identify suitable stages regarding the light-dependent C_4 gene-expression programme for potential transcriptome analysis.

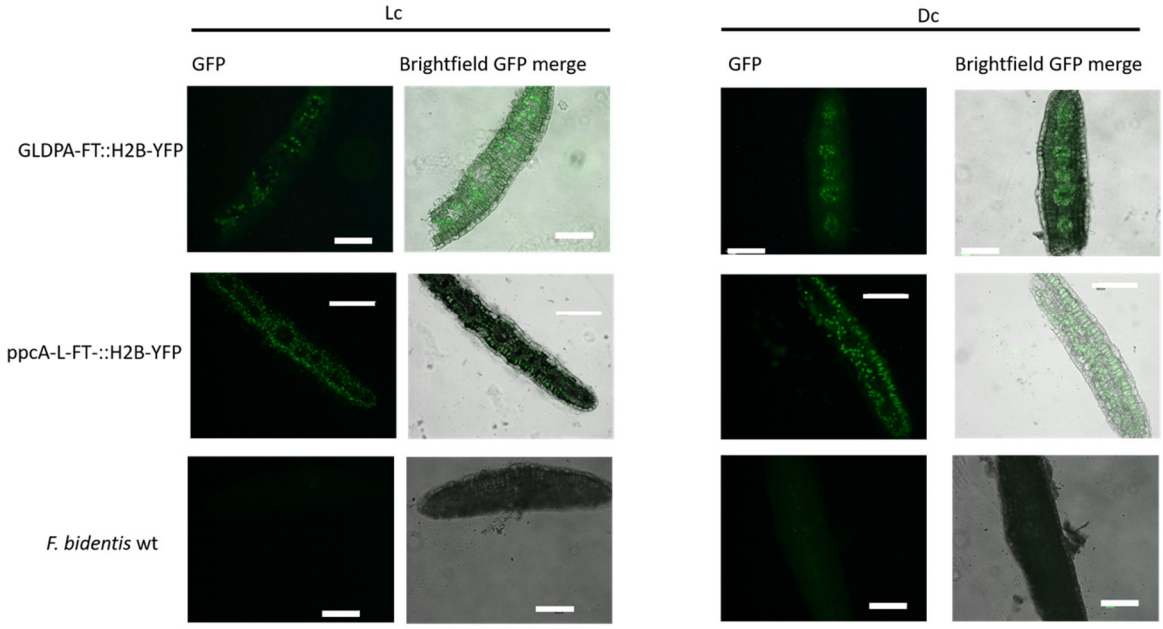

Figure 9 Cell-type-specific expression of reporter genes in *F. bidentis* (C_4).
YFP-signal of GLDPA-FT-::H2B-YFP and ppcA-L-FT-::H2B-YFP in cross-sections of F.bidentis (C_4) cotyledons. Seedlings were grown in continuous light (Lc) and in darkness (Dc) for 4 days. Representative pictures of the GFP-channel and the GFP-channel merged with bright field are displayed. Since YFP and GFP signals show similar excitation and emission values, the GFP filter of the microscope was used for detection of the YFP signal.

The YFP-signal was found in the BSC for the GLDPA::YFP-expressing seedlings and in the MCS for the PPCA::YFP-expressing seedlings in both dark and light grown cotyledons, respectively (Figure 9). Cross-sections of dark-grown plants were produced under green safety light to prevent light-induced changes of the expression during the procedure of cutting the cotyledons. *Flaveria* plants were analysed from day 1 to day 10 after sowing. Expression was

found to be similar at all stages; therefore, representative results from 4 days after germination are shown.

2.1.3 Expression of GLDPA-Ft::YFP is not light-dependent in *Arabidopsis*

The expression of the *F. trinervia* (C_4) derived GLDPA::YFP promoter was analysed in the heterologous system *A. thaliana* to investigate whether the C_4-derived promoter functions similarly in the C_3 plant *Arabidopsis* as in the C_4 plant. The GLPDA::GFP signal was, as reported in adult leaves of *F. bidentis* (C_4) and *A. thaliana* (Engelmann *et al*., 2008), located close to the veins, putatively in the BSCs (Figure 10). For this construct, plants grown in darkness or in light, respectively from day 1 to 10 after sowing were analysed and showed similar expression in the BSCs. Expression was found to be similar in all assessed stages, therefore representative results from eight days after sowing are shown.

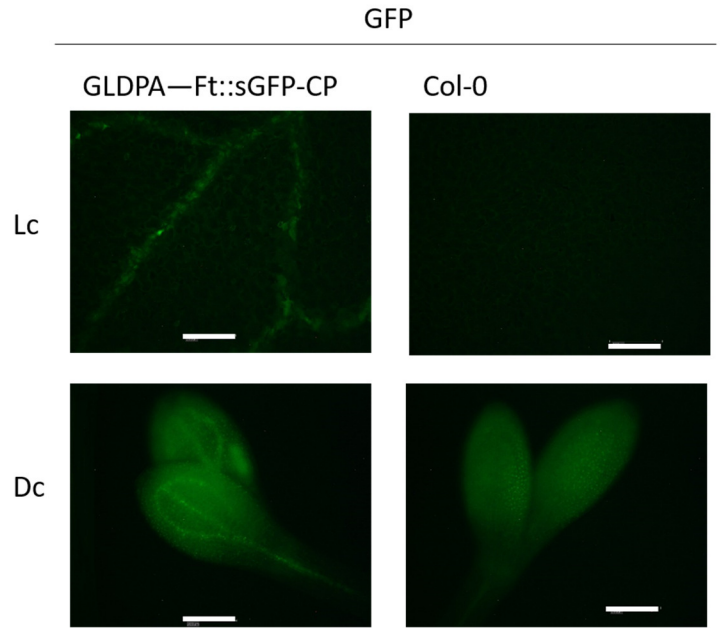

Figure 10 Tissue-specific expression of GLDPA-FT::sGFP-CP in *A.thaliana.*
YFP-signal of GLDPA-FT::sGFP-CP and Col-0 grown in continuous light (Lc) and in continuous darkness (Dc) for 8 days, respectively. Bar represents 200 µm.

In sum, the cell type-specific expression of both analysed C_4 genes was not light-dependent in *F. bidentis* (C_4) and in *Arabidopsis*. All assessed *Flaveria* species showed light-dependent BSC area increase. The goal of these experiments was to identify suitable stages for transcriptome analyses comparing light-dependent leaf differentiation in seedlings of C_3, C_3-C_4 and C_4 *Flaveria* species. Because of the results displayed in this thesis, transcriptome analysis was not performed.

2 Results

2.2 Analysis of leaf traits in *Arabidopsis* using a QTL approach

The aim of this project was to identify regulators of leaf traits. As a first step, experiments were performed to identify *Arabidopsis* accessions differing in leaf thickness, leaf vein density and palisade cell length. The second part of the project used QTL analysis to identify of putative candidate genes for leaf vein density.

2.2.1 Variation of estimated leaf thickness and leaf vein density in 33 *Arabidopsis* accessions

C_4 plants exhibit higher photosynthetic capacity than C_3 plants under more extreme conditions, that is high-light and high temperatures. Since the transition from C_3 to C_4 occurred several times independently in the plant kingdom, a certain potential for C_4-ness can be seen as given for all plants. Therefore, I aimed to identify *Arabidopsis* lines that show a high phenotypic variation in leaf traits when grown under high-light conditions.

To investigate whether *Arabidopsis* accessions display variation in leaf thickness and leaf vein density, 33 *Arabidopsis* accessions from worldwide locations were grown under 300 µmol m^{-2} s^{-1} under long day conditions. This condition is referred to as a high-light treatment in this thesis, as *Arabidopsis* plants can thrive and complete a healthy life cycle under these conditions but show high-light adaptations such as anthocyanin accumulation and leaf architecture changes (Supplemental Figure 1; Figure 18). For experiments, 3rd or 4th true leaves were analysed, since these leaves complete the largest part of their development before the onset of the flowering process of the plants under these conditions. The induction of flowering leads to altered gene expression that underlies the switch from vegetative to reproductive growth: thus, the analysis of leaf development experiments had to be performed before the switch occurred.

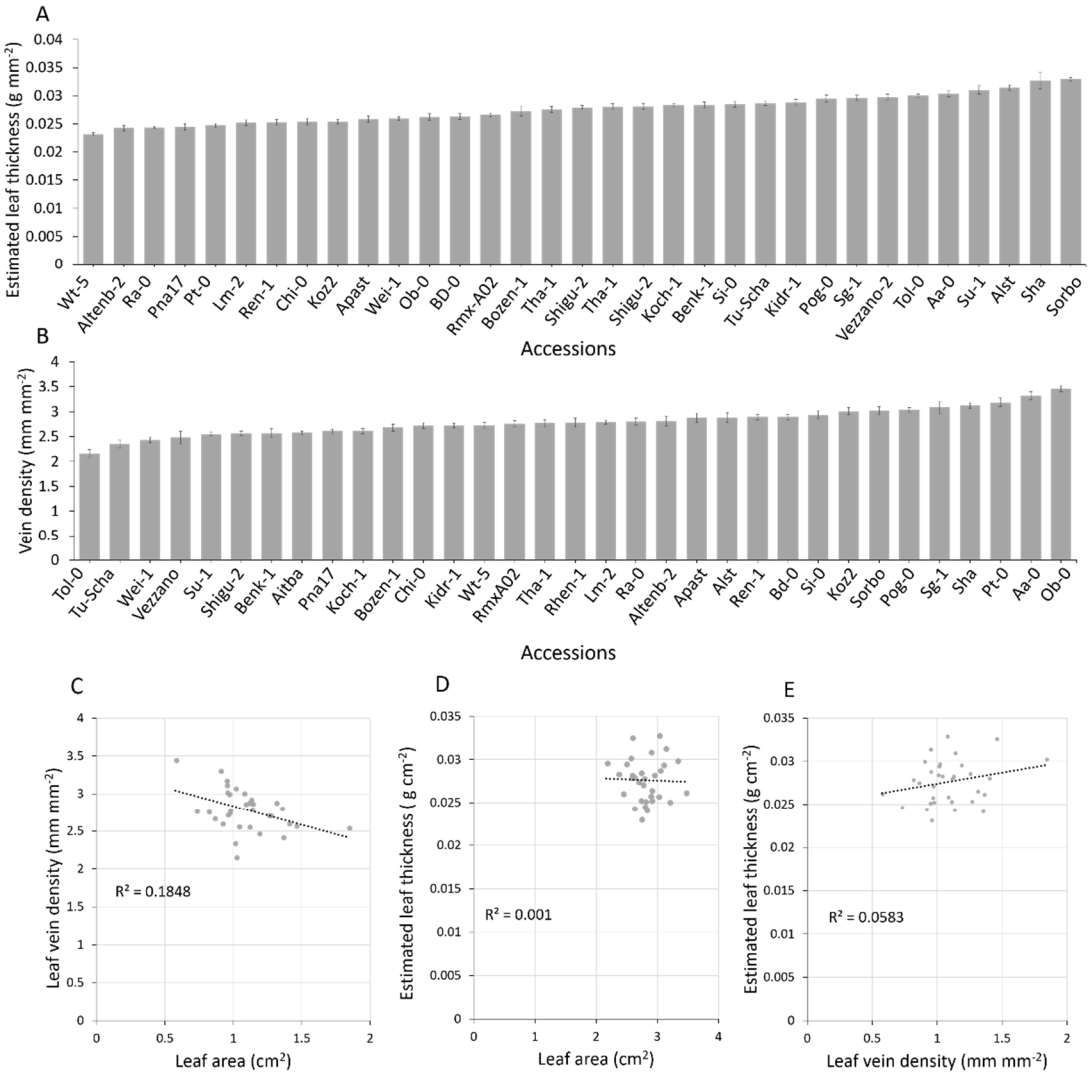

Figure 11 Leaf traits of 33 *Arabidopsis* accessions grown under high-light conditions.
A: Estimated leaf thickness and B: leaf vein density of 33 *Arabidopsis* accessions. C: Correlation study of leaf vein density and leaf area, D: estimated leaf thickness and leaf area and E: estimated leaf thickness and leaf vein density. Coefficient of determination of the linear trendline is indicated in each plot. Leaf vein density was measured on the 3rd true leaves of *Arabidopsis* accessions and leaf thickness was estimated using weight and area of the 4th true leaves of *Arabidopsis* accessions grown under 300 µmol m^{-2} s^{-1}. Displayed are mean values of 8–10 biological replicates. Error bars depict standard error.

Arabidopsis accessions showed variation in both estimated leaf thickness and leaf vein density (Figure 11A and B). Highest estimated leaf thickness was found for accessions Shakhdara, Aitba and Sorbo, while lowest estimated leaf thickness was found for accessions Wt-5, Altenb-2 and Ra-0. For leaf vein density, highest values were found for accessions Pt-0, Aa-0 and Ob-0. Lowest leaf vein density was found in accessions Tol-0, Tu-Scha and Wei-1. A low negative correlation was found between leaf vein density and leaf area (Figure 11C, R^2= 0.19), while estimated leaf thickness did neither correlate with leaf area (R^2=0.01, Figure 11D) nor leaf vein density (R^2= 0.06, Figure 11E). Interestingly, accessions with high estimated leaf thickness and leaf vein density have origins located in Central Asia: Both Sorbo and Shakhdara, with high leaf vein density and estimated leaf thickness originate from Tajikistan. Aitba has low leaf vein density but shows high values for estimated leaf thickness and derives from Marrakesh. However, Pt—0 and Aa-0, accessions showing high vein density, and Aa-0 also showing high estimated leaf thickness (Figure 11A and B), originate from Germany, indicating that there

might be bioecological backgrounds for each accession that cannot be defined by originating country alone.

2.2.2 Variation of estimated leaf thickness and leaf vein density of AMPRIL parental accessions

In the 33 analysed accessions, variation of the traits estimated leaf thickness and leaf vein density was found. However, from the accessions showing high and low vein density and leaf thickness, respectively, no recombinant inbred lines were available to facilitate QTL analysis. Therefore, the variation among the AMPRIL parental accessions (Huang *et al*., 2011) was assessed.

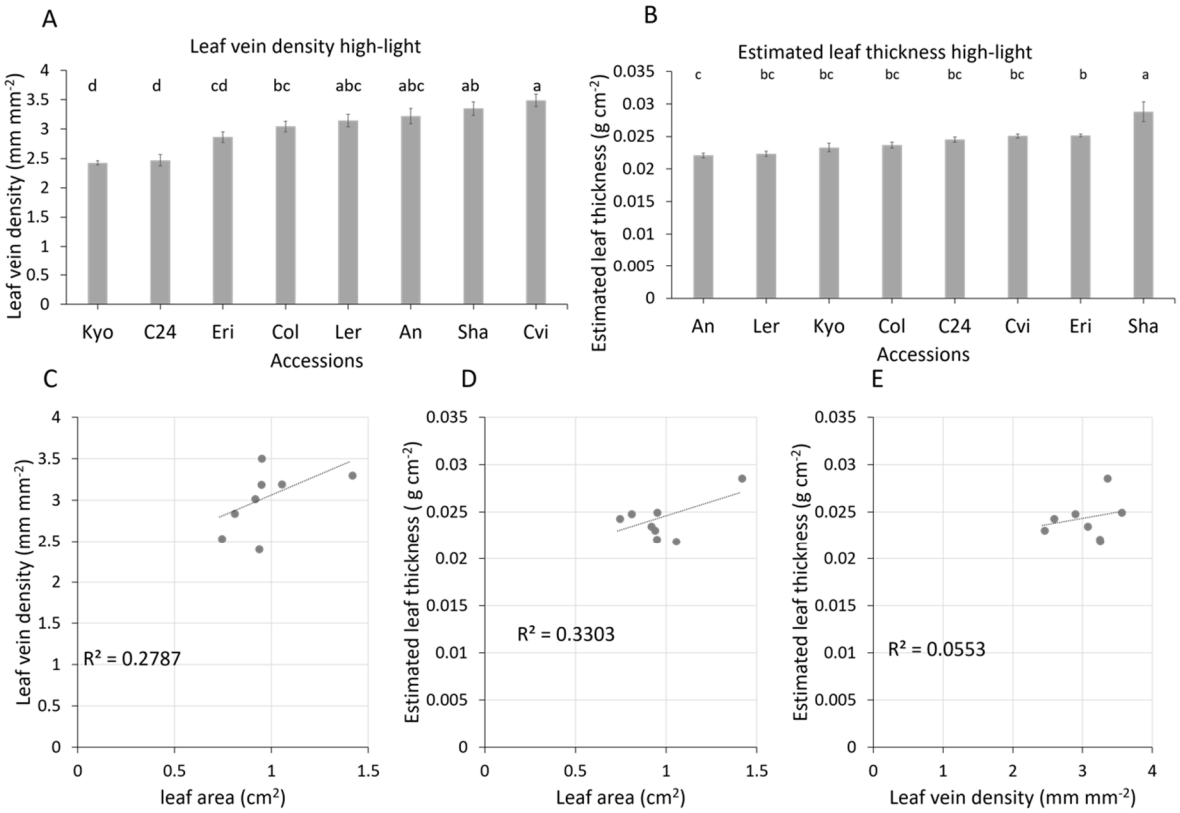

Figure 12 Leaf traits in AMPRIL parental accessions grown under high-light conditions.
A: Leaf vein density and B: estimated leaf thickness of 4th leaves of *Arabidopsis* accessions grown under 300 µmol m^{-2} s^{-1} in growth chamber. Displayed are mean values of 6–8 biological replicates. Error bars depict standard error. Statistics were performed using ANOVA and Tukey HSD post hoc testing p≤0.05. Same letters indicate no significant differences. C: Correlation of leaf vein density with leaf area, of D: estimated leaf thickness with leaf area and of E: estimated leaf thickness with leaf vein density. Coefficient of determination of the linear trendline is given in each plot.

Under high-light conditions, the AMPRIL founder accessions show similar maximum and minimum values for leaf vein density and estimated leaf thickness as the world-wide accessions (Figures 12 A and B, compare with Figure 11 A and B). Sha and Cvi showed high leaf vein density (3.2 and 3.5 mm mm^{-2}, respectively), while Kyo and C24 had low vein density (2.4 and 2.5 mm mm^{-2}, respectively). Estimated leaf thickness was high in Eri and Sha (0.028 and 0.025 g cm^{-2}, respectively), and low in An and Kyo (0.022 and 0.023 g cm^{-2}). Positive correlation was found between leaf vein density and leaf area (R^2: 0.3; Figure 12C), as well as between

estimated leaf thickness and leaf area (R^2: 0.3; Figure 12D). Estimated leaf thickness and leaf vein density did not show correlation (R^2: 0.06; Figure 12E).

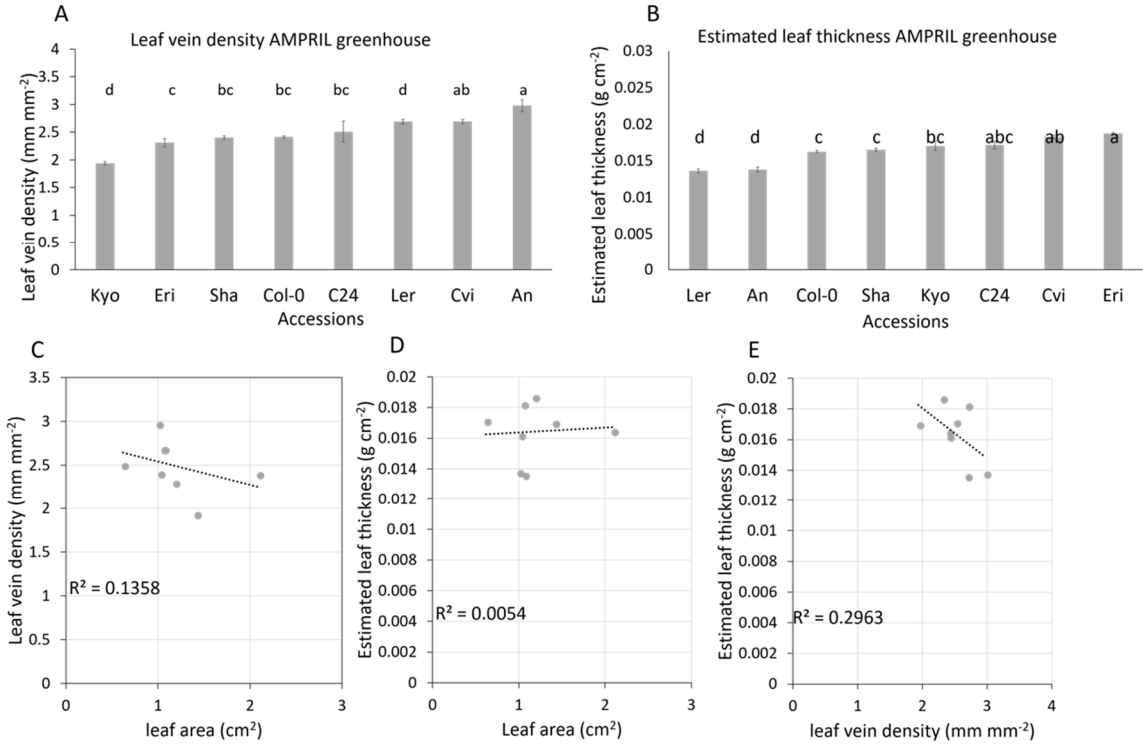

Figure 13 Leaf traits in AMPRIL parental accessions grown in greenhouse.
A: leaf vein density and B: estimated leaf thickness of the 4th true leaves of *Arabidopsis* accessions grown under greenhouse conditions. Displayed are mean values of 6–8 biological replicates. Error bars depict standard error. Statistics were performed using ANOVA and Tukey HSD post hoc testing p≤0.05. Same letters indicate no significant differences. Correlation studies C: of leaf vein density and leaf area, D: estimated leaf thickness and leaf area and E: estimated leaf thickness and leaf vein density. Coefficient of determination of the linear trendline is given in each plot.

The leaf architecture parameters were also analysed under greenhouse conditions, which was relevant for better comparability with other studies analysing similar leaf traits (Rishmawi *et al*., 2017). Also, greenhouse has larger capacities regarding plant growth which is important when it comes to large scale experiments such as QTL. Furthermore, leaves harvested under high-light conditions are more difficult to analyse for their vein density, as thicker leaves make photo-based leaf vein density analysis more difficult. Due to thicker leaves, the veins are not clearly visible as they are in thinner leaves which leads to more elaborate manual correction in the software PhenoVein (Bühler *et al*., 2015).
Light intensities are lower in the greenhouse (about 90–100 µmol m^{-2} s^{-1}). In plants grown under greenhouse conditions, estimated leaf thickness was high in Eri (0.0187 g cm^{-2}) and Cvi (0.0182 g cm^{-2}), and low in Ler (0.0136 g cm^{-2}) and An (0.0138 g cm^{-2}. Leaf vein density was high in Cvi and An 2.69 and 2.97 mm mm^{-2}, respectively, and low in Kyo and Eri, 1.93 and 2.3 mm mm^{-2}, respectively. Under greenhouse conditions, the variation of the traits was not as high as under high-light conditions (Figure 13A and B, compare with 12A and B). Negative correlation was found between leaf vein density and leaf area (Figure 13C), as well as between estimated leaf thickness and leaf vein density (Figure 13E). Estimated leaf thickness and leaf area did not show correlation under these conditions (Figure 13D).

The results indicate that both vein density and estimated leaf thickness are environment-dependent, since both traits show higher values and values varied in a larger range in high-light than under greenhouse conditions.
The AMPRILs GxF and FxG with the parental accessions An, Kyo, Ler and Sha were chosen for QTL mapping experiments, as the four accessions show the highest variation in both leaf traits (Figures 12 and 13).

2.2.3 QTL analysis of leaf traits of *Arabidopsis* grown in high fluence rate

The first experiments using AMPRIL parental accessions showed a high variation in estimated leaf thickness and leaf vein density. To identify leaf anatomy regulators, QTL analysis using AMPRIL GxF and FxG was performed under greenhouse and high-light conditions. As an additional parameter of leaf architecture, leaf petiole length was added. Petiole length is a trait highly responsive to environmental conditions. Leaf vein density, estimated leaf thickness and petiole length were assessed in greenhouse, and estimated leaf thickness and petiole length were analysed in high-light grown lines. Leaf vein density was only assessed in one condition, since the analysis of this trait is time-consuming, and plants grown under high-light exhibit thicker leaves which restrains proper leaf vein density analysis Leaf vein density was also recently studied using MAGIC lines and GWAS analysis (Rishmawi *et al*., 2017), therefore using AMPRIL could help identify additional regulators of leaf vein density.
With this experimental approach it is possible to compare QTLs for leaf traits in two different environments and possibly identify different regulators of anatomical traits.
QTL analysis aims to identify molecular markers that correlate with a quantitative trait of interest. The first experiment aims to identify genes in linkage disequilibrium for estimated leaf thickness and petiole length in AMPRILs grown under high-light conditions. Both leaf thickness and petiole length reportedly change under increasing fluence rates, increasing and decreasing, respectively (Lichtenthaler *et al*., 1981; Tsukaya *et al*., 2002). Petiole length was already object of numerous QTL investigations usually under normal light conditions (approx. 100 µmol m^{-2} s^{-1}; Jiménez-Gómez *et al*., 2010; Pérez-Pérez *et al*., 2002).
Plants were grown under long-day conditions and high-light at 350 µmol m^{-2} s^{-1} and sown in a randomized fashion in 77x trays, watered and turned daily. 6–8 plants per RIL were analysed. For statistical testing analysis, mean values of two independent experiments were analysed. This experiment shows results for petiole length of high-light grown leaves.

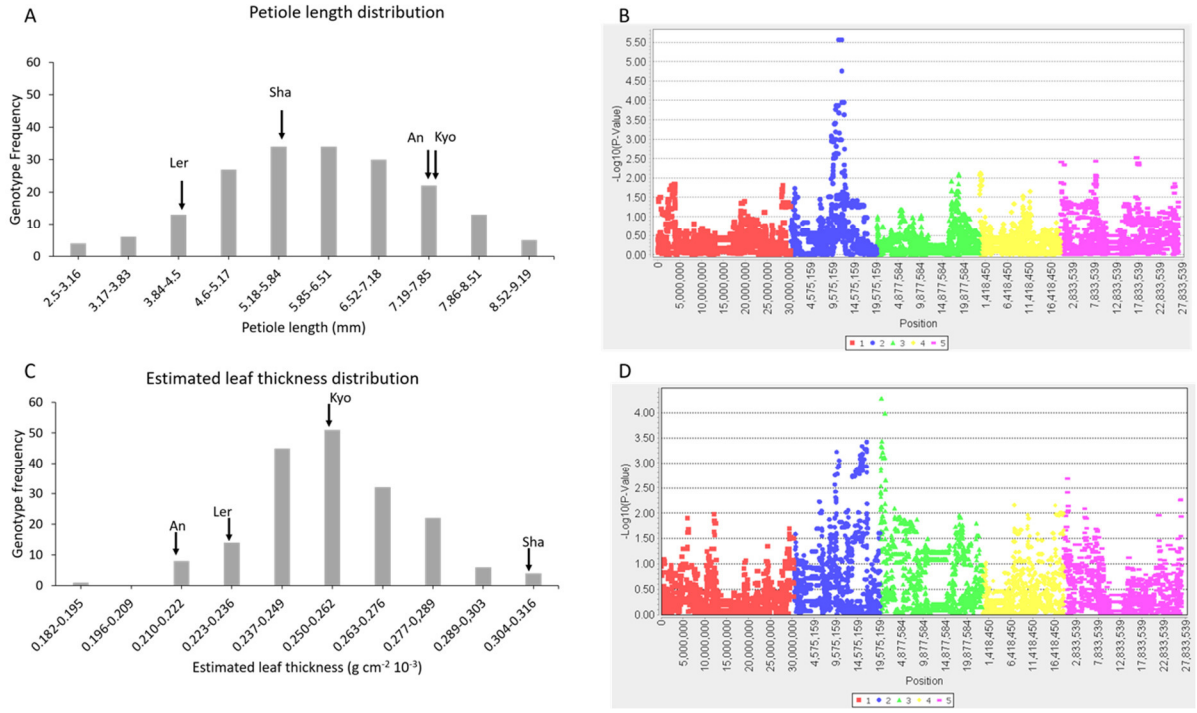

Figure 14 QTL analysis for leaf traits of high-light grown AMPRILs.
A: Frequency distribution of petiole length and C: estimated leaf thickness of AMPRIL FxG and GxF grown under high-light conditions. Arrows indicate values of parental accessions. Manhattan plots displaying SNP positions on the 5 *Arabidopsis* chromosomes and -logP-values on y-axis. B: Petiole length, D: estimated leaf thickness of 4th adult leaves grown at 350 µmol m^{-2} s^{-1} and long days. -logP-values deriving from MLM analysis of two experiments are shown.

Both petiole length and estimated leaf thickness followed a normal distribution (Figure 14A; C). Petiole length and estimated leaf thickness were assessed in RILs of AMPRIL grown under high-light conditions. Mean values of 2 experiments were used for analysis. Figure 14B shows a peak on chr.2, that could be annotated to ERECTA locus (Pérez-Pérez *et al.*, 2002). Manhattan plot for estimated leaf thickness shows two peaks on chromosome 2 and one peak at chromosome 3 (Figure 14D). Broad sense heritability for petiole length was 0.6 and for estimated leaf thickness it was 0.41. The -logP value of the peaks for estimated leaf thickness MLM were lower than 5, therefore the peaks were not considered to contribute to major QTLs, also because of the low heritability values. The R^2 value is a measure for the % of phenotypic variation that is explained by the marker variation. For petiole length under high-light conditions, the peak explained 20.75 % of total phenotypic variation. R^2 for estimated leaf thickness was 22.96 % for the peak on chromosome 3. For the peaks on chromosome 2 R^2 was 1.5 % and 5.1 %, from left to right.

2.2.4 QTL-analysis of leaf traits of AMPRIL grown in greenhouse

The same RILs were also grown under greenhouse conditions to compare QTLs of high-light-grown plants and greenhouse-grown plants. Also, leaf vein density was used as an additional trait.

Plants were sown in a randomized fashion in 77x trays and trays were turned to random positions every day. After 24 days of growth, the 4th true leaves were harvested for further analysis.

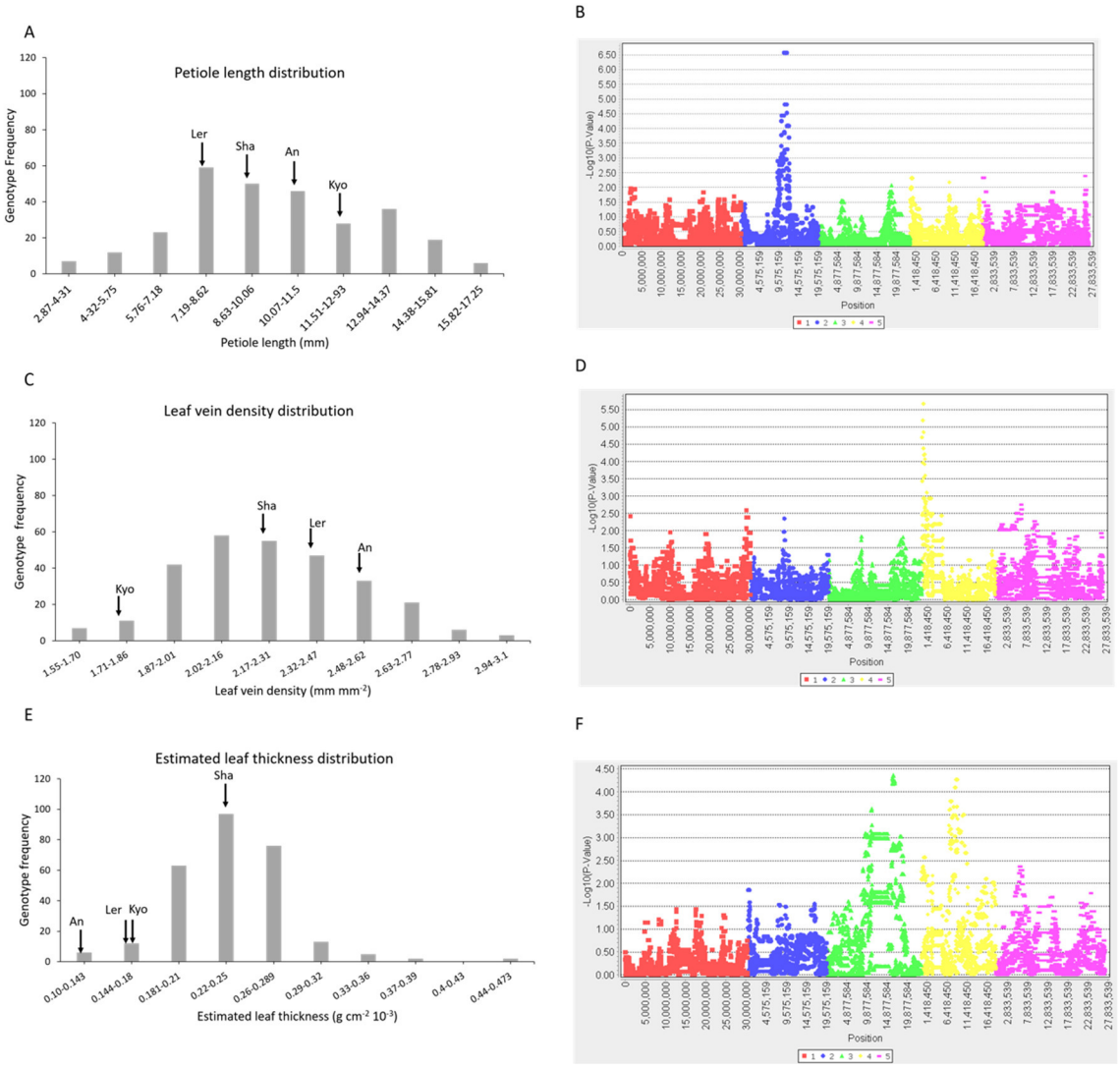

Figure 15 QTL analysis for leaf traits of greenhouse-grown AMPRILs.
A: Frequency distribution of petiole length, C: leaf vein density and E: estimated leaf thickness of AMPRIL FxG and GxF grown under greenhouse conditions. Arrows indicate values of parental accessions. Manhattan plots displaying SNP positions on the 5 *Arabidopsis* chromosomes on x-axis and -logP-values on y-axis. Manhattan plots for B: petiole length, D: vein density and F: estimated leaf thickness of plants grown in greenhouse. -logP-values deriving from MLM analysis of three replicate experiments are shown.

Petiole length of plants grown under greenhouse conditions show a right-skewed distribution, while leaf vein density is normally distributed and estimated leaf thickness shows a left-skewed distribution (Figure 15A, C and E).

For petiole length, a distinct peak on chromosome 2 was found after QTL analysis. This peak can potentially be accounted for the *ERECTA* locus, which is known to map to locus 11208183..11213971 (TAIR). The same region was also identified in the high-light experiments (Figure 14B). In this analysis, the marker variation of this QTL peak explains 33.3 % of total phenotypic variation (R^2). For petiole length, broad sense heritability was 0.75, for leaf vein

density heritability 0.69 and for estimated leaf thickness it was 0.47 under these experimental conditions. Estimated leaf thickness did not lead to the identification of one distinct peak but showed two peaks with -logP-value below 5 on chromosomes 3 and 4 (Figure 15F).
Vein density showed a distinct peak on chromosome 4 This QTL is from now on called QTL-VD. -logP-value for QTL-VD was above 5.5 and therefore, leaf vein density was chosen as a trait for further analysis. Although the -logP-value for vein density were not as high as the -logP values for petiole length, the peak was considered major peak due to the high heritability of leaf vein density. R^2 is 27.53 % for vein density. For petiole length, it is 33.3 % and for estimated leaf thickness 12.3 % for the peak on chromosome 3 and 15.7 % for the peak on chromosome 4.
Comparing the results from QTL under high-light conditions with green house conditions, the results for petiole length indicate that the regulation of petiole length is dependent on one major locus on chromosome 2 which is likely the *ERECTA* locus, in both greenhouse and high-light conditions.
For leaf thickness, under high-light conditions, QTL-analysis showed two peaks on chromosome 2 and one peak at the beginning of chromosome 3 (Figure 14B), in comparison to greenhouse conditions, for which the analysis revealed a peak in the middle regions of chromosome 3 and chromosome 4, respectively. This indicates, that the regulation of leaf thickness might be a trait regulated by multiple genes and that there might be light-quantity related regulations.

2.2.5 Selection of lines for fine mapping of leaf vein density QTL

For fine-mapping of QTL-VD, a heterogenous inbred family (HIF) approach was followed. HIFs are lines that are isogenic for most regions except for the region of interest (Tuinstra *et al*., 1997). Using the segregating lines near isogenic lines (NILs) can be identified and used for fine-mapping. SNP data provided by the Koornneef lab were analysed using TASSEL software. Heterozygous regions were indicated by the software. The whole genomic data set was analysed to identify lines only heterozygous for the region of interest. Before fine-mapping, it was necessary to confirm, that the segregating lines show significant variation in leaf vein density. The AMPRIL contained three eligible HIF lines that display a near isogenic genotype for the genome except for a heterozygous region on chromosome 4 (Figure 16A). To this end, individual plants of the lines GF33, GF07 and FG18 were genotyped using four PCR-based markers covering the heterozygous region of the QTL-VD and one marker on the downstream region of the heterozygous region, while GF07 was analysed using two markers, because of the smaller size of the heterogenous region. Plants that were identified homozygous for either parental allele were phenotyped. For FG18, the marker at about 218,000 bp on chromosome 4 showed always An phenotype (Supplemental Figure 4) indicating that for this line, the heterozygous region was smaller than expected. The other markers however showed segregation as expected and phenotyping was conducted according to the other markers, as the next marker confirmed heterozygous genotypes still in the QTL-VD region (Supplemental

Figure 4, Table15). For FG18 and GF07, parental alleles were identified as An and Kyo, while GF33 contains An and Sha alleles in QTL-VD (Figure 16A).

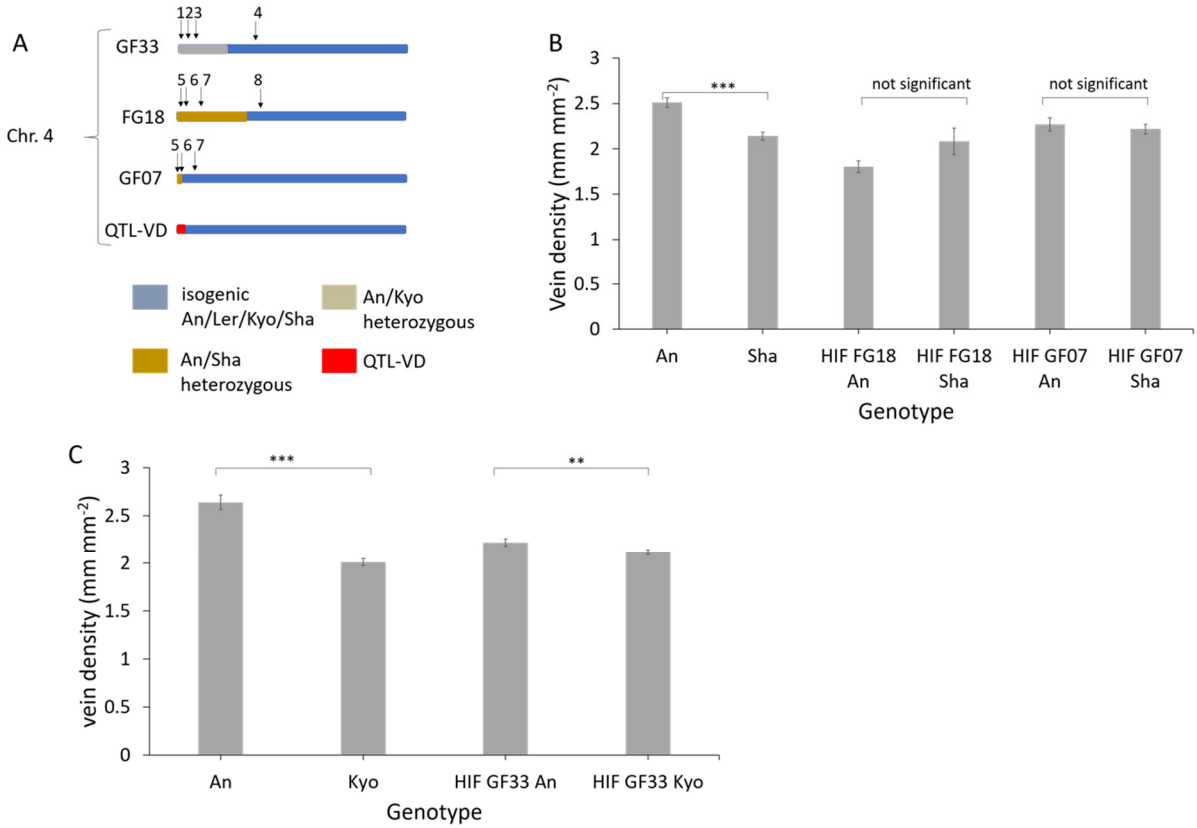

Figure 16 HIFs used for NIL analysis and T-DNA mutant candidate analysis.
A: Schematic overview of three lines chosen from AMPRIL populations GF and FG for NIL analysis. Displayed are chromosomes 4 as the other chromosomes are isogenic. Highlighted in red is the region of QTL-VD. Heterozygous regions are highlighted in grey and yellow for An/Kyo and An/Sha heterozygous regions, respectively. Arrowheads indicate marker locations for mapping of segregating lines. 1–4: Markers used for genotyping GF33: GF33_1, GF33_I, GF33_II, GF33_III an GF33_IV. 5–8: Markers used for genotyping FG18 and GF07: FG18/GF07_1, FG18/GF07_II, FG18/GF07_III and FG18/GF07_IV (Table 15). B: Leaf vein density does not differ in HIF lines FG18 and GF07 when homozygous for either parental allele compared to wild types An and Sha. C: Leaf vein density is significantly different in GF33 lines homozygous for QTL-VD. Displayed are mean values of 6–8 biological replicates. Error bars indicate standard error. Asterisks indicate statistical significance after pairwise t-test p≤0.05: *, p≤0.01: **, p≤0.001: ***.

FG18 and GF07 plants that were homozygous An or Sha in QTL-VD did not show significant difference in leaf vein density compared to parental accessions An and Sha (Figure 16B). Plants of GF33 homozygous for An in QTL-VD showed significantly higher leaf vein density than plants of GF33 homozygous for Kyo in QTL-VD (Figure 16C). The accession An also had significantly higher leaf vein density than the accession Kyo. However, although the difference was statistically significant, compared to the parental accessions An and Kyo the differences could not be identified by eye which would impede fast identification. Also, fine-mapping requires the assessment of segregating lines for the QTL-VD. It is possible, that the phenotypic differences will become smaller in the segregating lines and would render the differences not significant.

2.2.6 SNP-based polymorphism analysis of parental accessions

Instead of traditional fine-mapping, a SNP-based computational approach was followed, comparing the SNPs of parental accessions using the POLYMORPH 1001 webtool to identify mutations and premature stop codons leading to aberrant protein sequences. All genes contained in QTL-VD in a range of 75,000–1,400,000 bp were analysed. Genes with impact on cell differentiation and auxin metabolism were chosen for further analysis and are listed in the Appendices (Supplemental Table 1).

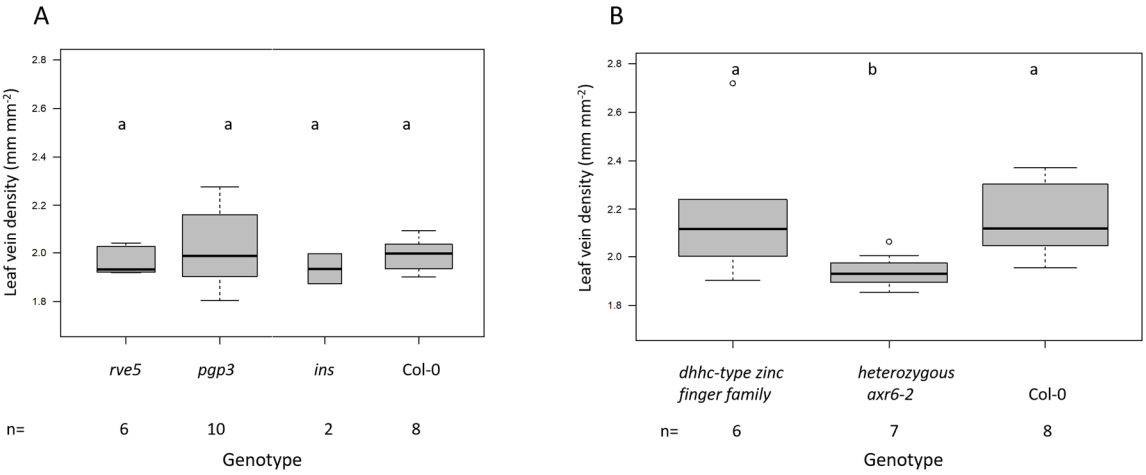

Figure 17 Leaf vein density of T-DNA mutants and *axr6-2*.
A: Four T-DNA mutant lines do not show significantly different leaf vein density compared to wild-type Col-0. B: axr6-2 heterozygous mutants show significantly lower leaf vein density compared to wild-type Col-0. Same letters indicate no statistical significance after pairwise t-test (p=0.05). numbers of individual 4th true leaves are indicated below each panel.

T-DNA mutants for four of candidate genes were chosen from their annotated function in auxin and hormone signalling or cell cycle regulation. The differentiation of major veins is started during the transition from primary to secondary morphogenesis in the leaf and changes of cell cycle and cell growth influence venation (Malinowski, 2013) and therefore genes involved in the regulation of cell cycle can be involved in vein growth and formation.
REVEILLE 5 (*RVE5*) is a member of the MYB transcription factor family proteins. *RVE5* is reported to be involved in photoperiodic and tissue-specific growth regulation in the petiole (Gray *et al*., 2017). Some members of the REVEILLE gene family also have functions in rosette size control (Gray *et al.,* 2017), however the involvement of RVE5 in leaf vein density has not been assessed yet. *PGP3* encodes for ABC protein of p-glycoprotein subfamily. While its function is yet unknown, members of the same protein family have been shown to be involved in auxin transport, *PGP1* for export and *PGP4* for import (Geisler *et al*., 2006). *AXR6* (*CULLIN1*) is a component of an SCF ubiquitin ligase complex and involved in mediating auxin and jasmonic acid response (Esteve-Bruna *et al*., 2013). I analysed *axr6-2*, a mutant derived from diepoxybutane mutagenization and subsequent 6-time backcrossing to Col-0 (Hobbie *et al*., 2000). indole synthase (*INS*) shows 65 % amino acid identity to thioredoxin peroxidase *TSA1*, which is involved in tryptophan-dependent indole synthesis and possibly auxin biosynthesis

(Zhang *et al*., 2008). DHHC-type zinc finger family protein might be involved in cytoplasmic vesicle transport. Its function however, is not known yet (Menges *et al*., 2002).
4th true leaves were harvested 24 d after germination, and vein density was assessed (Figure 17A and B). T-DNA mutants with T-DNA insertion located in exons were chosen (Supplemental Figure 3). Heterozygous mutants for *axr6-2* were identified according to their smaller rosette area as described by Hobbie and co-workers (2000). The homozygous mutants are seedling lethal (Hobbie *et al.,* 2000), therefore only heterozygous plants can be phenotyped. Mutants of *axr6-2* showed significantly different vein density when compared to the wild-type (Figure 17B), while the four assessed T-DNA mutant lines did not show significantly different leaf vein density when compared to Col-0 (Figure 17A). It is possible, that although the presence of the T-DNA insertion was verified by PCR, the T-DNA insertion does not influence the gene-expression of the targeted genes (Wang, 2008). Therefore, to verify the T-DNA insertion mutant analysis, the expression of the target genes should be assessed.
In sum, SNP-based analysis of polymorphisms was a helpful tool to identify candidate genes for QTL-VD. By searching the QTL-region for polymorphisms in between the four parental accessions of the AMPRIL lines and then filtering the candidate genes by their annotated function, it was possible to reduce the list of candidate genes to approximately 30 genes. The preliminary analysis of T-DNA mutants however did not show evidence that the analysed genes have function in the regulation of leaf vein density. The preliminary analysis of the diepoxybutane mutagenization-derived heterozygous mutants of *axr6-2* indicate a role for *axr6-2* in leaf vein formation, since the mutants showed reduced leaf vein density when compared to the wild-type (Figure 17B). However, the mutants were not confirmed by gene-expression analysis, yet.

2.3 Transcriptome analysis of high-light grown leaves

High-light has a great impact on the leaf architecture, however the regulators of these processes are yet not fully known. Plants grown under high-light conditions display adaptation changes such as increased leaf thickness and anthocyanin production (Kovinich *et al*., 2015; Weston *et al*., 2000) The aim of the experiment was to identify genes that are involved in high-light responses of leaf development.
To identify candidate genes for leaf thickness-regulators under high-light, RNA-sequencing was performed. In a first step, three developmental stages of leaves grown under low and high photon fluence rates were selected. To identify the high-light-dependent regulators of leaf anatomy, leaves of the same length were used in both conditions. Using leaf length as a criterium for sampling and not days after sowing was important, as plants grew slower under low-light conditions than plants grown under high-light conditions. Using leaf length therefore ensured comparable developmental stages of the assessed leaves. Three developmental stages were used for transcriptomic analyses. Small leaves at the onset of cell elongation were used as the first stage. The aim was to use the smallest leaves possible for analysis and which should place the leaves' development into the primary morphogenesis. The second stage was defined as the intermediate stage with leaves having reached half the length of adult leaves,

where cell elongation is mainly active. The third stage comprised adult leaves that reached their final size. This stage should serve as a control and give an overview of gene-expression in adult leaves. The goal of the transcriptomic analysis was to identify regulators of high-light-dependent leaf development.

2.3.1 Anatomical differences between high-light-and low-light-grown *Arabidopsis* leaves

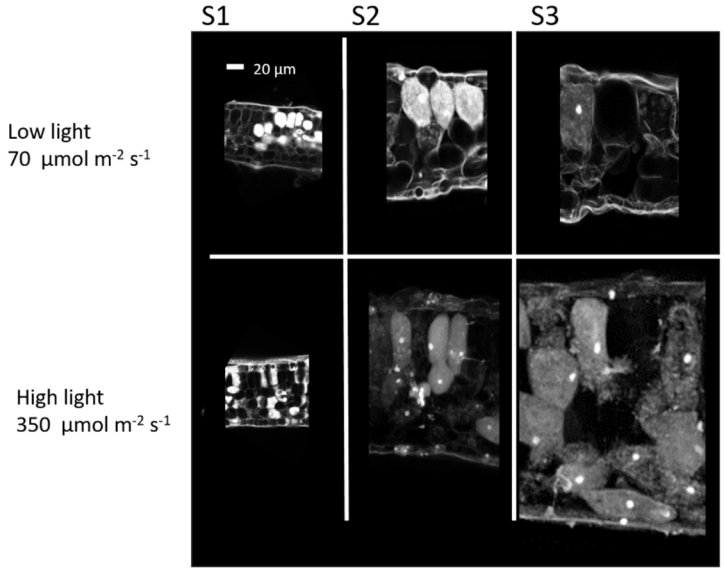

Figure 18 *Arabidopsis* cross-sections of leaves grown under two light-conditions.
Cross-sections of Col-0 4th leaves grown under low (70 µmol m^{-2} s^{-1}) and high-light (350 µmol m^{-2} s^{-1}). Sections were made from 1 mm (S1), 6–7 mm (S2) and 10–12 mm long leaves (S3). White bar represents 20 µm.

In a first step, three developmental stages of 4th leaves of plants grown under low- and high-light were analysed by cross-sectioning for their anatomical properties (Figure 18). The first stage (S1) represents 1 mm long leaves. Under low-light conditions, the palisade parenchyma cells were not as elongated as in high-light-treated leaves. Both low-light and high-light samples showed similar leaf thickness and the number of spongy parenchyma layers was the same. High-light treated plants showed elongated palisade parenchyma cells. Stage 2 (S2) represents 6–7 mm long leaves, that have reached approximately half of their final length. In low-light, palisade parenchyma cells were more isodiametric as compared to the cylinder-shaped palisade parenchyma cells of high-light grown leaves. Leaves of high-light grown plants were thicker in S2 than low-light-grown leaves. In the adult stage 3 (S3), low-light-grown leaves showed slightly elongated palisade cells and were generally thinner leaves than high-light-grown leaves. All three developmental stages showed light-dependent cell expansion. To identify regulators for high-light-dependent cell expansion, RNA-Sequencing was performed on samples deriving from these three developmental stages and light conditions.

2.3.2 RNA-sequencing of high-light and low-light grown *Arabidopsis* leaves

RNA-sequencing was performed at the Cologne Center for Genomics (CCG). Raw data analysis, genome assembly and differential gene expression analysis were executed by P. Wagle at the Cologne Graduate School of Ageing Research (CECAD, Wagle *et al*., 2015). A direct comparison of transcripts of the low-light grown samples with the high-light grown samples in a stage specific way revealed, at a stringency of FC≥2 and p≤0.05, for S1, 181 up-regulated and 213 down-regulated genes out of a total of 33,558 expressed genes. For S2, 542 up-regulated genes and 392 down-regulated genes were found and for S3, 2411 genes. were up-regulated and 2894 genes down-regulated (Figure 19B and C). Principle component analysis (PCA; Figure 19A) revealed that transcripts of low-light and high-light treated plants in the first two stages S1 and S2 shared similar components, while the distance between the high-light and low-light transcripts of the third stage was higher.

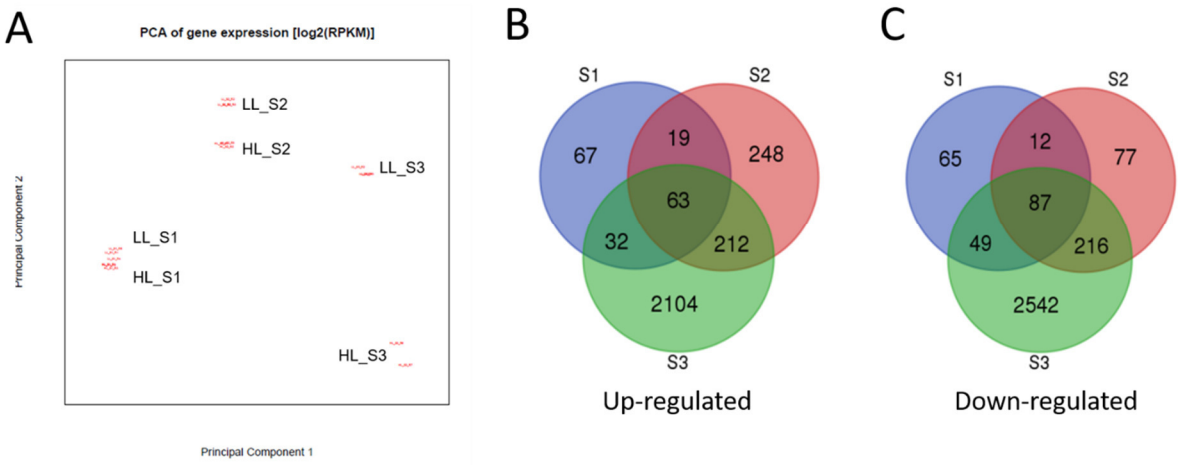

Figure 19 PCA and Venn diagrams of differentially expressed genes.
A: Principle component analysis of gene expression. X and Y axis represents principle component 1 and 2, respectively. In red, the averages of the 3 replicate samples are shown and in black the light-treatment Light treatment is indicated by LL: low-light, HL: high-light. Stage 1: S1, Stage 2: S2 and Stage 3: S3. For high-light treated samples in stage 3, 2 instead of 3 replicate samples were used. B–C: Venn diagrams of up (B) and (C) down-regulated genes of the differentially expressed genes. Stringency of FC≥2 and p≤0.05 were used. Stage-specific expression is indicated by non-overlapping regions. Stages are indicated by S1, S2 and S3 for stage 1, stage 2 and stage 3, respectively.

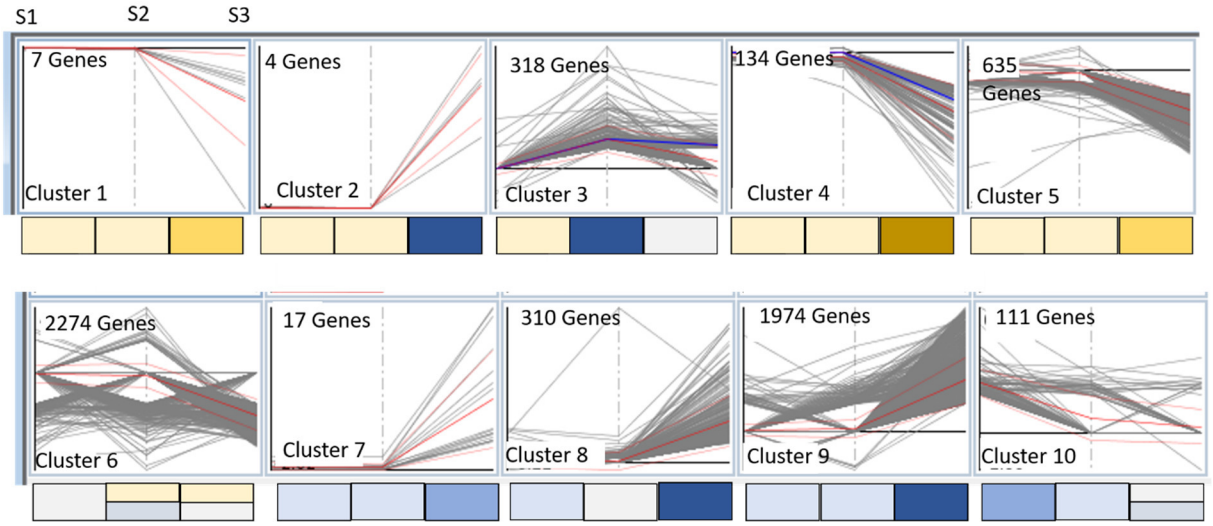

Figure 20 Cluster analysis of differentially expressed genes.

Genes expressed in high-light-grown samples were set relative to genes expressed in low-light-grown samples, which served as controls. *Arabidopsis* leaves in 3 developmental stages S1, S2 and S3. Top left corners: number of genes in the cluster, lower left: cluster number. Upper panel of cluster 1 indicates stages for all clusters. Cluster analysis was performed using the MapMan software with Euclidean distance. Middle red line indicates the empirical mean. Outer red lines indicate standard deviation. Grey lines indicate the genes present in the cluster. Colour panels indicate general trends of gene expression found in the cluster. Light blue: weak up-regulation of genes. Dark blue: strong up-regulation of genes. Light yellow: weak down-regulation of genes. Dark yellow: strong down-regulation. Light grey: no differentially regulation.

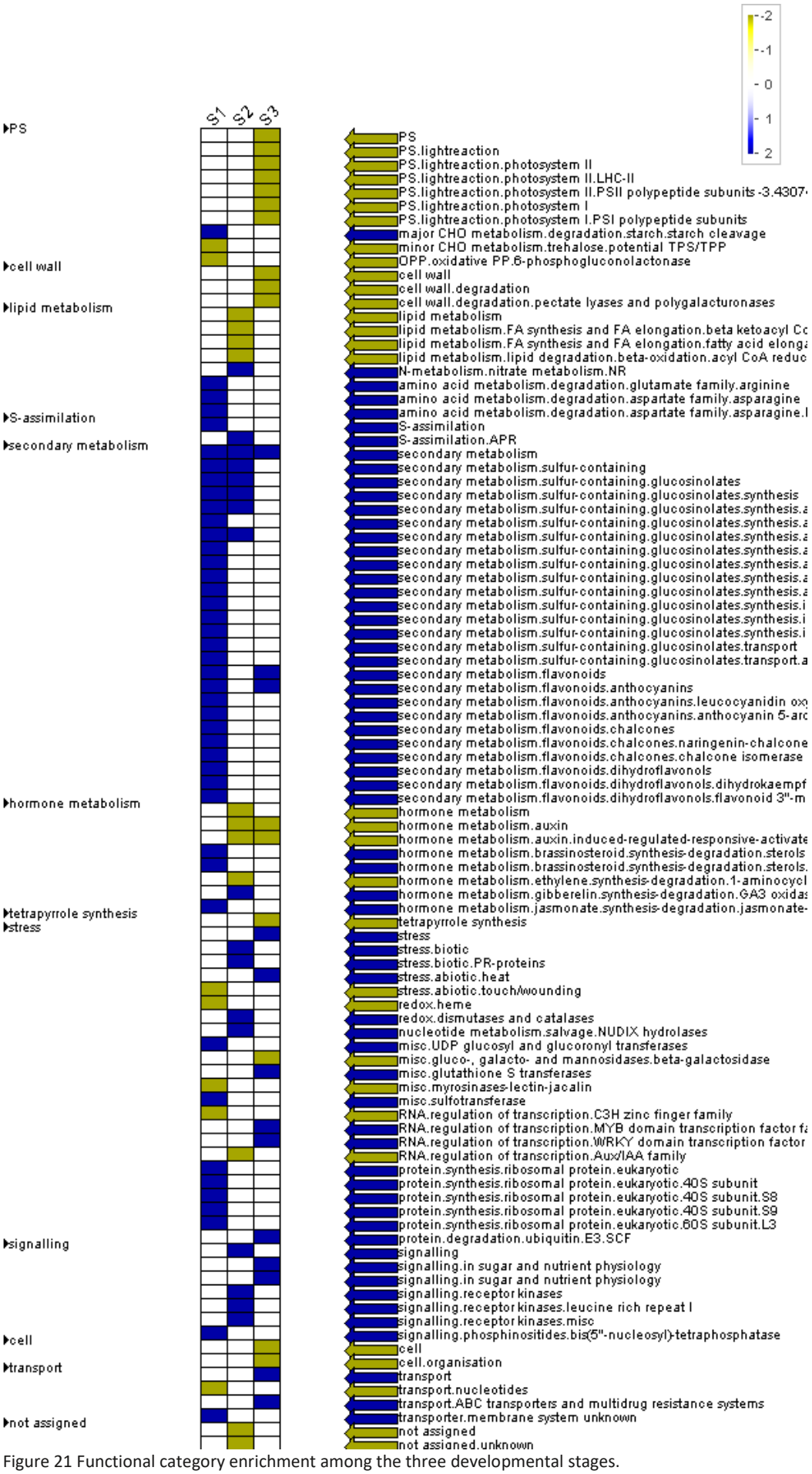

Figure 21 Functional category enrichment among the three developmental stages.

Enrichment of genes belonging to distinct functional categories (MapMan bins) was analysed using Wilcoxon statistic followed by the Benjamini-Hochberg correction. Blue: significantly up-regulated, yellow: significantly down-regulated.

Cluster analysis resulted in 10 clusters with differentially expressed genes following specific expression patterns over the three analysed growth stages. For example, genes of cluster 1 are down-regulated in stage 3, while non-regulated at stages 1 and 2 (Figure 20). Genes were grouped into functional categories, so-called MapMan bins, for cluster analysis using MapMan (Figure 21). Bin-identifier for each cluster shown can be found in the appendices (Supplemental Table 3). The aim of this experiment was to investigate which genes are potentially responsible for adjustment of the leaf morphology towards high-light. The third stage represents the adult stage of the leaf that does not show further increase in leaf area. Therefore, it is presumed that leaf growth and light-dependent adjustments of leaf anatomy take place in S1 and S2. Clusters that showed differential gene-expression in S1 and S2 were clusters 3, 6, 8 and 10. Cluster 3 includes genes lowly expressed in stages 1 and 3, but up-regulated in stage 2. This cluster contains a total of 318 genes, with genes involved in the bin categories stress (19 genes), protein (26 genes), RNA (32 genes) and signalling (33 genes). Cluster 6 contains genes of a more diverse pattern with genes showing no differentially expression in stage 1 but show up- or down-regulation in stage 2, with no or down-regulation in stage 3. This cluster contains the most genes with 2274 genes and their function can be summarized by functional categories of: RNA and protein metabolism, cell and signalling-reactions. In cluster 8, genes are differentially up-regulated in stage 1, not differentially regulated in stage 2 and up-regulated in stage 8. Cluster 10 (111 genes) shows genes highly up-regulated in stage 1 with a lower expression in the last two stages. Here, 15 genes involved in secondary metabolism are found (Supplemental Table 3).

Analysis of the differentially expressed genes showed that most genes are differentially expressed in the adult stage (Figure 19B and C), leaving a small number of genes that can be potentially involved in the morphological adaptations towards high-light.

Enrichment analysis of the differentially expressed genes was performed using PageMan analysis tool (Figure 21). Here, statistically enriched functional categories were displayed for all three developmental stages. In stage 1, secondary metabolism genes were up-regulated in this data set, which partially holds true for stage 2 as well. Also, hormone metabolism genes involved in brassinosteroid-, gibberellin- and jasmonate-metabolism were enriched in stages 1 and 2. Photosynthesis-involved genes were down-regulated in S3, as well as cell wall and auxin metabolism genes (Figure 21).

In the following sections, I will give an overview of gene families that show significant differences in fold changes of gene-expression in high-light conditions compared to low-light controls. Since the most distinct anatomical differentiation was achieved in the plants in the first two stages, I will focus on genes that show differential expression in high-light compared to low-light conditions in the first two stages.

GO-terms classify genes according to their annotated functions (du Plessis *et al*., 2011). Associated with GO-terms describing their functionality, genes can be grouped and identified based on the specific GO-term. This makes analysis of transcriptomic data sets better

comparable (du Plessis *et al*., 2011). For the formation of following tables, genes associated with GO-terms were assembled. Since genes can be annotated towards several GO-terms with different functions, lists were corrected for genes that have function in other biological processes than the GO-term in question.

Section 1: Genes involved in stress-responses

Genes that are differentially expressed under high-light conditions and are associated with GO-term high-light were found up-regulated in all three developmental stages. In S1, *ELIP1* shows the strongest up-regulation of the total up-regulated genes in stage 1. *ELIP2* also is highly up-regulated in stage 1. Both genes show high up-regulation in all three assessed stages. Only 1 gene associated with high-light shows down-regulation in the whole data set, a member of the RING/U-box superfamily protein family (Table 1).

Table 1 Genes associated with GO-term response to high-light intensity.
Displayed are fold changes of differentially expressed genes in high-light. S1: stage 1, S2: stage 2, S3: stage 3. Blue colours indicate up-regulated genes, yellow shades indicate down-regulated genes. Dark blue and yellow indicate higher or lower up and down-regulation, respectively. <2 indicate fold change levels lower than 2.

Genes associated with GO-term high-light				
Gene name	**ID**	**S1**	**S2**	**S3**
RING/U-box superfamily	AT1G14200	-2.07	<2	<2
TIN1	AT5G64510	2.43	2.42	24.62
ELIP2	AT4G14690	15.21	11.46	59.07
ELIP1	AT3G22840	32.79	29.79	389.59
ROF2	AT5G48570	<2	2.22	7.78
BIP3	AT1G09080	<2	3.53	10.74

The regulation of heat shock proteins is light-dependent (Al-Whaibi, 2011). Heat shock proteins are stress-induced and function in cell protection against many stress conditions (Kalmar & Greensmith, 2009). In this transcriptomic analysis, HSPs were found in clusters 3, 6, 8 and 9 (Figure 20). Most genes were up-regulated in the stage 3 (Table 2). 3 genes showed up-regulation over all three stages. This indicates a role for heat shock proteins in the later stages of leaf growth.

Table 2 Genes associated with GO-term heat shock protein.
Displayed are fold changes of differentially expressed genes in high-light. S1: stage 1, S2: stage 2, S3: stage 3. Blue colours indicate up-regulated genes, yellow shades indicate down-regulated genes. <2 indicate fold change levels lower than 2.

GO-term HSP				
Gene name	**ID**	**S1**	**S2**	**S3**
HSP17.4	AT3G46230	<2	<2	5.59
HSP20-like	AT5G51440	3.84	3.31	6.4
HSP23.6	AT4G25200	<2	<2	5.3
HSP23.5	AT5G51440	3.84	3.31	6.4
HSP70	AT3G12580	6.21	4.48	14.8
HSP70-2	AT5G02490	<2	2.08	10.01

HSP70-3	AT3G09440	<2	<2	4.05
HSP70-4	AT3G12580	6.21	4.48	14.8
HSP70-11	AT5G28540	<2	<2	3.74
HSP70-13	AT1G09080	<2	3.53	10.74
HSP81-2	AT5G56030	<2	<2	2.91
HSP81-3	AT5G56010	<2	<2	2.67
HSP90.1	AT5G52640	4.24	3.53	10.85
HSP101	AT1G74310	<2	<2	2.92
Unknown	AT3G04980	<2	<2	-2.41
SFP1	AT5G27240	<2	<2	-2.16
HSP70-17	AT4G16660	<2	<2	2.37
HSP20	AT5G47590	<2	<2	2.47
Unknown	AT2G20560	2.71	<2	6.4
DNAJ heat shock family protein	AT2G20560	2.71	<2	6.4
DNAJ heat shock family A2	AT2G26150	2.98	2.19	23.74

Reactive oxygen species (ROS) are important signalling compounds and are produced within seconds after high-light treatment (Moore *et al.,* 2014). Since ROS consist of free radicals, they are highly reactive and too much ROS leads to oxidative stress in the plant. Therefore, upon ROS production, de-toxification enzymes are up-regulated (You & Chan, 2015). Most ROS-related genes in this data set were differentially regulated in the S3. Only two ROS-related genes were differentially regulated in the S1, GST1 and PRXCA. Superoxide dismutase SOD was only differentially regulated in S2 (Table 3).

Table 3 Genes associated with GO-term ROS-detoxification and -response.
Displayed are fold changes of differentially expressed genes in high-light S1: stage 1, S2: stage 2, S3: stage 3. Blue colours indicate up-regulated genes, yellow shades indicate down-regulated genes. <2 indicate fold change levels lower than 2.

Genes associated with GO-term ROS				
Gene name	**ID**	**S1**	**S2**	**S3**
PRXCA	AT3G49110	-2.25	<2	6.12
RBOHD	AT5G47910	<2	2.68	2.86
SAG21	AT4G02380	<2	3.72	5.45
SROS	AT5G62520	<2	<2	5.12
DOX1	AT3G01420	<2	<2	6.22
APX4	AT4G09010	<2	<2	-7.026
APX5	AT4G35970	<2	<2	-2.99
GST1	At1G02930	6.94	2.3	7.38
CSD2	AT2G28190	<2	2.16	<2
ERF6	AT4G17490	<2	<2	-2.58
GAS14	AT5G14920	<2	<2	-5.83

Anthocyanins are protective pigments synthetized in plant organs and belong to the family of flavonoids. Flavonoids are involved in modulation of auxin transport (Peer & Murphy, 2007) and thereby have influence on plant development and growth. Under high-light conditions, their main function is probably to protect the leaves from excess light (Albert *et al.,* 2009). Anthocyanin synthesis genes were up-regulated from the S1 and reached their highest

expression in the adult stage S3 (Table 4). From the 186 genes up-regulated in S1, 17 were involved in flavonoid metabolism. This indicates that the flavonoid metabolism pathway is of high importance for the growth of *Arabidopsis* under high-light conditions. Anthocyanin synthesis genes were the most highly up-regulated genes found in the data set.

Table 4 Genes that are associated with GO-term Flavonoid metabolic process.
Displayed are fold changes of differentially expressed genes in high-light. S1: stage 1, S2: stage 2, S3: stage 3. Blue colours indicate up-regulated genes, yellow shades indicate down-regulated genes. Dark blue and yellow indicate higher or lower up and down-regulation, respectively. <2 indicate fold change levels lower than 2.

Genes associated with Flavonoid synthesis									
Gene name	ID	S1	S2	S3	**Gene name**	ID	S1	S2	S3
Hypothetical protein	AT2G30930	-3.06	-3.56	<2	*TOC64-III*	AT3G19030	<2	<2	-17.85
Hypothetical protein	AT3G27210	<2	<2	2.64	Hypothetical protein	AT5G57785	<2	<2	-8.9
ECT8	AT1G79270	2.27	<2	<2	*FAP3*	AT1G53520	<2	<2	-8.11
Uncharacterized	AT2G24550	-2.63	-2.74	-2.79	*PME53*	AT5G19730	<2	<2	-4.62
CPN21	AT5G20700	2.01	<2	<2	*SOT12*	AT2G03760	<2	<2	-3.72
TT3	AT5G42800	11.25	7.12	211.37	*CHI2*	AT5G66230	<2	<2	-3.53
TT4	AT5G13930	2.56	5.66	239.94	*ADT4*	AT3G44720	<2	<2	2.19
TT5	AT3G55120	2.08	<2	2.75	*BLH1*	AT2G35940	<2	<2	2.28
TT7	AT5G07990	18.95	2.6	71.99	*DGK3*	AT2G18730	<2	<2	2.47
TT8	AT4G09820	5.75	2.31	389.8	Acyl-transferase family member	AT1G28680	<2	<2	2.6
TT18	AT4G22880	7.23	5.67	291.51	*T22E16.130*	AT3G55470	<2	<2	2.61
UGT73B2	AT4G34135	<2	2.75	3.88	*UGT72B1*	AT4G01070	<2	<2	2.62
UGT78D2	AT5G17050	2.14	<2	5.11	AFG1-like ATPase family protein	AT2G25530	<2	<2	2.93
UGT79B1	AT5G54060	18.24	4.28	1006.2	*MYC2*	AT1G32640	<2	<2	2.97
UGT89C1	AT1G06000	2.32	3.02	4.65	*PSK5*	AT5G65870	<2	<2	3
CYP98A3	AT2G40890	<2	<2	-2.22	*CAD5*	AT4G34230	<2	<2	3.15
MYB12	AT2G47460	2.08	<2	10.64	*NFYA4*	AT2G34720	<2	<2	3.4
FLS1	AT5G08640	2.19	10.14	8.18	GDSL esterase/lipase	AT1G28570	<2	<2	3.59
PAL1	AT2G37040	2.38	<2	4.68	*MPC3*	AT4G05590	<2	<2	4.4
BIC1	AT3G52740	2.55	<2	<2	RING/U-box superfamily protein	AT5G41400	<2	<2	7.55
4CL3	AT1G65060	<2	2.21	25.88	*RHM1*	AT1G78570	<2	2.46	<2
CHIL	AT5G05270	<2	4.98	29.74	*PAP1*	AT1G56650	5.4	<2	52.35
					PAP2	At4g22240	<2	<2	<2

<u>Section 2: genes involved in signal transduction</u>

Photoreceptors and genes related to light signal transductions modulate the information of the absorbed photons and modulate biological activity. Upon high-light treatment, the regulation of genes responsible for photoreceptors is not changed much. Regarding genes

involved in light-signalling, ATBBX32 and HYH show up-regulation in all three stages. The third stage shows highest up- and down-regulation compared to stages 1 and 2 (Table 5).

Table 5 Photoreceptor genes and genes related to light signal transduction expression.
Displayed are fold changes of differentially expressed genes in high-light. S1: stage 1, S2: stage 2, S3: stage 3. Blue colours indicate up-regulated genes, yellow shades indicate down-regulated genes. <2 indicate fold change levels lower than 2.

Genes associated with photoreceptors and light signalling									
Gene name	**ID**	**S1**	**S2**	**S3**	**Gene name**	**ID**	**S1**	**S2**	**S3**
CRY1	AT4G08920	<2	<2	-2	*HFR1*	AT1G02340	<2	-2.46	-14.47
CRY3	AT5G24850	<2	<2	2.8	*PKS3*	AT1G18810	<2	-2.44	-7.83
PHOT1	AT3G45780	<2	<2	-2.67	*PKS2*	AT1G14280	<2	-2.33	-3.73
FKF1	AT1G68050	<2	<2	-4.03	*PIF7*	AT5G61270	<2	-2.04	<2
HY5	AT5G11260	<2	<2	4.22	*PIF3-like 2*	AT3G62090	<2	<2	2.48
PIF4	AT2G43010	-2.56	<2	-2.78	*NFYA5*	AT1G54160	<2	<2	2.52
PKS1	AT2G02950	-2.17	<2	-3.42	*RAX2*	AT2G36890	<2	<2	7.16
ATBBX32	AT3G21150	2.07	2.81	12.77	*RPT3*	AT5G64330	<2	<2	-2.54
HYH	AT3G17609	3.07	2.63	4.03	*PIF1*	AT2G20180	<2	<2	-2.32
PKS4	AT5G04190	-2.87	<2	-4.37	*PIF3*	AT1G09530	<2	<2	-2.23
					HBP2	AT2G37970	<2	<2	2.23

Section 3: Genes involved in leaf developmental processes

Cytochromes P450 are hemeproteins and have monooxygenase function in multiple metabolic pathways, including hormone metabolism as well as formation of precursors of structural macromolecules such as suberin and lignin (Bak *et al*., 2011). In this data set, six genes showed up-regulation in stage 1 and no differentially expression in the other two stages indicating a role specific for early stage development of these genes. Stage 3 contained 12 genes down-regulated in the high-light compared to the low-light, with 6 genes specifically up-regulated in this stage (Table 6).

Table 6 Cytochrome P450 superfamily genes.
Cytochrome P450 superfamily genes. Displayed are fold changes of differentially expressed genes in high-light. S1: stage 1, S2: stage 2, S3: stage 3. Blue colours indicate up-regulated genes, yellow shades indicate down-regulated genes. Dark blue and yellow indicate higher or lower up and down-regulation, respectively <2 indicate fold change levels lower than 2.

Cytochrome P450									
Gene name	**ID**	**S1**	**S2**	**S3**	**Gene name**	**ID**	**S1**	**S2**	**S3**
Putative cytochrome P450	AT3G26165	-4.2	-2.17	<2	*CYP86A8*	AT2G45970	<2	<2	-3.28
CYP76C2	AT2G45570	-2.65	<2	9.4	*CYP97C1*	AT3G53130	<2	<2	-2.95
CYP71B22	AT3G26200	-2.44	5.84	3.06	*CYP734A1*	AT2G26710	<2	<2	-2.86
CYP708A3	AT1G78490	-2.05	<2	<2	*CYP86C2*	AT3G26125	<2	<2	-2.69
CYP71A13	AT2G30770	2.2	<2	3	*CYP71B24*	AT3G26230	<2	<2	-2.57
CYP79F1	AT1G16410	2.34	<2	<2	*CYP711A1*	AT2G26170	<2	<2	2.13
CYP83A1	AT4G13770	2.35	<2	<2	*CYP81D5*	AT4G37320	<2	3.13	2.34
CYP707A4	AT3G19270	2.56	<2	<2	*CYP71A12*	AT2G30750	<2	2.51	2.98
CYP79B3	AT2G22330	2.77	<2	<2	*CYP707A2*	AT2G29090	<2	5.97	3.86

Cytochrome P450 superfamily protein	AT1G66540	3.02	<2	<2	*CYP94C1*	AT2G27690	<2	-2.87	5.9
CYP79B2	AT4G39950	3.62	<2	<2	*CYP81G1*	AT5G67310	<2	<2	8.28
Cytochrome P450 superfamily protein	AT3G44970	6.76	8.58	12.63	*CYP71B15*	AT3G26830	<2	<2	8.98
CYP81D11	AT3G28740	<2	<2	-27.59	*CYP704B1*	AT1G69500	<2	<2	15.72
CYP78A8	AT1G01190	<2	<2	-10.99	*CYP722A1*	AT1G19630	<2	<2	18.47
CYP71A24	AT3G48290	<2	-3.4	-10.49	*CYP79A4P*	AT5G35920	<2	<2	21.23
CYP718	AT2G42850	<2	<2	-7.02	*CYP710A1*	AT2G34500	<2	<2	23.62
CYP90A1	AT5G05690	<2	<2	-6.36	*CYP705A19*	AT3G20100	<2	-2.11	<2
CYP96A12	AT4G39510	<2	<2	-3.95	*CYP710A2*	AT2G34490	<2	<2	<2
CYP71B29	AT1G13100	<2	<2	-3.72	*CYP71B23*	AT3G26210	<2	2.61	<2
CYP709B3	AT4G27710	<2	<2	-3.44	*CYP79F2*	AT1G16400	<2	3.04	<2
CYP76C1	AT2G45560	<2	<2	-3.38	*CYP81F2*	AT5G57220	<2	2.62	<2
KLUH/KW/CYP78AS	AT1G13710	<2	<2	<2					

Stomata are pores in the epidermis of plants and are surrounded by two epidermal guard cells that function as valves to regulate gas exchange in plants. Stomata development is regulated by a series of cell division and cell-state transition (Pillitteri & Dong, 2013). Their development and aperture are light-dependent, and alterations of stomata distribution has high impacts on internal leaf temperature and water-usage efficiency (Dietrichs *et al*., 2001; Hronková *et al*., 2015; Yoo *et al*., 2011). In S1, expression of genes involved in stomata development did not differ between high-light and low-light. In S2, *SPEECHLESS,* a basic helix-loop-helix - transcription factor that is involved in the first asymmetric division of protoderm cells in the epidermis, is up-regulated in the high-light grown compared to the low-light grown samples. Also, *MUTE*, which is required for termination of amplifying divisions shows significant fold-change increase in S2. Also, other genes involved in stomata development were up-regulated in the S2 (Table 7). This indicates that stomata development in stage 2 under high-light conditions might be enhanced.

Table 7 Genes associated with GO-term stomata.
Displayed are fold changes of differentially expressed genes in high-light. S1: stage 1, S2: stage 2, S3: stage 3. Blue shades indicate up-regulated genes, yellow shades indicate down-regulated genes. <2 indicate fold change levels lower than 2.

Genes associated with stomata				
Gene name	**ID**	**S1**	**S2**	**S3**
CYCA2;3	AT1G15570	<2	<2	-2.97
MUTE	AT3G06120	<2	2.69	<2
SPEECHLESS	AT5G53210	<2	3.09	<2
ERECTA	AT2G26330	<2	<2	-3.89
STOMAGEN	AT4G12970	<2	<2	-8.49
TOO MANY MOUTHS	AT1G80080	<2	3.01	<2
BASL	AT5G60880	<2	2.39	<2
MPKK4	At1g51660	<2	<2	3.37
ERECTA-LIKE 1	AT5G62230	<2	2.44	<2

This experiment was performed to identify high-light dependent regulators of leaf development. Therefore, the analysis of genes associated with the GO-term leaf development is a must. For this GO-term, only 4 genes that are differentially expressed were identified (Table 8). One gene is up-regulated in S1 and S2. Two genes are only up-regulated in S2, while 1 gene is down-regulation in stages 2 and 3 (Table 8).
Differential expression values for genes mentioned in various literature sources responsible for leaf development are shown in supplemental Table 4.

Table 8 Genes associated with leaf development GO term.
Displayed are fold changes of differentially expressed genes in high-light. S1: stage 1, S2: stage 2, S3: stage 3. Blue colours indicate up-regulated genes, yellow shades indicate down-regulated genes. <2 indicate fold change levels lower than 2.

Genes associated with leaf development GO term				
Gene name	ID	S1	S2	S3
NGAL3	AT5G06250	2.85	2.03	<2
WAK1	AT1G21250	<2	6.02	<2
PKS2	AT1G14280	<2	-2.33	-3.73
GRF4	AT3G52910	<2	2.04	<2

Cell wall and cell cycle genes are important for cell development. The GO-term contains genes with functions as xyloglucan endotransferases, xylosidases and fucosyltransferases that regulate cell wall expansion and composition (Goujon *et al*., 2003). Fold-change values showed down-regulation of cell wall related genes in the first stage analysed in this data set (Table 9). In the second stage, about half of the genes found in the data set was up-regulated, the other half was down-regulated. Most down-regulated genes showed stronger down-regulation in the third stage.
The high number of genes involved in cell wall synthesis and modification differentially regulated in stages 1 and 2 indicate a high activity of cell expansion rate. Also, the fact that 17 genes involved in cell wall organization were up-regulated in the S2, and only 4 genes were up-regulated in the S1, gives hint that the main part of high-light dependent leaf-expansion was present in the S2.

Table 9 genes differentially expressed with association to GO-term cell wall and cell cycle.
Displayed are fold changes of differentially expressed genes in high-light. S1: stage 1, S2: stage 2, S3: stage 3. Blue colours indicate up-regulated genes, yellow shades indicate down-regulated genes. Dark blue and yellow indicate higher or lower up and down-regulation, respectively. <2 indicate fold change levels lower than 2.

Genes associated with cell wall and cell cycle GO-term									
Gene name	**ID**	**S1**	**S2**	**S3**	**Gene name**	**ID**	**S1**	**S2**	**S3**
GGT1	AT4G39640	-2.54	-2.04	-7.81	*BGAL6*	AT5G63800	<2	-2.07	-3.27
XTR7	AT4G14130	-2.53	-3	-12.27	Mannose-binding lectin family	AT5G18470	<2	<2	3.27
PER33	AT3G49110	-2.25	<2	6.12	*MEKK3*	AT4G08470	<2	2.01	<2
XTH22	At5g57560	-2.07	<2	<2	*PER71*	AT5G64120	<2	2.07	<2
XTH31	At3g44990	2.03	<2	-5.46	*MED37D*	AT5G02490	<2	2.08	10.01
XTH6	AT5G65730	-2.07	<2	-5.14	*SEP1*	AT5G15800	<2	2.09	2.72

EXL2	AT5G64260	-2.07	<2	<2	*ECS1*	AT1G31580	<2	2.11	<2
BXL2	AT1G02640	-2.05	<2	-8.97	*PRP2*	AT2G21140	<2	2.15	-2.45
NRT1.1	AT1G12110	2.06	<2	4.67	*EXT3*	AT1G21310	<2	2.17	5
ARP2	AT1G61580	2.48	<2	<2	*SKS9*	AT4G38420	<2	2.18	<2
MBL1	AT1G78850	-3.22	<2	-10.49	*XTH24*	AT4G30270	<2	2.21	<2
EXP8	AT2G40610	-3.15	-3.7	-28.07	*BGAL11*	AT4G35010	<2	7.21	-2.01
LRX10	AT2G15880	-2.96	<2	-3.46	Unknown	AT3G03060	<2	2.28	<2
EP1-like glycoprotein 2	AT1G78830	<2	<2	-12.64	*HHT1*	AT5G41040	<2	2.32	<2
PER32	AT3G32980	<2	-4.19	-77.62	*CEL1*	AT1G70710	<2	2.46	<2
GRP5	AT3G20470	<2	-3.08	-4.29	*FUT4*	AT2G15390	<2	2.7	2.34
PME2	AT1G53830	<2	-2.73	-2.29	*GEF4*	AT2G45890	<2	2.71	<2
EXP11	AT1G20190	<2	-2.49	-29.74	*PME12*	AT2G26440	<2	3.01	<2
DGR2	AT5G25460	<2	-2.46	-43.44	*PME41*	AT4G02330	<2	3.99	<2
BXL1	AT5G49360	<2	-2.45	-32.8	*PNP-A*	AT2G18660	<2	4.45	11.81
EXPB1	AT2G20750	<2	-2.42	-40.77	Extensin-like family protein	AT2G43150	<2	5.09	2.32
XTH25	AT5G57550	<2	-2.39	-18.52	*WAK1*	AT1G21250	<2	6.02	<2
EXLA1	AT3G45970	<2	-2.38	<2	**Cell cycle**				
DUF1680	AT5G12950	<2	-2.38	-3.17	*CYCP4;1*	AT2G44740	-2.07	-3.01	-11.02
Unknown	AT3G05900	<2	-2.28	<2	*PATL1*	AT1G72150	<2	-2.57	-3.4
Carbohydrate-binding X8	AT1G09460	<2	-2.25	<2	*PATL3*	AT1G72160	<2	-2.13	-2.09
LRX2	AT1G62440	<2	-2.2	-9.98	*HDG12*	AT1G17920	<2	-2.01	-2.25
MRO11.21	AT5G23750	<2	-2.16	<2	*DMC1*	AT3G22880	<2	2.66	2.47

Section 4: Genes involved in hormone metabolism

Auxin plays a crucial role in the plant's growth and development. Therefore, the dataset was screened for genes associated with the GO-term auxin. In functional category enrichment analysis, auxin metabolism genes were significantly down-regulated in stages 2 and 3 (Figure 21). In stage 1, equal numbers of genes are up- and down-regulated, respectively. However, the genes down-regulated in stages 2 and 3 were not significantly differentially regulated in stage 1 (Table 10). Genes only differentially expressed in stage 3 are not shown, due to space limitations.

Genes exclusively differentially expressed in stage 1 were not detected except for auxin resistant 3 (AXR3). AXR3 acts as transcriptional regulator repressing auxin-inducible gene-expression. Mutant allele *icu6* of *AXR3* showed smaller leaves than wild-type, and more elongated palisade cells than wild-type (Pérez-Pérez *et al*., 2010), indicating that *AXR3* plays a role in palisade cell elongation. 3 genes showed up-regulation in stages 1 and 3, but not in stage 2. One of them is *PIN4*, an auxin efflux protein. Most genes differentially expressed were found in stages 2 and 3 and show down-regulation. These genes contain IAA-inducible genes as well as members of SAUR-gene family (Table 10).

Table 10 genes differentially expressed with association to GO-term auxin.
Displayed are fold changes of differentially expressed genes in high-light. S1: stage 1, S2: stage 2, S3: stage 3. Blue colours indicate up-regulated genes, yellow shades indicate down-regulated genes. Dark blue and yellow indicate higher or lower up and down-regulation, respectively <2 indicate fold change levels lower than 2.

Genes associated with auxin GO-term					Genes associated with auxin GO-term				
Gene name	**ID**	**S1**	**S2**	**S3**	**Gene name**	**ID**	**S1**	**S2**	**S3**
SAUR66	AT1G29500	-3.49	-3.49	-36.83	SAUR12	AT2G21220	<2	3.15	<2
GH3.5	AT4G27260	-2.86	<2	2.14	SAUR15	AT4G38850	<2	-2.22	-4.57
PIF4	AT2G43010	-2.56	<2	-2.78	SAUR19	AT5G18010	<2	-2.94	-12.15
EIR1	AT3G26760	-2.08	-2.72	-6.45	SAUR20	AT5G18020	<2	-2.63	-16.38
PIN2	AT5G57090	-2.08	<2	<2	SAUR21	AT5G18030	<2	-3.01	-13.68
XTH22	AT5G57560	-2.07	<2	<2	SAUR22	AT5G18050	<2	-3.62	-21.62
MYB3	AT1G22640	-2.04	-2.33	<2	SAUR23	AT5G18060	<2	-3.18	-27.78
PIN4	AT2G01420	-2.01	<2	-6.29	SAUR24	AT5G18080	<2	-2.95	-8.13
GH3.15	AT5G13370	2.12	<2	-4.79	SAUR27	AT3G03840	<2	-2.89	-18.4
AXR3	AT1G04250	2.15	<2	<2	SAUR28	AT3G03830	<2	-2.86	-12.13
FLS1	AT5G08640	2.19	10.14	8.18	SAUR29	AT3G03820	<2	-2.61	-17.78
PILS5	AT2G17500	2.41	2.34	3.48	SAUR3	AT4G34790	<2	-2.17	-11
JMT	AT1G19640	2.69	2.17	2.57	SAUR46	AT2G37030	<2	-2.75	-7.61
CYP75B1	AT5G07990	18.95	2.6	71.99	SAUR51	AT1G75580	<2	2.3	<2
AAE18	AT1G55320	<2	2.47	2.57	SAUR62	AT1G29430	<2	-2.84	-6.88
ARF11	AT2G46530	<2	-2.06	-3.02	SAUR63	AT1G29440	<2	-3.05	-8.19
AUX1	AT2G38120	<2	<2	-5.4	SAUR67	AT1G29510	<2	-2.84	-64.29
BT5	AT4G37610	<2	-3.14	-14.1	SAUR68	AT1G29490	<2	-2.3	-6.33
CYP94C1	AT2G27690	<2	-2.87	5.9	SAUR72	AT3G12830	<2	2.94	<2
ERF11	AT1G28370	<2	2.73	7.54	SAUR64	AT1G29450	<2	-3.47	-8.95
HAT2	AT5G47370	<2	-2.61	<2	SAUR57	AT3G53250	<2	-2.58	-48.06
IAA14	AT4G14550	<2	-2.99	-2.34	SAUR65	AT1G29460	<2	-3.42	-11.92
IAA19	AT3G15540	<2	-2.88	-2.48	YUCCA 3	AT1G04610	<2	-2.1	<2
IAA2	AT3G23030	<2	-2.77	-2.21	YUCCA 8	AT4G28720	<2	-2.39	-4.66
IAA29	AT4G32280	<2	-3.42	-12.03	YUCCA 9	AT1G04180	<2	-3.11	-3.72
IAA3	AT1G04240	<2	-2.29	-2.23	NPF7.3	AT1G32450	<2	2.1	<2
IAA34	AT1G15050	<2	-2.7	-2.86	RHM1	AT1G78570	<2	2.46	<2
DRM2	AT2G33830	-26.59	-12.78	-10.36	APG	AT3G16370	<2	-2.26	-10.4
DRMH3	AT1G56220	-2.82	-2.03	-2.94	IAA6	AT1G52830	<2	-2.86	-4.85
MYBD	AT1G70000	2.07	<2	8.62	MPK11	AT1G01560	<2	3.94	<2
MYB12	AT2G47460	2.08	<2	10.64	NOV	AT4G13750	<2	2.2	<2
PIN4	AT3G55120	2.08	<2	2.75	MDR15	AT1G27940	<2	2.66	<2
TT4	AT5G13930	2.56	5.66	239.94	NPY1	AT4G31820	<2	-3.37	-4.25
L31	AT5G27420	<2	2.34	2.74	ROPGAP3	AT2G46710	<2	-2.07	-6.99
MDAR3	AT3G09940	<2	2.05	14					

Cytokinin plays a key role in regulation of the cell proliferation by positively regulating cell division (Perilli *et al.*, 2010). Cytokinins regulate leaf developmental processes together with

auxin. Again, only genes differentially expressed in the first two stages and not exclusively in the third stage are shown. One gene was up-regulated in the first stage and 3 genes were up-regulated from stage 2 onwards. A higher number of cytokinin-associated genes were down-regulated throughout all three stages (Table 11).

Table 11 genes differentially expressed with association to GO-term cytokinin.
Displayed are fold changes of differentially expressed genes in high-light. S1: stage 1, S2: stage 2, S3: stage 3. Blue colours indicate up-regulated genes, yellow shades indicate down-regulated genes. <2 indicate fold change levels lower than 2.

Genes associated with cytokinin GO-term				
Gene name	**ID**	**S1**	**S2**	**S3**
ARR5	AT3G48100	<2	-2.89	-3.02
ARR6	AT5G62920	2.01	<2	-14.39
ARR9	AT3G57040	<2	<2	-4.73
ARR11	AT1G67710	<2	-2.68	<2
ARR14	AT2G01760	<2	<2	-2.82
IPT3	AT3G63110	<2	<2	-5.11
IPT5	AT5G19040	<2	<2	-2.41
IPT7	AT3G23630	<2	<2	16.06
CKX5	AT1G75450	<2	<2	2.48
CKX7	AT5G21482	<2	<2	2.07
ARR11	AT1G67710	<2	-2.68	<2
UGT76C2	AT5G05860	<2	-2.37	-7.02
SOB5	AT5G08150	-2.27	-3.63	-5.25
F-box/kelch-repeat protein	AT1G80440	-2.79	-7.17	-15.27

Gibberellic acid regulates cell proliferation and cell expansion in *Arabidopsis* (Cowling & Harberd, 1999). Functional classification analysis showed, that genes involved in gibberellic acid metabolism were up-regulated in the stage 2 (Figure 21). In stage 2, up-regulation of genes involved in gibberellic acid synthesis (GA20OX3, GA3OX1 and GA3OX3) and gibberellic acid response was found (Table 12). In the third stage, the fold change decreases for some of the genes and was highly down-regulated for two of them.

Table 12 genes differentially expressed with association to GO-term gibberellic acid.
Displayed are fold changes of differentially expressed genes in high-light. S1: stage 1, S2: stage 2, S3: stage 3. Blue colours indicate up-regulated genes, yellow shades indicate down-regulated genes. Dark blue and yellow indicate higher or lower up and down-regulation, respectively <2 indicate fold change levels lower than 2.

Genes associated with gibberellic acid				
Gene name	**ID**	**S1**	**S2**	**S3**
GASA6	AT1G74670	-3.39	-5.2	-42.83
GASA9	AT1G22690	2.35	2.19	-2.03
GA3OX1	AT1G15550	2.66	2.35	<2
RGL3	AT5G17490	<2	-2.97	-3.3

FMO GS-OX-like 6	AT1G12130	<2	-2.19	-3.45
GASA7	AT2G14900	<2	-2.03	-2.31
GASA13	AT3G10185	<2	4.17	2.31
MYB13	AT1G06180	<2	2.21	8.65
ATMYB31	AT1G74650	<2	2.33	19.63
WRKY27	AT5G52830	<2	2.49	<2
TRM13	AT2G45900	<2	2.8	<2
GA20OX3	AT5G07200	<2	2.87	-21.25
GIS	AT3G58070	2.91	3.02	2.5
GA3OX2	AT1G80340	<2	3.75	-4.51
SOC1	AT2G45660	-2.02	<2	-2.41

This analysis comparing transcriptome data of low-light- and high-light-grown leaves of *Arabidopsis* plants gave a first insight into the transcriptional changes in long-term high-light-grown plants. High-light treatment changed many aspects of the plant's transcriptome including hormone metabolism, stress-responses and developmental processes. To assess, which regulators are responsible for the high-light induced growth adaptations, further analyses need to be conducted.

3 Discussion

3.1 C_4 anatomy differentiation and regulation

3.1.1 Light-dependent C_4 cotyledon differentiation in *Flaveria* species

The understanding of the developmental formation of C_4 photosynthesis is of high agricultural interest, since the implementation of C_4 photosynthesis in a C_3 crop such as rice could increase yield sufficiently to meet the rising needs of the world's human population (von Caemmerer *et al*., 2012; Hibberd *et al*., 2008; Sheehy *et al*., 2000). C_4 photosynthesis is the evolutionary answer to high temperatures, high photon fluence rates and dry habitats (Edwards *et al*., 2010). With most of the C_4 photosynthesis genes identified and their function understood, the development however of the C_4 photosynthesis-specific Kranz anatomy is not yet fully understood. Kranz anatomy is defined by close vein spacing and large BSCs surrounding the veins. BSC and MCs are in close contact and show a decreased ratio of MC to BSC compartments (Dengler & Taylor, 2000; McKown & Dengler, 2007). Both MC and BSC show cell-type-specific expression of C_4 genes to obtain a spatial separation of a primary CO_2 fixation forming a C_4 compound in the MCs and a decarboxylation of the C_4 compound for re-fixation in the Calvin-Benson cycle in the BSC with the advantage of reduced photorespiration (reviewed in Sage *et al*., 2012).

Analysing cotyledons can be of advantage when it comes to light-dependent studies, since adult leaves of most plant species are not able to grow in the darkness (Shu *et al*., 1999). However, developmental processes might be different in cotyledons than in adult leaves. In cotyledons, cell proliferation occurs during embryogenesis, meaning the growth of the cotyledon post-germination is only dependent on cell expansion (Tsukaya *et al*., 1994). In this study, the light-dependent BSC area increase was confirmed for all analysed *Flaveria* species, as it was shown for *F. trinervia* (C_4; Shu *et al*., 1999). The original goal of this experiment was to perform transcriptome analyses on developing cotyledons in C_3, C_3-C_4 and C_4 *Flaveria* species grown in darkness or in light with the precondition, that the BSCs in the C_3 species do not show light-dependent or less light-dependent cell area increase. Since the results obtained in this thesis indicate a light-dependent BSC area increase in all assessed species, the RNA-Sequencing approach was not followed further.

In cotyledons of *Flaveria* species, the ratio of the compartments of mesophyll : bundle sheath is similar in all species, although absolute BSC area differs between species (Figures 6 and 7). In adult leaves, the reported ratio of the compartments of M : BS is low in C_4 species and also in *F. ramosissima* (C_3-C_4) but is high in *F. robusta* (C_3) and in *F. pringlei* (C_3), indicating that the MC-compartment is larger than the BSC compartment (McKown & Dengler, 2007). Unlike their first identification as true C_3 *Flaveria* species (Sage *et al*., 2013), analyses have shown recently, that *F. pringlei* and *F. robusta* might display so called "proto-Kranz" features, including large BSCs and increased organelle number in adult leaves (McKown & Dengler, 2007; Sage *et al*., 2013). Both *F. pringlei* (C_3) and *F. robusta* (C_3) contain two copies of the gene encoding the GLDP subunit, *GLDPA* and *GLDPB*, with BSC-specific expression and ubiquitous expression in

all leaf cells, respectively (Schulze *et al*., 2013; Wiludda *et al*., 2012). Despite this pre-conditioning, both species were characterized as C_3 by CO_2-compensation rates (Alonso-Cantabrana & von Caemmerer 2016; Ku *et al*., 1991).
C_4 plants have higher vein density than C_3 plants (Christin *et al*., 2013; Kajala *et al*., 2011). It would be interesting to analyse the cotyledons vein density to gain an idea of whether in cotyledons, "proto-Kranz" also involves higher vein density. Since the overall cells appear to be larger in the C_3 species, it is possible that the compartment ratio is similar, however the vein density is lower in the C_3 plants than in the C_4. To further investigate, whether the "proto-Kranz" anatomy is present in the analysed C_3 species it would be necessary to investigate the number and positioning of BSC organelles in the cotyledons, since these traits are important features for "proto-Kranz" (Sage *et al*., 2013).
Up to date, photosynthesis in *Flaveria* cotyledons has not been analysed. It would be interesting to assess photosynthesis rates in the cotyledons to investigate, whether C_3, C_3-C_4 intermediate and C_4 species show differences in their photosynthesis rate. According to the anatomical study performed here, with the M to BSC ratio similar in all species, I suggest that the photosynthesis rates of *Flaveria* cotyledons will be similar across all species.

3.1.2 Expression of C_4-related genes is not light-dependent in *F. bidentis* (C_4) and *Arabidopsis* (C_3)

Light is an important regulator of gene-expression and of anatomical changes. I showed that in *Flaveria*, light plays an important role in the cell expansion of the BSCs. However, light does not play a role in the cell-type-specific expression of the *F. trinervia* (C_4)-derived GLDPA and PPCA promoters in *F. bidentis* (C_4) and *A. thaliana*. Expression of an *FtGLDPA::GUS* reporter construct was BSC-specific in adult leaves of *F. bidentis* (C_4) and in *A. thaliana* (Engelmann *et al*., 2008). While the expression of *FtPPCA::FYP* loses MC-specificity when introduced into *A. thaliana*, it shows MC-specificity *in F. bidentis* (C_4). In growing cotyledons of *F. bidentis*, the *FtGLDPA::YFP* and *FtPPCA::YFP* showed cell-specific expression in BSC and MC, respectively in both light and darkness. In *A. thaliana*, the *FtGLDPA::YFP* also showed BSC-specific expression independent of the light-condition. This indicates, that the promoter region of the *F. trinervia*-derived *GLDPA* gene contains regulatory elements that enable cell-specific expression even in C_3 plant *Arabidopsis*.
FtPPCA-promoter loses cell-type specificity when introduced into *Arabidopsis*. Also, other C_4 genes have promoter sequences that lose cell-type specificity when introduced into C_3 plants, as does the NADP-dependent malic enzyme- and the PEP-CK- promoter from maize when introduced into rice. (Engelmann *et al*., 2008; Nomura *et al*., 2000). This indicates, that the promoter sequences contain signals specific for C_4 plants to cause cell-type-specificity, but not for C_3 plants. Akyildiz and co-workers (2007) identified a cis-regulatory module MEM1 for mesophyll-specific expression of PPCA. Further analyses will shed light on similar modules in other C_4 plants to broaden the understanding of cell-specificity of C_4-gene expression.
In *F. trinervia*, the cell-specific accumulation of mRNA was shown as a light-dependent process in growing cotyledons for RuBisCO and PEPC (Shu *et al*., 1999), however with low

accumulation of mRNA detectable also in the dark. My results are solely qualitative, and no quantification of the GFP-signals were performed. It might therefore be possible, that dark-grown seedlings show less-GFP signal than light-grown. In follow-up experiments it would be interesting to quantify the GFP-signals and compare the signal intensities between dark- and light-grown cotyledons.

Due to their numerous independent evolutionary origins, C_4 plants show a lot of different solutions of gene-expression and anatomical adaptations on the way to C_4 photosynthesis. Light-dependent C_4-gene expression was found for FbNADP-ME, PCK in *Urochloa panicoides* and for the small subunit of RuBisCO in maize (Finnegan *et al*., 1999; Marshall *et al*., 1996, Nomura *et al*., 2000). However, other C_4 genes are known not to be regulated by light: *Amaranthus hypochondriacs* cotyledons do not show light-dependent formation of Kranz anatomy and cell-type specific expression of C_4 enzymes such as PEPC, RuBisCO and PPDK (Wang *et al*., 1993). NAD-ME, however, did show light-dependent expression in *Amaranthus* cotyledons, being expressed in both light- and dark-growing germinating cotyledons in the first 7d after germination, then down-regulated in the dark-grown cotyledons with light being able to trigger up-regulation in light-shifted seedlings (Long & Berry, 1996). Gene-expression of C_4 genes can be up-regulated not only by light, but also by high nitrogen availability as nitrogen-induced expression was reported for PDK and PEPC of maize, sorghum and *Amaranthus* (Suzuki *et al*., 1994; reviewed in Sheen, 1999). Therefore, it would be interesting to test whether the expression of FtGLDPA::- and FtPPCA::reporter constructs might be regulated by other abiotic stimuli e.g. nitrogen or ABA-treatment.

3.2 Analysis of leaf traits in *Arabidopsis*

3.2.1 Variation of leaf traits in 33 accessions and in AMPRIL parental accessions

Leaf thickness is a trait that has been found to positively correlate with several important parameters for efficient plant growth such as leaf water content and photosynthesis rates in some species (Afzal *et al*., 2017; McMillen & McClendon, 1983). Also, leaf thickness is smaller in between veins in C_4 leaves than in C_3 leaves (Dengler *et al.,* 1994; Lundgren *et al*., 2014). Leaf vein density is an important trait of C_4 photosynthesis, enabling the Kranz anatomy and thus the C_4 photosynthesis to work efficiently. In this study, the variation of the two traits, leaf thickness and leaf vein density among *Arabidopsis* accessions was determined.

Both AMPRIL parental accessions as well as the 33 analysed accessions showed variation in similar ranges (Figures 11A and 12A and B). This could be, because AMPRIL parental accessions have different world-wide origins (Huang *et al*., 2011), in a similar way as the 33 analysed accessions.

Although there was no clear correlation between origin of the accessions and their phenotypes regarding estimated leaf thickness and leaf vein density, local climate parameters at their habitats of origin might play a role in their phenotypes. For example, cool temperature and high-light was found to influence both leaf thickness and vein architecture in *Arabidopsis* (Cohu *et al*., 2013). Also, precipitation, and the general floral neighbour community can

influence plant development and lead to adaptations of inbred lines at the site. Therefore, investigation of the detailed climatic conditions in the habitats of the accessions' origins would be interesting.

3.2.2 QTL analysis of petiole length under greenhouse and high-light conditions

Both under greenhouse conditions and under high-light conditions, QTL analysis of petiole length of *Arabidopsis* plants identified a prominent peak on chromosome 2. A peak on chromosome 2 at approximately 11.2 MBp was found in several studies associated with petiole length as well and was identified as the *ERECTA* locus (Pérez-Pérez *et al*., 2002; Huang *et al*., 2011). The strain L*er* carries a mutation in the *ERECTA* gene and derives from the accession La-1 (Zapata *et al*., 2016). Since the parental accessions of the used AMPRIL contain L*er*, it is likely that the *ERECTA* allele is responsible for the phenotype. Also, the peak position matches with the reported *ERECTA* position (TAIR). Since one of six AMPRIL subpopulations was used for the experiments, it is possible that the accuracy and the power of the QTL analysis is reduced (Beavis, 1998). Since petiole length is a complex trait that has been analysed before, it was used as a control for QTL accuracy. As it was possible to detect the putative *ERECTA* locus using one of six populations, the accuracy of the QTL was regarded as sufficient. Petiole length showed the highest heritability under both growth conditions compared to the other two traits analysed. However, there are more loci regulating petiole length, which were not identified in this study (Tsukaya *et al*., 2002). Interestingly, also the usage of more populations of the AMPRIL failed to identify other loci than ERECTA (Huang *et al*., 2011). This might be because of the strong effect of *ERECTA* on petiole length. Since Ler is one of the eight parental accessions, it would be interesting to analyse petiole length using populations without L*er* as parental accessions. This could help to identify other genes affecting petiole length.

3.2.3 QTL analysis of estimated leaf thickness under greenhouse and high-light conditions

QTL analysis on estimated leaf thickness under greenhouse conditions led to the identification of three peaks, two on chromosome 3 and one on chromosome 4. Overall, estimated leaf thickness showed low values for heritability. A recent study on RILs deriving from crosses of L*er* and Cvi also led to the identification of a QTL peak on chromosome 3 for leaf thickness (Coneva & Chitwood, 2018). Leaf thickness is associated with the levels of endoreduplication and is also dependent on the elongation of palisade parenchyma cells (Coneva & Chitwood, 2018). This indicates, that leaf thickness is regulated by multiple genes.
QTL analysis of estimated leaf thickness under high-light conditions resulted in two peaks on chromosome 2 and one peak on chromosome 3. However, broad sense heritabilities were low, indicating not a genetic basis for leaf thickness. Since QTLs detected under greenhouse conditions differ from those detected under high-light conditions, it is assumed that leaf thickness is a highly environment-dependent multi-gene regulated trait.

3.2.4 QTL analysis of leaf vein density under greenhouse conditions

Experiments were performed using AMPRIL in the greenhouse to be able to compare results with previous studies. A recent analysis of QTLs in world-wide accession GWAS as well as in multiparent RIL MAGIC revealed several putative major QTLs and one candidate for leaf vein density, the salt- and cold-inducible gene *RC12c* (Rishmawi *et al*., 2017). T-DNA mutants *rci12c* showed reduced vein density (Rishmawi *et al*., 2017). Other recent genetic screens identified *COTYLEDON VASCULAR PATTERN* 1 and 2 (*CVP1*, *CVP2*) and *FORKED* (*FKD1*) as further players in leaf vein development (Carland *et al*., 1999; Steynen & Schultz, 2003). Since Rishmawi and co-workers (2017) used both GWAS and a multiparent approach and found 33 potential QTLs that did not overlap in both systems for leaf vein density. Leaf vein density appears to be a trait regulated by multiple genes. In the present study, QTL analysis gave rise to one distinct peak for leaf vein density in AMPRIL grown in the green house. The absence of further QTLs could be due to the low number of RILs used in this study, since 90 RILs do not display the full potential of the AMPRIL, which contains approx. 550 RILs (Huang *et al*., 2011). To increase potential QTL number, experiments should be repeated including more RILs. This was not done in this study, since the analysis of leaf vein density is very time-consuming. As eight biological replicates were used, one option to reduce time for analysis is to use fewer biological replicates. Rishmawi and co-workers (2017) used four biological replicates and a higher number of RILs and were able to detect more QTLs.

Rishmawi and co-workers (2017) showed that, using different approaches analysing natural variation such as GWAS and QTL mapping can lead to the identification of different SNPs. Using GWAS, a higher number of alleles can be analysed in comparison to QTL, where only the allelic diversity introduced by the parental lines can be assessed (Korte & Farlow, 2013). Therefore, by increasing the size of the analysed accessions to approximately. 60–100 and performing GWAS analysis it could be possible to identify other SNPs. Compared to QTL analysis, GWAS has the advantage of the simple use of genetic variation without needing to produce mapping populations (Bergelson & Roux, 2010; Korte & Farlow, 2013). For further analysis more accessions could be included, and also more parameters of vein phenotypes could be measured, such as number of ending point density and areole number density, which are parameters that can give information about the increase of vein density dependent on secondary or tertiary veins (Rishmawi *et al*., 2017). Including GWAS could lead to the identification of more potential candidate SNPs or could help fine-mapping because of overlapping regions between QTL- and GWAS-derived SNP regions.

Vein density was higher in high-light-grown plants compared to the greenhouse-grown plants. Both high-light chamber and greenhouse display two differing conditions including ventilation, light-spectrum and watering regime, therefore it is not recommended to directly compare leaf vein densities. However, a trend was visible for the high-light grown leaves to have larger leaf vein density values than from plants grown in the greenhouse. That increase of photon fluence rate can alter leaf vein density was shown for shade-and light-grown leaves before (Adams *et al*., 2006; 2007). To verify the influence on high-light on leaf vein density,

experiments should be repeated using low- and high-light in the same growth chamber to reduce other environmental factors influencing the outcome.

3.2.5 *AXR6* is candidate for leaf vein density QTL

Fine-mapping of the QTL peak for leaf vein density on chromosome 4 could be possible with line GF33. However, the differences between the genotypes cannot be seen by eye and fine-mapping would therefore have been very time-consuming. The segregating HIF GF07 and FG18 did not show significant differences in leaf vein density. Since high-light did show to influence leaf vein density, it would be interesting to assess phenotypes again under high-light. Also, the parental accessions of AMPRIL showed a wider range of vein density when grown under high-light. It could be possible, that high-light will increase the difference between homozygous HIFs for each parental allele to allow phenotyping for fine-mapping under these conditions.

A different approach was chosen by comparing the coding sequences of the parental accessions and screening for mutations. From this data set, genes were chosen according to their function in hormone signalling or metabolism. With this method, a candidate gene list of approx. 30 genes was established (Supplemental Table 1). Due to time limitations, a preliminary T-DNA mutant analysis of four candidate genes was performed, however did not show statistically significant differences in leaf vein density between T-DNA mutants and Col-0. However, heterozygous plants of the diepoxybutane-mutagenization-derived *axr6-2* line, carrying a mutation in the *axr6-2* locus, showed statistically significant lower leaf vein density than Col-0, indicating that this gene might play a role in vein density in *Arabidopsis* (Figure 17B).

AXR6 encodes CULLIN1 (CUL1), which is a member of the TIR1-containing SKP, Cullin, F-box complex (SCF^{TIR1}). SCF^{TIR1} is an E3-ubiquitin ligase complex involved in the ubiquitination of proteins involved in the auxin response, labelling them for degradation at the proteasome (Gray *et al*., 1999). Under low auxin concentrations, Aux/IAA proteins inhibit the transcription of auxin-responsive genes. In the presence of auxin, Aux/IAA proteins interact with TIR1 and are ubiquitinated by the SCF^{TIR} E3 ubiquitin ligase and subsequently degraded in the 26S proteasome: thus, auxin-responsive gene-expression is enabled. SCF^{TIR1} contains AtCUL1, SKP-1 related proteins ASK1 and ASK2, and F-box-protein TIR1 (del Pozo *et al*., 2002). CUL1 is a scaffolding protein and *cul1* mutants axr6-1 and axr6-2 show reduced auxin response (Hellmann *et al*., 2003; Hobbie *et al*., 2000). Alleles of *axr6* show different phenotypes. Homozygous mutant alleles *axr6-1*, *axr6-2* and *axr6-3* are seedling lethal, Heterozygous *axr6-1* and *axr6-2* show reduced leaf and cotyledon vein density (Hobbie *et al*., 2000).

The analysis of the T-DNA mutant only comprised genotyping. It was not tested, whether the expression of the genes was indeed affected. Wang investigated 2008 the effectiveness of T-DNA mutagenesis and found that in 10% of analysed T-DNA insertion lines, gene expression was still detectable (Wang, 2008). To verify an effect of the T-DNA on the respective gene, gene-expression analysis for these lines is necessary.

Although *AXR6/CUL1* might be a candidate gene for the identified QTL on leaf vein density, the mutation identified by sequence comparisons was different to the *axr6-2* mutation (Supplemental Figure 1). While the *axr6-2* allele leads to an F->I substitution at amino acid 111, Kyo and L*er* both contain a methionine at position 415 instead of a threonine which is present in Col-0, Sha and An (Supplemental Figure 1). The human CUL1 consists of a 415 aa-long n-terminal helical region that binds the Skp1-F-box^{SKP2}complex. The c-terminus consists of a 360 aa-long c-terminal globular α/β-domain that binds RBX1. The axr6-1 and axr6-2 substitutions are within the SKP1-F-box module-interaction region of CUL1, based on human SCF^{SKP2} crystal structure (Zheng *et al*., 2002). The T -> M substitution in Kyo and Ler are in another domain than the *axr6-1* and *axr6-2* mutant alleles.

Interestingly, Kyo and Ler have the same genotype at amino acid position 415 but differ in their leaf vein density (Figures 12A, 13A). The analysis of coding sequences does not take into account potential mutations in non-coding regulatory regions or possible post-transcriptional regulations that might act in the parental accessions analysed in the QTL experiments. The mutation found in the coding sequence of *CULLIN1* is likely not to be responsible for the observed phenotype on the plant level because of the different phenotypes observed in the accessions Kyo and L*er*. Therefore, promoter sequences should be also analysed. By introducing the promoter and gene sequences from Kyo to L*er* and vice versa, the influence of the alleles can be assessed by phenotypic analysis.

To assess whether *AXR6* is a true candidate gene for the QTL, it would be interesting to test the abundance of the protein in the parental accessions and also compare the promoter sequences. Since CUL1 is member of the SCF^{TIR}-complex that is involved in the auxin-response, it would be interesting to test the expression levels of auxin-responsive genes in the Kyo, Ler and Col, with *axr6-2* as control.

In sum, the QTL-analysis of leaf vein density using AMPRIL gave rise to a candidate region on chromosome 4. By using sequence data of parental accessions from which the AMPRIL derived and preliminary analysis of mutants, it was possible to identify a putative candidate gene for the QTL. Further analyses to identify whether *AXR6* is the true candidate for this QTL or whether there might be another candidate, need to be conducted. For this, more T-DNA mutants should be analysed from the candidate gene list and for line *ins*, more plants need to be assessed (Figure 17A). Also, the absence of gene-expression in the T-DNA lines should be confirmed.

3.3 Transcriptome analysis of *Arabidopsis* leaves grown under different light conditions

The aim of this part was to identify candidate transcripts responsible for the anatomical adaptations including palisade cell elongation and increase of overall leaf thickness in *Arabidopsis* plants. For this, *Arabidopsis* plants were grown under low- and high-light conditions and three developmental stages were analysed comprising 1 mm long, 6-7 mm long and 10–12 mm long leaves, which represent an early, intermediate and adult leaf growth stage. The connection of leaf thickness with palisade cell elongation was shown before, indicating that under high-light, the main part of an increase of leaf thickness is due to the

elongation of the palisade parenchyma cells (Gotoh *et al*., 2018; Kozuka *et al*., 2011; Weston *et al*., 2000). The slenderness of a cell is synonymous to increased elongation of cells, which renders them more cylindrical. Palisade cell slenderness is regulated by PHOT1 and PHOT2 and also mutants of *an* display thicker leaves and elongated and slender palisade parenchyma cells, indicating a function of *AN* in cell development. Under the chosen conditions for this experiment, *Arabidopsis* plants did not produce a second layer of palisade cells in all assessed growth stages (Figure 18). The changes of leaf thickness are thereby accounted for by the increase in cell slenderness and size.

In the transcriptomic data set, transcript of *PHOT1* were only differentially regulated in the adult stage S3 and *PHOT2* did not show differentially expression in the high-light compared to the low-light (Table 5). *AN*, a protein involved in lateral cell expansion, leaf lamina formation and also in leaf thickness control was not differentially expressed in the data set of this transcriptomics approach (Gotoh *et al*., 2018; Horiguchi *et al*., 2005; Supplemental Table 4). Also, other genes reported to be involved in leaf development were not differentially regulated in the high-light compared to the low-light over the developmental gradient (Supplemental Table 4). High-light treatment seems to trigger different pathways for leaf development than the reported ones.

For the first analysed stage, 1 mm long leaves were used. The goal of this experiment was, to use for this stage leaves undergoing the process of primary morphogenesis. Since this stage is an early developmental stage which is difficult to track down (Andriankaja *et al*., 2012), it might be possible that the stage analysed was already in the process of secondary morphogenesis. One hint that this might be the case are the already elongated palisade cells in the first stage (Figure 18). For a follow-up experiment, even smaller leaves could be used in transcriptomic analysis. However, transcriptomes of S1 and S2 showed a diverse pattern of expressed genes indicating that both developmental stages do differ strongly in their gene-expression and represent therefore different developmental stages (Figure 19).

In general, for the transcriptomics data set it should be noted, that S1 had the least number of differentially expressed genes of all three stages. The differentially expressed data-set represents genes that are up- or down-regulated in the high-light-treated samples which holds true for all three stages. However, from stage 2 up to stage 3, the number of differentially expressed genes increases with the highest number of genes differentially expressed in the adult S3. This could indicate, that under these conditions gene expression does not differ that much during the growth of the leaves but gets more variable and adapted towards the light conditions in the adult stage of the leaf.

<u>Genes involved in stress-responses</u>

Genes that show the highest up-regulation in the first stage and showed a constantly high up-regulation over all three stages were members of the chlorophyll a/b binding protein family ELIP1 and ELIP2 (Table 1). They have photoprotective properties by binding free chlorophyll. Chlorophyll is released under high-light stress due to the degradation of damaged photosystems and is a generator of singlet oxygen in the light (Adamska, 2006; Hutin *et al*., 2003). The constant presence of transcripts in the high-light treated plants versus the low-

light treated plants indicates an important role of *ELIPs* also in relatively moderate high-light conditions. *ELIPs* are also up-regulated by other abiotic stresses such as desiccation and high temperatures (Adamska, 2006). In the high-light growth chamber, the temperature increased during the day due to the heating of the light bulbs, therefore increased temperature also plays a role in the expression of genes in this data set and might explain the high expression of *ELIPs* due to a combined effect of temperature and high-light.

Heat shock proteins (HSPs) are up-regulated in response to heat but are also responsive to several other stresses as for example osmotic stress, cold and wounding (Swindell *et al*., 2007). HSPs function as molecular chaperones regulating the folding and accumulation of proteins, as well as regulators of degradation of damaged or misfolded proteins (Al-Whaibi, 2010).

In this data-set, heat shock proteins showed higher expression in the high-light treated adult samples compared to the low-light samples (Table 2). In the first stage the leaf was maybe too small to be totally exposed to the high-light and surrounding temperature due to the close distance to the SAM and other developing leaves that could have a shading function. In the adult high-light stressed leaf, the need of HSPs is more apparent, since the adult leaf is a fully functional photosynthetic unit. High-light triggers expression of HSP in *Arabidopsis* plants shifted to high-light (Rossel *et al*., 2002). Our results indicate that HSP play an important role for adult leaves in the high-light, however not so much in developing leaves. These results should be confirmed by quantitative PCR.

Abiotic stresses such as high-light also lead to the formation of ROS (reviewed in Pospíšil, 2016). Besides their harmful properties due to their free radical nature that can lead to apoptosis, they are also known as signalling compounds under moderate stress (You & Chan, 2015). ROS also show involvement in cell elongation during organ growth (Carol & Dolan, 2006). Enzymes associated with the GO-term ROS were mainly differentially expressed in the S3, similarly to the heat shock proteins (Tables 2 and 3). *GST1* encodes glutathione transferase, which is induced by ROS and is involved in detoxifying processes (Edwards *et al*., 2000). In this dataset, *GST1* is up-regulated in all three developmental stages. Interestingly, most genes involved in detoxification of ROS are not differentially expressed in early developmental stages S1 and S2, although the plants were continuously treated with an 16h high-light 8 h darkness regime. It is possible, that the high-light stress and the resulting need of photoprotection in the plant was taken care of by ELIPs in the first stage (Juvaney *et al*., 2013). ROS are also accumulated at the onset of leaf senescence (Jajic *et al*., 2015), and it might be possible, that due to the high-light stress, high-light treated leaves start senescing earlier than low-light treated leaves. To test this hypothesis, it would be necessary to analyse the gene-expression of senescence-associated genes by RT-qPCR. *WRKY53*, a transcription factor involved in the regulation of senescence and expressed early during senescence is up-regulated in the S2 in this data set and shows slight lower up-regulation in the S3 (Fold changes S2: 2.7 and S3: 2.33; Lim *et al*., 2003).

Gene-expression of genes associated with GO-terms HSPs and ROS was enhanced in the adult stage S3, which was also the case for genes associated with flavonoid synthesis. Flavonoids comprise a class of secondary metabolites involved in the pigmentations of plants. Flavonoids also play a role in the modulation of auxin transport and thereby regulating leaf development

(Peer & Murphy, 2007). The anatomical properties of flavonoids mutants grown under high-light conditions will give insights into the role of flavonoids on leaf development.

Anthocyanins are end products of the flavonoid biosynthesis pathway (Saito *et al*., 2013). Genes involved in anthocyanin biosynthesis showed very high differential regulation in all three developmental stages (Table 4). *TT7* and *UGT79B1* showed the third- and fourth-highest differential expression of all genes in S1. Anthocyanin accumulation protects the cells and specifically the photosynthetic apparatus from reactive components that can lead to photoinhibition (Das *et al*., 2011, Hughes *et al*., 2007). The up-regulation of anthocyanin biosynthesis and modification genes in early stages indicates an early role for anthocyanins protection of the leaves under high-light conditions. In the S2, both *TT7* and *UGT79B1* do not show very high expression with only 2 and 3-fold higher expression than under low-light conditions, which changes in the S3, where *UGT79B1* shows third-highest expression of all genes differentially expressed in S3 (Table 4). Transcription factors *MYB12*, *PAP1* and *PAP2* are involved in early flavonoid biosynthesis modulation and anthocyanin biosynthesis control (Broun *et al.,*2005; Mehrtens *et al.,* 2005). In this data set, *MYB12* and *PAP1* were differentially up-regulated in both S1 and S3, but not in S2. Both *PAP1* and *PAP2* are strongly up-regulated in response to strong light (Cominelli *et al.,* 2008), which was seen for *PAP1* in this data set, but not for *PAP2* (Table 4). Interestingly, MYB112 a high-light induced TF for regulation of anthocyanin biosynthesis (Lotkowska *et al.,* 2015) was not differentially expressed in this data set. To verify this result, gene-expression should be verified for the mentioned genes. To investigate, whether in the second stage anthocyanin-levels are lower than in S1 and S3, it would be necessary to quantify and qualify levels of anthocyanins in all three stages.

<u>Genes involved in signal transduction</u>

Photoreceptors and genes involved in light signal transduction are important for the plant to sense the environmental light conditions and adapt its development accordingly (reviewed in Mawphlang & Kharshiing, 2017). In this data set, the expression of genes involved in signal transduction did not show drastic changes. *BBX32* and *HYH* showed up-regulation and *PIF4*, *PKS1* and *PKS4* were down-regulated in the S1. While the expression of *BBX32* and *HYH* was higher in the high-light-grown samples for all three developmental stages analysed, in the second stage genes involved in light signalling were down-regulated. The highest regulation was found in the adult stage S3. The low abundance of differentially expressed genes in the light signal transduction involved genes is interesting, given the importance of light signalling to the plants. *HYH* encodes HY5 homolog. *HY5* is only differentially expressed in the S3, while *HYH* shows up-regulation in all three stages (Table 5). Genes like *ELIP1* and *ELIP2*, that are induced by *UVR8* through *HY5* are in this data-set strongly up-regulated in all three stages, while *UVR8* and *HY5* are not or only differentially expressed in the S3, respectively (Brown & Jenkins, 2008; Hayami *et al*., 2015). This suggests other regulatory mechanisms under high-light for the induction of the high-light responsive genes, maybe through HYH.

Genes involved in leaf development

The search for genes in S1 and S2 involved in the GO-term leaf development resulted four genes differentially expressed (Table 7). Searching for GO-term associated genes can have the draw-back, that the search relies on the correct annotation of the genes to the correct function. Also, multiple functions can be annotated to one gene. Genes known to be involved in leaf development might not be annotated to the GO-term leaf development (e.g. auxin-responsive genes). Therefore, there are more genes involved in leaf development that are found in this table, however they were not found as they are not labelled with the GO-term leaf development.

One gene associated with the GO-term leaf development showed up-regulation in the S1 and S2, but no differentially regulation in the S3. *NGAL3* is involved in the leaf shape formation, as well as seed size (Engelhorn *et al*., 2012; Zhang *et al*., 2015). NGAL3 is a putative transcriptional repressor of *CUC2*, which is involved in leaf serration (Engelhorn *et al*., 2012; Nikovics *et al*., 2006). In this data-set, the expression of *CUC2* was found to be not differentially expressed in all three stages (Supplemental Table 4). Other leaf shape-regulating genes such as *PIN1* and *miR165* (Engelhorn *et al*., 2012) showed up- and down regulation only in the third stage, respectively (Supplemental Table 4). The close relative to *NGAL3*, *SOD7*, which is involved in the seed size by restricting cell proliferation in the developing seeds showed up-regulation in the S3, but no differential expression in S1 and S2 (Supplemental Table 4). Maybe *NGAL3* has a high-light inducible function in leaf development that has not yet been reported, as in this data set, it is up-regulated before the flowering of the plants. Also, *ngal3 sod7* double mutant plants have larger leaves, which indicates a function in leaf development for both genes (Zhang *et al*., 2015).

From the cell wall-associated genes up-regulated in the S1, several have functions that could be associated with the phenotype of high-light-grown leaves: XTH31 could play a role in cell wall loosening by working as a xyloglucanase. It is known to be expressed highly in the first 14 days of *Arabidopsis* growth and is expressed in highly elongating tissues (Kaewthai *et al*., 2013). XTH31-mutants in *Arabidopsis* did not show phenotype under high temperature, sucrose-treatment or normal conditions (Kaewthai *et al*., 2013). It would be interesting, to test the effect of high-light onto these mutants.

ARP2 is a member of the Arp2/3 complex responsible for actin polymerization. Mutants of *ARP2* were found to display trichome defects and aberrant leaf epidermis pavement cells (Li *et al*., 2003).

Genes that are associated with the GO-terms cell wall and cell cycle showed 15 genes up-regulated only in stage 2 (Table 9). Two of them are involved in pathogen responses (AT5G64120 and AT2G33580). A common response of high-light treatment is the up-regulation of pathogen infection and HL oxidative stress response genes (Mühlenbock *et al.*, 2008; Rossel *et al*., 2007; Szechyńska-Hebda & Karpiński, 2013). Why these pathways are both induced by high-light remains elusive to this point (Gordon *et al*., 2013). From the 15 genes only up-regulated in S2, several are involved in cell elongation and cell expansion: CELLULASE1 is a 1,4 beta-glucanase involved in cell-elongation (Shani et a., 2006). *CELL WALL-ASSOCIATED*

KINASE 1 (*WAK1*) shows highest up-regulation of cell wall-associated genes in S2. *WAK1* expression is linked to leaf cell expansion and knock-down mutants display no changes in rosette size for *wak1* (Wagner & Kohorn, 2001). These results indicate, that in the S2, cell elongation was stronger up-regulated in the high-light compared to the low-light treated plants. The mentioned genes could play a role in high-light-dependent anatomical changes.

Stomata associated genes were up-regulated in S2 in high-light grown plants compared to low-light grown samples (Table 7). Interestingly, the up-regulation was only present in this stage. No differentially expressed genes showed significant fold changes in the S1. In the S3, genes up-regulated in the S2 were not differentially expressed, but others were down-regulated (Table 7). Stomata development is a tightly regulated process that involves cell division and cell differentiation Since genes responsible for stomata development show significant fold changes in the second stage, it would be interesting to analyse, whether the number of stomata changes in the high-light compared to the low-light in S2 compared to S1. Stomata density increases with the light intensities (Pillitteri & Dong, 2013). If stomata density changes from S1 to S2 under high-light conditions, this would shed light on the developmental timing of stomata density development.
Cytochromes have a multitude of functions in the plant cells, including pathogen defence mechanisms, anthocyanin biosynthesis and brassinosteroid synthesis (Bak *et al*., 2011). With a very diverse functional pattern, the expression of cytochrome P450-genes was also diverse in the high-light treated samples in comparison to the low-light treated samples. In the S1, six cytochrome P450 genes showed significant fold-change induction, but not in the other two stages. While also the S3 contained genes specifically higher expressed in the high-light than in the low-light, the S2 shared some of the differentially expressed genes with the other stages (Table 6). CYP79F1 was up-regulated in the S1 and is involved in the biosynthesis of aliphatic glucosinolates (Reintanz *et al*., 2001). Mutants of CYP79F1 have increased levels of IAA and show reduced secondary vein formation as well as crinkled leaves (Reintanz *et al*., 2001). This indicates an important role for CYP79F1 in the plant's development. Since CYP79F1 was found to be higher expressed in high-light grown samples, it might have an influence on the light-dependent anatomical adaptations. Other genes encoding cytochrome P450 enzymes showed also involvement in hormone signalling such as *CYP707A4* in ABA catabolism *CYP79B3* and *CYP79B2* in IAA biosynthesis (Hull *et al*., 2000; Saito *et al*., 2004). These genes show only up-regulation in the S1, not in S2 or S3 (Table 6). The mentioned genes might play a role in the adaptations towards high-light. Phenotyping of the corresponding T-DNA mutant lines would be interesting to investigate whether they are involved in leaf thickness and leaf vein density formation under high-light.

<u>Genes involved in hormone metabolism</u>
Auxin is involved in several biological processes including leaf vein and leaf shape formation by polar auxin transport through pin-formed (PIN) proteins and the formation of local auxin maxima (Scarpella *et al*., 2010) In this data set, most genes were differentially expressed in S2 and S3 (Table 10). Among the 24 differentially expressed genes in the S1, 16 are down-

regulated. The highest down-regulation was found for *DRM2*, a gene involved in seed dormancy (Yazdanpanah *et al*., 2017). Also, other dormancy-associated genes were found down-regulated, as for example AT1G56220, which is down-regulated in all three stages (table 9).

Gretchen-Hagen protein 3.15 was up-regulated in S1 and down-regulated in S3 and encodes for an IBA-specific acyl acid amido-synthetase that might be involved in auxin homeostasis modulating IBA-levels for conversion to IAA in the peroxisome (Sherp *et al*., 2018). Other Gretchen-Hagen genes were found differentially regulated: *WES1* was down-regulated throughout the three stages and is involved in modulation of auxin and pathogen pathways (Table 10; Westfall *et al*., 2016). The only gene up-regulated specifically in S1 is *AXR3* that has a role in palisade cell elongation (Pérez-Pérez *et al*., 2002).

Differential expression of GO-term auxin involved genes in the S2 and S3 indicates higher regulation of auxin-associated genes in the later developmental stages compared to S1 under high-light conditions. Small auxin-upregulated (SAUR) genes were mostly down-regulated in this data set (Table 10). While the function of SAURs is diverse, SAUR19 and SAUR63 have a positive regulatory role in cell elongation (Ren & Grey, 2015), but are down-regulated in high-light grown leaves compared to low-light grown leaves in stages 2 and 3.

As auxin is a hormone that controls developmental processes by building a gradient throughout tissues (Qi *et al*., 2014; Tsiantis *et al*., 1999), it is difficult to pinpoint a specific gene that shows differentially regulation in total leaves to a function in auxin-dependent development. To gain further insights into auxin-dependent leaf development under high-light conditions, it would be interesting to investigate gene-expression of auxin-biosynthesis candidate genes over leaf gradients or investigate the expression of reporter genes in high-light and low-light treated leaves.

Cytokinins are responsible for regulation of cell proliferation by the cell cycle in the shoot and maintenance of the SAM and regulation of leaf senescence, as well as vasculature development (Kieber & Schaller, 2014; Schaller *et al*., 2014). Most genes associated with the GO-term cytokinin showed down-regulation throughout all three developmental stages. Most of the cytokinin-response genes were down-regulated from S2 to S3, only *Arabidopsis* Response Regulator 6 (*ARR6*) which is involved in negative regulation of cytokinin signalling (To *et al*., 2004) was up-regulated in S1 but down-regulated in S3 (Table 11). In the third stage, 2 of 3 IPT-cytokinin biosynthesis genes were down-regulated in the high-light-grown compared to the low-light-grown samples. Also, 2 enzymes involved in the oxidation of cytokinins were up-regulated in the S3 in high-light-grown compared to low-light-grown samples which reduces bioactive cytokinin (Werner *et al*., 2003). In summary, cytokinin is down-regulated in the high-light-grown samples compared to the low-light-grown samples. Interestingly, cytokinin has a role in light-stress response in *Arabidopsis*. Plants with reduced perception of cytokinin or cytokinin deficient plants show a higher susceptibility towards high-light stress including a stronger photoinhibition that non-stressed plants (Cortleven *et al*., 2014). However, the high-light stress used in the publication from Cortleven was much higher than the stress conditions chosen for this experiment (1000 µmol m^{-2} s^{-1} versus 350 µmol m^{-2}

s^{-1} in this thesis). Why most of the cytokinin-associated genes are down-regulated in the high-light samples however, remains elusive.

Gibberellic acid is involved in several developmental processes such as seed germination, transition from meristem to shoot growth, from juvenile to adult leaf stage and the onset of flowering (Gupta & Chakrabarty, 2013). Gibberellic acid upregulates expression of xyloglucan endotransglucosylases (XET) and expansins. XET enhances plasticity of cell wall because it is involved in xyloglucan reorganization through cleaving and re-ligating polymers in the cell wall (Sun, 2010). In this RNA data set gibberellic acid synthesis genes such as *GA3OX2* and *GA3OX1* were found to be expressed more in the high-light grown leaves than in the low-light grown leaves in stages 1 and 2 and stage 2, respectively (Table 12). Interestingly, S2 shows an up-regulation of genes involved in gibberellic acid-associated genes, which is not present in S1 and S3. This differential expression pattern indicates a role for gibberellic acid in the high-light-dependent development of *Arabidopsis* in the early stage of development when leaves are transitioning from young to adult leaves. Whether gibberellic acid signalling has an influence of leaf architecture remains elusive to this point and should be tested by using mutants of gibberellic acid synthesis genes and facing them with high-light. Also, the expression of gibberellic acid genes should be verified by quantitative RT-PCR.
High-light-grown leaves show anatomical adaptations towards high-light. This experiment aimed to gain understanding of regulator of the leaf development by comparing transcriptomes of high-light-and low-light-grown *Arabidopsis* leaves, comparing samples of different leaf developmental stages. Having an overview of the transcriptome, the next steps need to be the further analysis of candidate genes identified in this thesis. These contain genes such as *GH3.15*, *AXR3*, *GA3OX2*, *CELLULASE1*, *WAK1* and *NGAL3*. Candidate genes were differentially expressed in the S1 and the S2 and are known to be involved in developmental processes. Gene-expression of these genes should be verified using q-PCR. By using T-DNA mutants of these genes and assessing their leaf anatomy both under low-light and high-light, it will be possible to identify leaf-anatomy regulators.

4 Material and Methods

4.1 Material

4.1.1 Chemicals and antibiotics

Chemicals and antibiotics in research/pro analysis grade were obtained from AppliChem GmbH (Darmstadt, Germany), BD Biosciences (Heidelberg, Germany), Bio-Rad Laboratories GmbH (Munich, Germany), Carl Roth GmbH (Karlsruhe, Germany), Colgate-Palmolive GmbH (Hamburg, Germany), Duchefa Biochemie B.V. (Haarlem, Netherlands), Honeywell Riedel- de-Haen Specialty Chemicals Seelze GmbH (Seelze, Germany), Life Technologies GmbH (Karlsruhe, Germany), Merck KGaA (Darmstadt, Germany), Roche Diagnostics GmbH (Mannheim, Germany), SERVA Electrophoresis GmbH (Heidelberg, Germany), Sigma- Aldrich Chemie GmbH (Munich, Germany), Thermo Fisher Scientifc (Schwerte, Germany) and VWR International GmbH (Darmstadt, Germany).

4.1.2 Databases and Software

A plasmid editor (ApE) Software was used as database for genomic sequences downloaded from 1001 genome project and for primer design (http://biologylabs.utah.edu/jorgensen/wayned/ape/ (link downloaded 01.2018) version 02. 0.53, by M. W. Davis).
Coding Sequences from *Arabidopsis thaliana* accessions were acquired from *Arabidopsis* 1001 genomes project GE browser 3.0.
Cleaved amplified polymorphic sequences (CAPS) between accessions were identified using the CAPS designer of the Sol Genomic Network (SGN) webtool (Fernandez-Pozo *et al*., 2015).
Polymorphisms between *Arabidopsis* accessions were identified using the Polymorph 1001 variant browser from the 1001 Genomes Project (http://tools.1001genomes.org/polymorph/, link from 01.2018).
Association mapping was performed using TASSEL software (Bradbury *et al*., 2007).
Quantification of images was performed using the Fiji software (Schindelin *et al*., 2012).
Leaf vein density and leaf area was acquired using PhenoVein (Bühler *et al*., 2015), as a plugin of MeVisLab (MeVis Medical Solutions AG).
Venn diagrams were produced using the web interface of bioinformatics & evolution (http://bioinformatics.psb.ugent.be/webtools/Venn/ on 29.01.2018)

4.1.3 Plant material

Arabidopsis thaliana
Arabidopsis accessions used are listed in Supplemental Table 2.
GLDPA—Ft::sGFP-CP (Döring, PhD thesis 2016) *Arabidopsis* seeds in T5 were kindly provided by Udo Gowik University of Düsseldorf.
AMPRIL GF and FG seeds F7 were kindly provided by Marteen Koornneef, Max Planck Institute for Plant Breeding Research (Huang *et al*., 2011).

T-DNA mutant lines were obtained by the Nottingham *Arabidopsis* Stock Center.

Flaveria
Seeds of wild-type species *F. robusta* (C_3), *F. pringlei* (C_3), *F. ramosissima* (C_3-C_4), *F. bidentis* (C_4) and *F. trinervia* (C_4) were obtained from Udo Gowik, University of Düsseldorf.
Seeds of transgenic *F. bidentis* UG5 and CWc carrying the constructs PPCA-L-Ft::H2B-YFP (Stockhaus *et al.,* 1994) and GLDPA-Ft::H2B-YFP (Wiludda *et al.,* 2012) respectively, both in T1, were obtained from Udo Gowik, University of Düsseldorf.

4.1.4 Molecular weight markers

GeneRuler 1 kb DNA Ladder and GeneRuler Low Range DNA Ladder (Thermo Fisher Scientific, Schwerte, Germany) were used as size standard in agarose gel electrophoresis.

4.1.5 Media

Murashige & Skoog (MS) medium
4.44 g /L MS salts
For solid medium, 10 g/L agarose was added to the liquid medium before autoclaving. The pH was adjusted with KOH. For *Arabidopsis* growth a pH of 5.8 was used and for *Flaveria* a pH of 7.0.

4.1.6 Buffers and solutions

All buffers and solutions were prepared with double-distilled water (ddH_2O), if not stated otherwise. Buffers were stored at room temperature (RT) if not stated otherwise. Buffers are only listed in table 1, if they do not represent a simple dilution or a dilution of a stock chemical.

Table 13 Buffers and Solutions.

Buffer /Solution	**Components**
DNA extraction buffer (Thompson method**)**	200 mM Tris/HCl pH 7.5 250 mM NaCl 25 mM EDTA 0.5 % (w/v) SDS
DNA loading dye	0.25 % (w/v) Bromophenol Blue 30 % (v/v) glycerol

PCR reaction buffer	100 mM Tris/HCl pH 9.0 500 mM KCl 15 mM $MgCl_2$
Seed sterilization *Arabidopsis* (*Flaveria*)	20 % (22.5 %) (v/v) Klorix 0.03% (v/v) Triton X-100
TE buffer	10 mM Tris/HCl pH 8.0 1 mM EDTA
1xTAE	40 mM Tris/HCl pH 7.6 20 mM acetic acid 1 mM EDTA
Leaf clearing solution (Rishmawi *et al*., 2017)	55 % methanol 2 % acetic acid

4.2 Methods

4.2.1 *Arabidopsis* growth

4.2.1.1 *Arabidopsis* sterile cultures

Arabidopsis seeds were surface sterilized with sterilization solution for 8 min. Supernatant was discarded working under a sterile hood and the seeds were rinsed five times with sterile ddH_2O. After sowing to MS plates with or without the corresponding antibiotics, the seeds were subjected to stratification at 4 °C for 5 days to break dormancy. Subsequently, plates were incubated in a light chamber at 21 °C for 3 h before light and dark treatment.

4.2.1.2 *Arabidopsis* growth on soil

A 3:1 mixture of soil (Einheitserde Classic, Einheitserde Werkverband e.V, Sinntal-Altengronau, Germany) and vermiculite (Basalt Feuerfest, Linz, Germany). was used as substrate. Seeds were mixed with 0.1 % agarose, or directly sown on soil, watered and kept at 4 °C for and incubated in darkness for 5 days to break dormancy. Plants were grown in greenhouse under long day conditions at approx. 40 % humidity and a temperature regime of 21 °C during the day and 18 °C during the night.

High-light chamber
Seeds were sown on 77x multiplates (Nitsch & Sohn, Kreuztal, Germany, each hole approximately 4 cm x 4 cm x 5.2 cm, length x width x height) in a randomized fashion. Plates were incubated under different fluence rates in a walk-in growth chamber (Johnson Controls, Milwaukee, WI, USA). Fluence rates were generated by white-light halide lamps MT400DL/BH (EYE LIGHTNING INTERNATIONAL INC., Mentor, OH, USA).
For seed germination, plates were incubated for 3 days at 150 µmol m^{-2} s^{-1} and then transferred to the corresponding final fluence rate. Plates were turned every day, including altering of the position to avoid position-dependent growth changes. To avoid plant damages due to fungus gnat larvae, a suspension containing nematodes was applied every week directly onto the soil (Fa. Sautter und Stepper, Ammerbuch).
Plants were grown for 19 days under long day conditions (16 h light, 8 h dark), with 21°C during day and night.

4.2.2 *Flaveria* growth

Flaveria seeds were surface-sterilized using sterilization solution for 20 min. The supernatant was discarded under a sterile hood and the seeds were rinsed five times with sterile ddH_2O. Seeds were plated on MS plates pH 7 and stratified for five days at 4°C. Plates were incubated for three hours in light before subjected to light or dark treatment.

4.2.3 *Arabidopsis* leaf architecture analysis

The identity of the adult 4th leaf was recorded for each plant after 14 days of growth in the green house and 10 days of growth in the high-light chamber, respectively. After 19 days in the high-light chamber and 23 days in the green house, the 4th true leaves were detached from the plants using a scalpel blade (Swann-Morton, Sheffield, UK) and the petiole was removed. The leaves were weighed individually and glued to a sheet of paper to remove unevenness. Pictures were taken with a digital camera. Leaves were subsequently removed from the paper and incubated in 2 mL reaction tube filled with 96 % denatured ethanol for up to 3 weeks at 4 °C. The supernatant was discarded, and leaf clearing solution was applied to the leaves, incubated for 2 days at 4 °C and subsequently removed. Leaves were then stored in 96 % denatured ethanol. For picture acquisition, leaves were rinsed in ddH_2O for 2 min and then

transferred to a cover slide, with the adaxial side facing upwards. Using a light box in an otherwise dark room pictures were taken from the leaves using a digital camera. Pictures were imported into PhenoVein for measurement of the leaf area and total leaf vein density.

4.2.4 Confocal microscopy of cross-sections of *Flaveria* cotyledons

Cross-sections

Cross-sections of *Flaveria* cotyledons were produced by detaching the cotyledons from the hypocotyl using a razor blade (0.1 mm blade thickness; Dorco, San Diego, USA). The cotyledons were carefully placed between two slices of Styrofoam using forceps. The basal part of the cotyledons was placed protruding to the outside of the Styrofoam. A drop of water was placed on the edge of a razor blade to allow smooth cutting. With seesaw movements, the blade was then moved through the Styrofoam and through the specimen. After several cuttings, the Styrofoam was turned by 180° to allow more straight cuts. After cutting, the resulting leaf sections and Styrofoam debris were collected in a drop of water on a specimen slide. Using binocular and forceps, the debris was discarded. 50 µg/ mL propidium iodide was applied towards the leaf sections and a 1.5 mm thick cover glass was carefully lowered on the sample.

Image acquisition

Images were acquired using SP8 as well as DM6000 confocal laser scanning microscopes (Leica microsystems) using the Leica Application Suite software (Leica Microsystems, Wetzlar, Germany). Propidium iodide (PI)-stained samples were excited using the argon laser at 561 nm and the fluorescence was detected with the default settings for PI. Z-axis stacks were taken with a step size between 0.7 and 2 µm. ImageJ was used to combine stacked pictures to produce a sum picture and also to add the scale bars.

4.3. Molecular biology methods

4.3.1 Extraction of nucleic acids

4.3.1.1 Genomic DNA extraction from plant material

Single leaves were either snap-frozen in liquid nitrogen and stored at -80°C until usage, or immediately used for DNA extraction. Frozen plant material was ground to a fine powder using plastic pistils before adding 400 µL Thompson DNA extraction buffer, or fresh leaves were immediately ground in 400 µL extraction buffer and mixed by vortexing.

Samples were centrifuged at 20 000 *g* for 3 min, 200 µl of the supernatant was transferred to a new reaction tube, mixed with 200 µl isopropanol and incubated at RT for 2 min. Samples were then centrifuged at 20 000 *g* for 10 min, the supernatant was removed by inverting the reaction tubes and the pellets were air-dried for 15 min before being resuspended in 75 µL ddH_2O or TE buffer. Samples were stored for further usage at 4 °C or for long term storage at -20 °C.

4.3.1.2 RNA extraction from plant material

The RNAeasy Plant Mini Kit (Qiagen, Hilden, Germany) was used for isolation of total RNA from 50-100 mg of snap-frozen *Arabidopsis* leaves. Extraction was performed according to the manufacturer's instructions.
RNA concentrations were measured using a Nanodrop ND-1000 spectrophotometer (Thermo Fisher Scientific, Schwerte, Germany). To verify the integrity of the RNA, it was analysed on a 1 % agarose gel to check for the presence of clear 28S and 18S rRNA bands. RNA samples were stored until usage at -80 °C.

4.3.2 Oligonucleotides

Oligonucleotides were designed using Primer 3 or ApE software and lyophilized powder oligonucleotides were obtained from Sigma Aldrich (Munich, Germany). Oligonucleotides were re-suspended in ddH_2O following the manufacturer's instructions to obtain a concentration of 100 µM and stored at -20 °C. Oligonucleotides used for mapping are listed in Table 15.

4.3.3 Molecular markers

CAPS markers were identified using the CAPS Designer software from Sol Genomics Network (Fernandez-Pozo *et al*., 2015). Sequences of the accessions were obtained from 1001 genome Project and up-loaded in the SGN tool. This tool screens for polymorphisms between sequences that lead to creation or abolishment of restriction endonuclease restriction sites. The output of the tool was screened for suitable restriction enzymes. Using ApE, suitable PCR primers were designed in a way that the resulting PCR product was about 400- 800 bp long and that the restriction site was approximately in the middle of the PCR product to simplify optical verification of the marker.
PCR-products were loaded on 1 % gel to verify quantity before subjecting the PCR-products to CAPS-specific restriction digest. Restriction digests were performed using 10 µL PCR product, 2 µL 10x buffer according to the manufacturer's recommendation and 0.5µL enzyme in a total 20 µL reaction volume. Digests were incubated over night at the recommended temperature. The digests were analysed on a 1–4 % agarose gel, depending on the fragment sizes.

4.3.4 Identification of HIF lines in AMPRIL

The identification of heterozygous regions in the AMPRIL lines were performed using TASSEL 5. Genotype data of the AMPRIL population kindly provided by the Koornneef group were imported into TASSEL. Data consist of all SNPs of parental lines and RILs used for genotyping the AMPRIL population (Huang *et al.,* 2011). Data were screened for heterozygous regions indicated by the software. To assign the SNPs present in the RILs with parental alleles, up to

30 SNPs of the heterozygous regions were compared with the parental SNPs and by exclusion process, the parental SNPs of the heterozygous regions were identified. Using CAPS markers, the SNPs were verified, as most markers were specific for polymorphisms present in either parent. The whole data set was screened to identify lines only segregating in the region of interest on chromosome 4.

4.3.5 Polymerase chain reaction (PCR)

The polymerase chain reaction technique (Mullis & Faloona 1987) was used for mapping of the HIF lines as well as for verification of the T-DNA mutants.
A standard PCR reaction contained a mixture of 1 x PCR reaction buffer, 0.5 µM forward and reverse primers, and 125 µM dNTPs and 1 µL of Taq DNA Polymerase and 1 µL genomic DNA in a 20 µL total reaction volume.
The initial denaturation step was set to 95 °C for 5 min. Then, 40 cycles of denaturation (30 s), primer hybridization at 55 °C (30 s), and catalytic elongation of the nucleic acids by the polymerase at 72 °C (30 s / 500 bp) were programmed. A final elongation step was performed after the last cycle at 72 °C for 5 min. PCR products were stored at 4 °C or at -20 °C. Primers for the genotyping of T-DNA insertion lines are listed in table 2, primers for CAPS-marker analysis are listed in table 3. For Go Taq G2 Polymerase, the PCR cycling conditions were adjusted according the manufacturer's recommendations.

4.3.6 Agarose gel electrophoresis

Nucleic acids were separated in agarose gels based on 1 x TAE buffer according to standard protocols (Sambrook *et al*., 2001). Depending on the DNA fragment size, 1–4 % (w/v) agarose was boiled in 1x TAE-buffer, mixed with 0.25 µg / mL ethidium bromide after cooling to approx. 50 °C with and then casted.
Nucleic acids were mixed with 1x DNA loading dye and gels were run in 1x TAE as running buffer. For visualization of nucleic acids, a GEL Stick "Touch" imager (INTAS Science Imaging Instruments, Göttingen, Germany) was used.

4.3.7 genotyping of T-DNA mutants

For genotyping of T-DNA *Arabidopsis* mutants, genomic DNA was isolated. To genotype T-DNA insertion mutants, the presence of the wild-type and the mutant allele was tested by two independent PCR reactions containing either wild-type specific primers or a combination of T-DNA- and wild-type-specific primer.
Primer combinations used for genotyping T-DNA insertion mutants are given in Table 14.

4.4. QTL-Analysis

4.4.1 Mixed Linear Model for QTL analysis

QTL-Analysis was performed using default settings of the program TASSEL (Bradbury *et al*., 2007): Matrixes containing the kinship data and SNP identities of the AMPRIL were kindly provided by Marteen Koornneef (MPI, Cologne, Germany). To perform QTL analysis, the mean values for all lines were imported and a numerical factor was added to identify the replicates. The Mixed linear Model was used for association analysis.
Using the Henderson matrix annotation, the model can be displayed as follows:
$y = X\beta + Zu + e$
With y being the vector of observations, β an unknown vector of fixed effects, but including genetic marker and population structure. Random additive genetic effects from multiple background QTL for individuals/lines are represented by vector u. X and Z are the known design matrixes, while e is the unobserved vector of random residuals.
This model includes random and fixed effects. It also takes the genetic marker-based kinship matrix into account, which increases the statistical power of this model. Furthermore, TASSEL implemented a compression method in the mixed linear model analysis. This reduces the dimensionality of the kinship matrix, reduces computational time and improves model fitting. With compression level set to 1, no compression is used, and each taxon belongs to its own distinct group. With maximum compression (compression =n), all taxa are joint in one group and it is not possible to estimate random effects independently of error.
After computation, the results were displayed in a Manhattan blot.

4.4.2 calculation of broad sense heritability

The broad sense heritability H^2 is a statistic measure to estimate the degree of genetically based variation of a phenotypic trait in a population. Broad sense heritability is defined as

$$\mathrm{H}^2 = \frac{V_G}{V_P} = \frac{V_G}{V_G + V_E}$$

With
V_P: Phenotypic variance = $1/n \sum (x_i - \bar{x})^2$ with phenotypic data $=x_i \ldots x_n$
V_G: genetic variance $1/n \sum (x_{vp} - \bar{x}_{vp})^2$
V_E environmental variance.

4.5 RNA-Sequencing

Total isolated RNA samples were given to CCG institute for DNase treatment and library formation. In the following a summary of the workflow is listed.
Quality of RNA was confirmed by Agilent 4200 TapeStation (Agilent, Santa Clara, USA). Only RNA samples with an RNA integrity number (RIN) higher than eight was used. Poly-A-

containing mRNA was isolated, and first and second strand cDNA was synthesized following instructions provided from the TruSeq stranded mRNA kit (Ilumina, Cambridge, UK). 3' ends were adenylated to prevent them from self-ligation. Consequently, adapters were ligated to the ends of the ds cDNA fragments for preparation of hybridization onto a flow cell. DNA fragments with fragments on both 3' and 5' ends were enriched by PCR using only 14 cycles to prevent skewing of library representation of the fragments. Library quantity was checked, considering size, purity and concentration of the libraries using KAPA Library Quantification kit for Illumina platforms (qPCR; Illumina, Cambridge, UK). The expected library has a size of approximately 260bp and indexed DNA libraries were normalized to 2ng/µl. RNA Sequencing was performed using the Illumina HiSeq 4000 system, creating 33,33Mio Reads per sample.

Statistical analysis of RNA Sequencing data set was performed by Prerana Wagle, CECAD and are listed in Wagle *et al*., 2015.

Table 14 Primer for T-DNA mutant genotyping.

Primer	T-DNA insertion mutant line	Sequence (5' → 3')	Reference
SALK_047540C_LP	*pgp3*	TATTAACCGACGTCGCATTTC	Salk institute
SALK_047540C_RP	*pgp3*	CTTTCGTGACCTATGTTTCGC	Salk institute
SALK_026326_LP	*ins*	CTGCGACGAGGAGTAGAGAAC	Salk institute
SALK_026326_RP	*ins*	TTCGGAACCCGAAAAATCTAC	Salk institute
SALK_202706_LP	*axr6*	CTGTAAACGGACTCTGATGCC	Salk institute
SALK_202706_RP	*axr6*	TTTTAATGTTCGGCGATTGAG	Salk institute
Wiscseq_DsLox507B01.1_LP	*dhhc-type zinc-finger family*	TTCTCAGCTGCTTGTAGAGCC	Salk institute
Wiscseq_DsLox507B01.1_RP	*dhhc-type zinc-finger family*	AGCATTGCAGGACATGTAACC	Salk institute
Wiscseq_LBP	Used with Wiscseq primers	AACGTCCGCAATGTGTTATTAAGTTGTC	Salk institute
SAIL_769_A09_LP	*rve5*	TTTTGGCAGATTTGTCGATTC	Salk institute
SAIL_769_A09_RP	*Rve5*	TCCACGCGGACATCTTTATAG	Salk institute
LBP1.3	T-DNA-specific primer	ATTTTGCCGATTTCGGAAC	Salk institute
SAIL_769_LBP	T-DNA-specific primer	ATT AGG CAC CCC AGG CTT TAC ACT TTA TG	Salk institute

Table 15 Primer for CAPS marker analysis

Primer	Sequence (5'→3')	Marker name	Reference	Accessions	Restriction site location (bp)	PCR product size (digest size)	Restriction enzyme
Prim_sin_fwd	AAATCTGAATGACTTGAAAACGAAG	GF33_I	This study	An, Kyo	110711	247 (176 + 71)	*Sac*II in Kyo
Prim_sin_rev	TGTGGTGTTAGTTAGTTACGATGGA						
GF33_right_2_fwd	GATTGGTTAAAGGAGCGTGCAAGG	GF33_III	This study	An, Kyo, Sha	1260707	818	*Xho*I in An-1
GF33_right_2_rev	CCCAAATCTAGTTTACCTACCAGC						
KpnI_1_AK_4.8M_fwd_1	CAATTCCTGCGTTCCGGTTAGATGC	GF33_IV	This study	An, Kyo	4840690	582 (332 + 250)	*Kpn*I in An-1
KpnI_1_AK_4.8M_rev_2	ATGTGGTGCTTTGGTTTAGGCTAC						
600k_NcoI_850_fwd	GTTGTTTTAGAAAGAAATGGGCT	GF33_III	This study	An, Kyo	608600	850 (644 +206)	*Nco*I in Kyo
600k_NcoI_850_rev	TGGATTAAAACCGAAACTTACCC						
EcoNI_fwd_2	TTGCTCAGAGTTTCCATGATGTCC	FG18/GF07_I	This study	An, Sha	218027	1061 (711 + 350)	*Sac*II in Sha
SacII_rev2	CTGTTGTGTGTTTCCCTTACTTGG						
Midri_AS_XhoI_533_fwd	TTTGGGCATACTCTAGCTAAAACAA	FG187GF07_II	This study	An, Sha	738585	563 (331 + 232)	*Xho*I in Sha
Midri_AS_XhoI_533_rev	ACATGGTCTAACAAAAGTCAAAGGA						
NheI_2_fwd_1	CATTGTTGGTCTAACTTGTGGGTCG	FG18/GF07_IIII	This study	An, Sha	1060727	620 (405 + 215)	*Nhe*I in An-1
NheI_2_rev_3	TTCCTCTCTTGGGTTATTGTCGTCG						
ApaI_fwd_1	AACACAACACAAGCCAATGAGAGC	FG18/GF07_IV	This study	An-1, Sha	7175592	791 (496 + 295)	*Apa*I in Sha
ApaI_rev_1	GTATATCTGGCGTTATCACTCACC						

5 References

Adams W.W., Zarter C.R., Mueh K.E., Amiard V., Demmig- Adams B. (**2006**) Energy dissipation and photoinhibition: a continuum of photoprotection. In Photoprotection, photoinhibition, gene regulation, and environment. Advances in photosynthesis and respiration, Demmig-Adams B., Adams, W.W., Mattoo, A.K., eds. (Dordrecht: Kluwer Academic Publishers), 49–64.

Adams, W.W., Watson, A.M., Mueh, K.E., Amiard, V., Turgeon, R., Ebbert, V., Logan, B.A., Combs, A.F., and Demmig-Adams, B. (**2007**). Photosynthetic acclimation in the context of structural constraints to carbon export from leaves. Photosyn. Res. 94, 455–466.

Adamska, I. (**1997**). ELIPs – Light-induced stress proteins. Physiol. Plant. 100, 794–805.

Afzal, A., Duiker, S.W., and Watson, J.E. (**2017**). Leaf thickness to predict plant water status. Biosyst. Eng. 156, 148–156.

Akyildiz, M., Gowik, U., Engelmann, S., Koczor, M., Streubel, M., and Westhoff, P. (**2007**). Evolution and function of a cis-regulatory module for mesophyll-specific gene expression in the C_4 dicot *Flaveria trinervia*. Plant Cell 19, 3391–3402.

Al-Whaibi, M.H. (**2011**). Plant heat-shock proteins: A mini review. J. King Saud Univ. Sci. 23, 139–150.

Albert, N.W., Lewis, D.H., Zhang, H., Irving, L.J., Jameson, P.E., and Davies, K.M. (**2009**). Light-induced vegetative anthocyanin pigmentation in Petunia. J. Exp. Bot. 60, 2191–2202.

Alonso-Blanco, C., and Koornneef, M. (**2000**). Naturally occurring variation in *Arabidopsis*: an underexploited resource for plant genetics. Trends Plant Sci. 5, 22–29.

Alonso-Cantabrana, H., and von Caemmerer, S. (**2016**). Carbon isotope discrimination as a diagnostic tool for C_4 photosynthesis in C_3-C_4 intermediate species. J. Exp. Bot. 67, 3109–3121.

Alsharafa, K., Vogel, M.O., Oelze, M.-L., Moore, M., Stingl, N., König, K., Friedman, H., Mueller, M.J., and Dietz, K.-J. (**2014**). Kinetics of retrograde signalling initiation in the high light response of *Arabidopsis thaliana*. Philos. Trans. R. Soc. Lond., B, Biol. Sci. 369, 20130424.

Anderson, J.M. (**1986**). photoregulation of the composition, function, and structure of thylakoid membranes. Annu. Revi. Plant Physiol. 37, 93–136.

Andersson, U., Heddad, M., and Adamska, I. (**2003**). Light stress-induced one-helix protein of the chlorophyll a/b-binding family associated with photosystem I. Plant Physiol. 132, 811–820.

Andreo, C.S., Gonzalez, D.H., and Iglesias, A.A. (**1987**). Higher plant phosphoenolpyruvate carboxylase. FEBS Lett. *213*, 1–8.

Andriankaja, M., Dhondt, S., De Bodt, S., Vanhaeren, H., Coppens, F., De Milde, L., Mühlenbock, P., Skirycz, A., Gonzalez, N., Beemster, G.T.S., (2012). Exit from proliferation during leaf development in *Arabidopsis thaliana*: a not-so-gradual process. Dev. Cell *22*, 64–78.

Arsovski, A.A., Galstyan, A., Guseman, J.M., and Nemhauser, J.L. (**2012**). Photomorphogenesis. TAB 10, e0147.

Aubry, S., Brown, N.J., and Hibberd, J.M. (**2011**). The role of proteins in C_3 plants prior to their recruitment into the C_4 pathway. J. Exp. Bot. 62, 3049–3059.

Bailey, S., Thompson, E., Nixon, P.J., Horton, P., Mullineaux, C.W., Robinson, C., and Mann, N.H. (**2002**). A critical role for the Var2 FtsH homologue of *Arabidopsis thaliana* in the photosystem II repair cycle in vivo. J. Biol. Chem. 277, 2006–2011.

5 References

Bak, S., Beisson, F., Bishop, G., Hamberger, B., Höfer, R., Paquette, S., and Werck-Reichhart, D. (**2011**). Cytochromes P450. *Arabidopsis* Book 9.

Bar, M., and Ori, N. (**2014**). Leaf development and morphogenesis. Development 141, 4219–4230.

Beavis, W. D., (**1998**). QTL analyses: power, precision, and accuracy. Mol. Dissection Complex Traits, 145–162.

Bergelson, J., and Roux, F. (**2010**). Towards identifying genes underlying ecologically relevant traits in *Arabidopsis thaliana*. Nat. Rev. Genet. 11, 867–879.

Berleth, T., and Jurgens, G. (**1993**). The role of the monopteros gene in organising the basal body region of the *Arabidopsis* embryo. Development 118, 575–587.

Blanco, A., Simeone, R., and Gadaleta, A. (**2006**). Detection of QTLs for grain protein content in durum wheat. Theor. Appl. Genet. 112, 1195–1204.

Bögre, L., and Beemster, G., ed. (**2008**). Plant Growth Signaling (Berlin, Heidelberg: Springer-Verlag).

Bolhàr-Nordenkampf, H.R., and Draxler, G. (**1993**). Functional leaf anatomy. In Photosynthesis and Production in a Changing Environment: A Field and Laboratory Manual, Hall, D.O., ed. (Dordrecht: Springer), 91–112.

Botha, C.E. (**1992**). Plasmodesmatal distribution, structure and frequency in relation to assimilation in C3 and C 4 grasses in southern Africa. Planta 187, 348–358.

Bowes, G., Ogren, W.L., and Hageman, R.H. (**1971**). Phosphoglycolate production catalyzed by ribulose diphosphate carboxylase. Biochem. Biophys. Res. Commun. *45*, 716–722.

Bradbury, P.J., Zhang, Z., Kroon, D.E., Casstevens, T.M., Ramdoss, Y., and Buckler, E.S. (**2007**). TASSEL: software for association mapping of complex traits in diverse samples. Bioinformatics 23, 2633–2635.

Brodribb, T.J., Feild, T.S., and Jordan, G.J. (**2007**). leaf maximum photosynthetic rate and venation are linked by hydraulics. Plant Physiol. 144, 1890–1898.

Broun, P. (**2005**). Transcriptional control of flavonoid biosynthesis: a complex network of conserved regulators involved in multiple aspects of differentiation in *Arabidopsis*. Curr. Opin. Plant Biol. 8, 272–279.

Brown, B.A., and Jenkins, G.I. (**2008**). UV-B signaling pathways with different fluence-rate response profiles are distinguished in mature *Arabidopsis* leaf tissue by requirement for UVR8, HY5, and HYH. Plant Physiol. 146, 576–588.

Brown, B.A., Cloix, C., Jiang, G.H., Kaiserli, E., Herzyk, P., Kliebenstein, D.J., and Jenkins, G.I. (**2005**). A UV-B-specific signaling component orchestrates plant UV protection. PNAS 102, 18225–18230.

Brown, W.V. (**1975**). Variations in Anatomy, Associations, and Origins of Kranz Tissue. Am. J. Bot. 62, 395–402.

Bühler, J., Rishmawi, L., Pflugfelder, D., Huber, G., Scharr, H., Hülskamp, M., Koornneef, M., Schurr, U., and Jahnke, S. (**2015**). phenoVein-A Tool for Leaf Vein Segmentation and Analysis. Plant Physiol. 169, 2359–2370.

Calvin, M., and Benson, A.A. (**1948**). The Path of Carbon in Photosynthesis. Science *107*, 476–480.

Carland, F.M., Berg, B.L., FitzGerald, J.N., Jinamornphongs, S., Nelson, T., and Keith, B. (**1999**). genetic regulation of vascular tissue patterning in *Arabidopsis*. The Plant Cell 11, 2123–2137.

5 References

Carol, R.J., and Dolan, L. (**2006**). The role of reactive oxygen species in cell growth: lessons from root hairs. J. Exp. Bot. 57, 1829–1834.

Chaves, I., Pokorny, R., Byrdin, M., Hoang, N., Ritz, T., Brettel, K., Essen, L.-O., van der Horst, G.T.J., Batschauer, A., and Ahmad, M. (**2011**). The cryptochromes: blue light photoreceptors in plants and animals. Annu Rev Plant Biol 62, 335–364.

Christin, P.-A., Osborne, C.P., Chatelet, D.S., Columbus, J.T., Besnard, G., Hodkinson, T.R., Garrison, L.M., Vorontsova, M.S., and Edwards, E.J. (**2013**). Anatomical enablers and the evolution of C4 photosynthesis in grasses. PNAS 110, 1381–1386.

Clarke, J.H., and Dean, C. (**1994**). Mapping FRI, a locus controlling flowering time and vernalization response in *Arabidopsis thaliana*. Mol. Gen. Genet. 242, 81–89.

Cohu, C.M., Muller, O., Demmig-Adams, B., and Adams, W.W. (**2013**). Minor loading vein acclimation for three *Arabidopsis thaliana* ecotypes in response to growth under different temperature and light regimes. Front Plant Sci 4, 240.

Cominelli, E., Gusmaroli, G., Allegra, D., Galbiati, M., Wade, H.K., Jenkins, G.I., and Tonelli, C. (**2008).** Expression analysis of anthocyanin regulatory genes in response to different light qualities in *Arabidopsis thaliana*. J. Plant Physiol. 165, 886–894.

Coneva, V., and Chitwood, D.H. (**2018**). Genetic and Developmental Basis for Increased Leaf Thickness in the *Arabidopsis* Cvi Ecotype. Front. Plant Sci. 9, 322.

Cortleven, A., Nitschke, S., Klaumünzer, M., AbdElgawad, H., Asard, H., Grimm, B., Riefler, M., and Schmülling, T. (**2014**). A novel protective function for cytokinin in the light stress response is mediated by the *Arabidopsis* HISTIDINE KINASE2 and *Arabidopsis* HISTIDINE KINASE3 Receptors1. Plant Physiol.164, 1470–1483.

Covshoff, S., and Hibberd, J.M. (**2012**). Integrating C4 photosynthesis into C_3 crops to increase yield potential. Curr. Opin. Biotechnol. 23, 209–214.

Covshoff, S., Burgess, S.J., Kneřová, J., and Kümpers, B.M.C. (**2014**). Getting the most out of natural variation in C_4 photosynthesis. Photosynth. Res. 119, 157–167.

Cowling, R.J., and Harberd, N.P. (**1999**). Gibberellins control *Arabidopsis* hypocotyl growth via regulation of cellular elongation. J. Exp. Bot. 50, 1351–1357.

Crawford, K.M., and Zambryski, P.C. (1999). Phloem transport: Are you chaperoned? Curr. Biol. *9*, R281-285.

Das, P.K., Geul, B., Choi, S.-B., Yoo, S.-D., and Park, Y.-I. (**2011**). Photosynthesis-dependent anthocyanin pigmentation in *Arabidopsis*. Plant Signal. Behav. 6, 23–25.

del Pozo, J.C., Boniotti, M.B., and Gutierrez, C. (**2002**). *Arabidopsis* E2Fc functions in cell division and is degraded by the ubiquitin-SCF(AtSKP2) pathway in response to light. Plant Cell 14, 3057–3071.

Dengler, N.G., and Nelson, T. (**1999**). Leaf Structure and Development in C_4 Plants. C_4 Plant Biology 133–172.

Dengler, N.G., and Taylor, W.C. (**2000**). Developmental Aspects of Photosynthesis. In Photosynthesis: Physiology and Metabolism, R.C. Leegood, T.D. Sharkey, and S. von Caemmerer, eds. (Dordrecht: Kluwer Academic Publishers), 471–495.

5 References

Dengler, N.G., Dengler, R.E., Donnelly, P.M., and Hattersley, P.W. (**1994**). Quantitative Leaf Anatomy of C3 and C4 Grasses (Poaceae): Bundle Sheath and Mesophyll Surface Area Relationships. Ann. Bot. 73, 241–255.

Dewitte, W., Scofield, S., Alcasabas, A.A., Maughan, S.C., Menges, M., Braun, N., Collins, C., Nieuwland, J., Prinsen, E., Sundaresan, V., (**2007**). *Arabidopsis* CYCD3 D-type cyclins link cell proliferation and endocycles and are rate-limiting for cytokinin responses. PNAS *104*, 14537–14542.

Dietrich, P., Sanders, D., and Hedrich, R. (**2001**). The role of ion channels in light-dependent stomatal opening. J. Exp. Bot. 52, 1959–1967.

Donnelly, P.M., Bonetta, D., Tsukaya, H., Dengler, R.E., and Dengler, N.G. (1999). Cell cycling and cell enlargement in developing leaves of *Arabidopsis*. Dev. Biol. 215, 407–419.

Döring, F. (**2017**). Understanding the Bundle Sheath in C4 Evolution–Forward Genetic and Transcriptomic Approaches. PhD thesis. Heinrich-Heine-Universität Düsseldorf.

du Plessis, L., Škunca, N., and Dessimoz, C. (**2011**). The what, where, how and why of gene ontology—a primer for bioinformaticians. Brief Bioinform. 12, 723–735.

Dunaeva, M., and Adamska, I. (**2001**). Identification of genes expressed in response to light stress in leaves of *Arabidopsis thaliana* using RNA differential display. Eur. J. Biochem. *268*, 5521–5529.

Edwards, E.J., Osborne, C.P., Strömberg, C.A.E., Smith, S.A., and Consortium, C.G. (**2010**). The Origins of C_4 Grasslands: Integrating Evolutionary and Ecosystem Science. Science 328, 587–591.

Ehleringer, J.R., Cerling, T.E., and Helliker, B.R. (**1997**). C_4 photosynthesis, atmospheric CO_2 and climate. Oecologia 112, 285–299.

Eklöf, J.M., and Brumer, H. (**2010**). The XTH gene family: an update on enzyme structure, function, and phylogeny in xyloglucan remodeling. Plant Physiol. 153, 456–466.

Ellis, R.J. (**1979**). The most abundant protein in the world. Trends Biochem. Sci. 4, 241–244.

Eloy, N.B., de Freitas Lima, M., Van Damme, D., Vanhaeren, H., Gonzalez, N., De Milde, L., Hemerly, A.S., Beemster, G.T.S., Inzé, D., and Ferreira, P.C.G. (**2011**). The APC/C subunit 10 plays an essential role in cell proliferation during leaf development. Plant J.. 68, 351–363.

Engelhorn, J., Reimer, J.J., Leuz, I., Göbel, U., Huettel, B., Farrona, S., and Turck, F. (**2012**). Development-related PcG target in the apex 4 controls leaf margin architecture in *Arabidopsis thaliana*. Development 139, 2566–2575.

Engelmann, S., Wiludda, C., Burscheidt, J., Gowik, U., Schlue, U., Koczor, M., Streubel, M., Cossu, R., Bauwe, H., and Westhoff, P. (**2008**). The gene for the P-subunit of glycine decarboxylase from the C4 species *Flaveria trinervia*: analysis of transcriptional control in transgenic *Flaveria bidentis* (C_4) and *Arabidopsis* (C_3). Plant Physiol. 146, 1773–1785.

Esau, K. (1977). Anatomy of seed plants (New York: Wiley).

Eshed, Y., Izhaki, A., Baum, S.F., Floyd, S.K., and Bowman, J.L. (**2004**). Asymmetric leaf development and blade expansion in *Arabidopsis* are mediated by KANADI and YABBY activities. Development 131,2997–3006.

Esteve-Bruna, D., Pérez-Pérez, J.M., Ponce, M.R., and Micol, J.L. (**2013**). incurvata13, a novel allele of AUXIN RESISTANT6, reveals a specific role for auxin and the SCF complex in *Arabidopsis* embryogenesis, vascular specification, and leaf flatness. Plant Physiol. 161, 1303–1320.

5 References

Favory, J.-J., Stec, A., Gruber, H., Rizzini, L., Oravecz, A., Funk, M., Albert, A., Cloix, C., Jenkins, G.I., Oakeley, E.J., (**2009**). Interaction of COP1 and UVR8 regulates UV-B-induced photomorphogenesis and stress acclimation in *Arabidopsis*. EMBO J. 28, 591–601.

Fernandez-Pozo, N., Rosli, H.G., Martin, G.B., and Mueller, L.A. (**2015**). The SGN VIGS tool: user-friendly software to design virus-induced gene silencing (VIGS) constructs for functional genomics. Mol. Plant. 8, 486–488.

Finnegan, P.M., Suzuki, S., Ludwig, M., and Burnell, J.N. (**1999**). Phosphoenolpyruvate Carboxykinase in the C_4 Monocot *Urochloa panicoides* Is Encoded by Four Differentially Expressed Genes. Plant Physiol. 120, 1033–1042.

Galvez-Valdivieso, G., Fryer, M.J., Lawson, T., Slattery, K., Truman, W., Smirnoff, N., Asami, T., Davies, W.J., Jones, A.M., Baker, N.R., (**2009**). The high light response in *Arabidopsis* involves ABA signaling between vascular and bundle sheath cells. Plant Cell 21, 2143–2162.

Gälweiler, L., Guan, C., Müller, A., Wisman, E., Mendgen, K., Yephremov, A., and Palme, K. (**1998**). Regulation of polar auxin transport by AtPIN1 in *Arabidopsis* vascular tissue. Science 282, 2226–2230.

Geisler, M., Kolukisaoglu, H.U., Bouchard, R., Billion, K., Berger, J., Saal, B., Frangne, N., Koncz-Kalman, Z., Koncz, C., Dudler, R., (**2003**). TWISTED DWARF1, a unique plasma membrane-anchored immunophilin-like protein, interacts with *Arabidopsis* multidrug resistance-like transporters AtPGP1 and AtPGP19. Mol. Biol. Cell 14, 4238–4249.

Gordon, M.J., Carmody, M., Albrecht, V., and Pogson, B. (**2013**). Systemic and Local Responses to Repeated HL Stress-Induced Retrograde Signaling in *Arabidopsis*. Front. Plant Sci. 3, 303.

Gotoh, E., Suetsugu, N., Higa, T., Matsushita, T., Tsukaya, H., and Wada, M. (**2018**). Palisade cell shape affects the light-induced chloroplast movements and leaf photosynthesis. Sci. Rep. 8, 1472–1480.

Goujon, T., Minic, Z., El Amrani, A., Lerouxel, O., Aletti, E., Lapierre, C., Joseleau, J.-P., and Jouanin, L. (**2003**). AtBXL1, a novel higher plant (*Arabidopsis thaliana*) putative beta-xylosidase gene, is involved in secondary cell wall metabolism and plant development. Plant J. 33, 677–690.

Gowik, U., Bräutigam, A., Weber, K.L., Weber, A.P.M., and Westhoff, P. (**2011**). Evolution of C4 Photosynthesis in the Genus *Flaveria*: How Many and Which Genes Does It Take to Make C4? The Plant Cell 23, 2087–2105.

Gray, J.A., Shalit-Kaneh, A., Chu, D.N., Hsu, P.Y., and Harmer, S. (**2017**). The *REVEILLE* clock genes inhibit growth of juvenile and adult plants by control of cell size. Plant Physiol.173, 2308–2322.

Gray, W.M., del Pozo, J.C., Walker, L., Hobbie, L., Risseeuw, E., Banks, T., Crosby, W.L., Yang, M., Ma, H., and Estelle, M. (**1999**). Identification of an SCF ubiquitin–ligase complex required for auxin response in *Arabidopsis thaliana*. Genes Dev. 13, 1678–1691.

Grbić, B., and Bleecker, A.B. (**1996**). An altered body plan is conferred on *Arabidopsis* plants carrying dominant alleles of two genes. Development 122, 2395–2403.

Gupta, R., and Chakrabarty, S.K. (**2013**). Gibberellic acid in plant: still a mystery unresolved. Plant Signal Behav. 8, e25504.

Hagemann, M., Eisenhut, M., Hackenberg, C., and Bauwe, H. (**2010**). Pathway and importance of photorespiratory 2-phosphoglycolate metabolism in cyanobacteria. Adv. Exp. Med. Biol. *675*, 91–108.

5 References

Harrar, Y., Bellec, Y., Bellini, C., and Faure, J.-D. (**2003**). Hormonal control of cell proliferation requires PASTICCINO genes. Plant Physiol. 132, 1217–1227.

Hatch, M.D. (**1988**). C4 photosynthesis: a unique blend of modified biochemistry, anatomy and ultrastructure. BBA 895: 81-106.

Hayami, N., Kimura, M., Tokizawa, M., Iuchi, S., Kurihara, Y., Matsui, M., Nomoto, M., Tada, Y., Sakai, Y., and Yamamoto, Y.Y. (**2015**). The Responses of *Arabidopsis* ELIP2 to UV-B, high light, and cold stress are regulated by a transcriptional regulatory unit composed of two elements. Plant Physiol. 169, 840–855.

Heijde, M., and Ulm, R. (**2012**). UV-B photoreceptor-mediated signalling in plants. Trends Plant Sci. 17, 230–237.

Hellmann, H., Hobbie, L., Chapman, A., Dharmasiri, S., Dharmasiri, N., del Pozo, C., Reinhardt, D., and Estelle, M. (**2003**). *Arabidopsis* AXR6 encodes CUL1 implicating SCF E3 ligases in auxin regulation of embryogenesis. EMBO J. 22, 3314–3325.

Hibberd, J.M., Sheehy, J.E., and Langdale, J.A. (**2008**). Using C_4 photosynthesis to increase the yield of rice-rationale and feasibility. Curr. Opin. Plant Biol. 11, 228–231.

Hobbie, L., McGovern, M., Hurwitz, L.R., Pierro, A., Liu, N.Y., Bandyopadhyay, A., and Estelle, M. (**2000**). The axr6 mutants of *Arabidopsis thaliana* define a gene involved in auxin response and early development. Development 127, 23–32.

Hoffmann, M. H. (**2002**). Biogeography of *Arabidopsis thaliana* (L.) Heynh. (Brassicaceae). Journal of Biogeography 29, 125–134.

Horiguchi, G., Kim, G.-T., and Tsukaya, H. (**2005**). The transcription factor AtGRF5 and the transcription coactivator AN3 regulate cell proliferation in leaf primordia of *Arabidopsis thaliana*. Plant J. 43, 68–78.

Hronková, M., Wiesnerová, D., Šimková, M., Skůpa, P., Dewitte, W., Vráblová, M., Zažímalová, E., and Šantrůček, J. (**2015**). Light-induced STOMAGEN-mediated stomatal development in *Arabidopsis* leaves. J. Exp. Bot. 66, 4621–4630.

Hu, Y., Xie, Q., and Chua, N.-H. (**2003**). The *Arabidopsis* auxin-inducible gene ARGOS controls lateral organ size. Plant Cell 15, 1951–1961.

Huang, X., Paulo, M.-J., Boer, M., Effgen, S., Keizer, P., Koornneef, M., and Eeuwijk, F.A. van (**2011**). Analysis of natural allelic variation in *Arabidopsis* using a multiparent recombinant inbred line population. PNAS 108, 4488–4493.

Hughes N. M., Morley C. B., and Smith W.K. (**2007**). Coordination of anthocyanin decline and photosynthetic maturation in juvenile leaves of three deciduous tree species. New Phytologist 175, 675–685.

Hull, A.K., Vij, R., and Celenza, J.L. (**2000**). *Arabidopsis* cytochrome P450s that catalyze the first step of tryptophan-dependent indole-3-acetic acid biosynthesis. Proc. Natl. Acad. Sci. U.S.A. 97, 2379–2384.

Hutin, C., Nussaume, L., Moise, N., Moya, I., Kloppstech, K., and Havaux, M. (**2003**). Early light-induced proteins protect *Arabidopsis* from photooxidative stress. Proc. Natl. Acad. Sci. U.S.A. 100, 4921–4926.

5 References

Jackson, D., Veit, B., and Hake, S. (**1994**). Expression of maize KNOTTED1 related homeobox genes in the shoot apical meristem predicts patterns of morphogenesis in the vegetative shoot. Development 120, 405–413.

Jajic, I., Sarna, T., and Strzalka, K. (**2015**). Senescence, Stress, and Reactive Oxygen Species. Plants 4, 393–411.

Jiménez-Gómez, J.M., Wallace, A.D., and Maloof, J.N. (**2010**). Network Analysis Identifies ELF3 as a QTL for the Shade Avoidance Response in *Arabidopsis*. PLoS Genet 6(9): e1001100.

John, G.P., Scoffoni, C., and Sack, L. (**2013**). Allometry of cells and tissues within leaves. Am. J. Bot. 100, 1936–1948.

Kaewthai, N., Gendre, D., Eklöf, J.M., Ibatullin, F.M., Ezcurra, I., Bhalerao, R.P., and Brumer, H. (**2013**). Group III-A XTH genes of *Arabidopsis* encode predominant xyloglucan endohydrolases that are dispensable for normal growth. Plant Physiol. 161, 440–454.

Kagawa, T., Sakai, T., Suetsugu, N., Oikawa, K., Ishiguro, S., Kato, T., Tabata, S., Okada, K., and Wada, M. (**2001**). *Arabidopsis* NPL1: a phototropin homolog controlling the chloroplast high-light avoidance response. Science 291, 2138–2141.

Kajala, K., Covshoff, S., Karki, S., Woodfield, H., Tolley, B.J., Dionora, M.J.A., Mogul, R.T., Mabilangan, A.E., Danila, F.R., Hibberd, J.M., (**2011**). Strategies for engineering a two-celled C_4 photosynthetic pathway into rice. J. Exp. Bot. 62, 3001–3010.

Kalmar, B., and Greensmith, L. (**2009**). Induction of heat shock proteins for protection against oxidative stress. Adv. Drug Deliv. Rev. 61, 310–318.

Kalve, S., Fotschki, J., Beeckman, T., Vissenberg, K., and Beemster, G.T.S. (**2014**). Three-dimensional patterns of cell division and expansion throughout the development of *Arabidopsis thaliana* leaves. J. Exp. Bot. 65, 6385–6397.

Kanai, R., and Edwards, G.E. (**1999**). The Biochemistry of C4 Photosynthesis. In C4 Plant Biology, R.F. Sage, and R.K. Monson, eds. (San Diego: Academic Press), 49–87.

Kausch, A.P., Owen, T.P., Zachwieja, S.J., Flynn, A.R., and Sheen, J. (**2001**). Mesophyll-specific, light and metabolic regulation of the C_4 PPCZm1 promoter in transgenic maize. Plant Mol. Biol. 45, 1–15.

Kellogg, E.A. (**2013**). C4 photosynthesis. Current Biology 23, 594–599.

Kerstetter, R.A., Bollman, K., Taylor, R.A., Bomblies, K., and Poethig, R.S. (**2001**). KANADI regulates organ polarity in *Arabidopsis*. Nature 411, 706–709.

Keurentjes, J., Bentsink, L., Alonso-Blanco, C., Blankestijn-de Vries, M.H.C., Effgen, S., Vreugdenhil, D., and Koornneef, M. (**2007**). Development of a near-isogenic line population of *Arabidopsis thaliana* and comparison of mapping power with a recombinant inbred line population. Genetics 175, 891–905.

Kieber, J.J., and Schaller, G.E. (**2014**). Cytokinins. TAB 12, e0168. Kim, G.-T., Tsukaya, H., Saito, Y., and Uchimiya, H. (**1999**). Changes in the shapes of leaves and flowers upon overexpression of cytochrome P450 in *Arabidopsis*. Proc. Natl. Acad. Sci. USA 96, 9433–9437.

Kim, W.-Y., Fujiwara, S., Suh, S.-S., Kim, J., Kim, Y., Han, L., David, K., Putterill, J., Nam, H.G., and Somers, D.E. (**2007**). ZEITLUPE is a circadian photoreceptor stabilized by GIGANTEA in blue light. Nature 449, 356–360.

5 References

Kimura, M., Yamamoto, Y.Y., Seki, M., Sakurai, T., Sato, M., Abe, T., Yoshida, S., Manabe, K., Shinozaki, K., and Matsui, M. (**2003**). Identification of *Arabidopsis* genes regulated by high light–stress using cDNA microarray. Photochem. Photobiol. 77, 226–233.

Kleine, T., Kindgren, P., Benedict, C., Hendrickson, L., and Strand, Å. (**2007**). Genome-wide gene expression analysis reveals a critical role for CRYPTOCHROME1 in the response of *Arabidopsis* to high irradiance. Plant Physiol. 144, 1391–1406.

Kong, S.-G., and Okajima, K. (**2016**). Diverse photoreceptors and light responses in plants. J. Plant Res. 129, 111–114.

Koornneef, M., Alonso-Blanco, C., and Vreugdenhil, D. (**2004**). Naturally occurring genetic variation in *Arabidopsis thaliana*. Annu. Rev. Plant. Biol. 55, 141–172.

Korte, A., and Farlow, A. (**2013**). The advantages and limitations of trait analysis with GWAS: a review. Plant Methods 9, 29–28

Kover, P.X., Valdar, W., Trakalo, J., Scarcelli, N., Ehrenreich, I.M., Purugganan, M.D., Durrant, C., and Mott, R. (**2009**). A Multiparent Advanced Generation Inter-Cross to fine-map quantitative traits in *Arabidopsis thaliana*. PLOS Genetics 5, e1000551.

Kovinich, N., Kayanja, G., Chanoca, A., Otegui, M.S., and Grotewold, E. (**2015**). Abiotic stresses induce different localizations of anthocyanins in *Arabidopsis*. Plant Signal. Behav. 10, e1027850.

Kozuka, T., Kong, S.-G., Doi, M., Shimazaki, K. -i., and Nagatani, A. (**2011**). Tissue-autonomous promotion of palisade cell development by Phototropin 2 in *Arabidopsis*. The Plant Cell 23, 3684–3695.

Ku, M.S., Wu, J., Dai, Z., Scott, R.A., Chu, C., and Edwards, G.E. (**1991**). Photosynthetic and photorespiratory characteristics of *Flaveria* species. Plant Physiol. 96, 518–528.

Ku, S.B., and Edwards, G.E. (**1977**). Oxygen inhibition of photosynthesis: II. kinetic characteristics as affected by temperature. Plant Physiol. 59, 991–999.

Langdale, J.A., Rothermel, B.A., and Nelson, T. (**1988**). Cellular pattern of photosynthetic gene expression in developing maize leaves. Genes Dev. 2, 106–115.

Li, S., Blanchoin, L., Yang, Z., and Lord, E.M. (**2003**). The Putative *Arabidopsis* Arp2/3 complex controls leaf cell morphogenesis. Plant Physiol. 132, 2034–2044.

Lichtenthaler, H.K., Buschmann, C., Döll, M., Fietz, H.J., Bach, T., Kozel, U., Meier, D., and Rahmsdorf, U. (**1981**). Photosynthetic activity, chloroplast ultrastructure, and leaf characteristics of high-light and low-light plants and of sun and shade leaves. Photosyn. Res. 2, 115–141.

Lim, P.O., Woo, H.R., and Nam, H.G. (**2003**). Molecular genetics of leaf senescence in *Arabidopsis*. Trends in Plant Science 8, 272–278.

Ljung, K., Bhalerao, R.P., and Sandberg, G. (**2001**). Sites and homeostatic control of auxin biosynthesis in *Arabidopsis* during vegetative growth. Plant J. 28, 465–474.

Long, J.J., and Berry, J.O. (**1996**). Tissue-specific and light-mediated expression of the c4 photosynthetic nad-dependent malic enzyme of amaranth mitochondria. Plant Physiol. 112, 473–482.

Lotkowska, M.E., Tohge, T., Fernie, A.R., Xue, G.-P., Balazadeh, S., and Mueller-Roeber, B. (**2015**). The *Arabidopsis* transcription factor MYB112 promotes anthocyanin formation during salinity and under high light stress. Plant Physiol. 169, 1862–1880.

5 References

Lundgren, M.R., Osborne, C.P., and Christin, P.-A. (**2014**). Deconstructing Kranz anatomy to understand C4 evolution. J. Exp. Bot. 65, 3357–3369.

Majeran, W., Friso, G., Ponnala, L., Connolly, B., Huang, M., Reidel, E., Zhang, C., Asakura, Y., Bhuiyan, N.H., Sun, Q., (**2010**). Structural and metabolic transitions of C_4 leaf development and differentiation defined by microscopy and quantitative proteomics in maize. The Plant Cell 22, 3509–3542.

Malinowski, R. (**2013**). Understanding of Leaf Development—the Science of Complexity. Plants 2, 396–415.

Mallmann, J., Heckmann, D., Bräutigam, A., Lercher, M.J., Weber, A.P.M., Westhoff, P., and Gowik, U. (**2014**). The role of photorespiration during the evolution of C4 photosynthesis in the genus *Flaveria*. Elife 3, 1–23.

Marshall, J.S., Stubbs, J.D., and Taylor, W.C. (**1996**). Two genes encode highly similar chloroplastic NADP-Malic Enzymes in *Flaveria* (implications for the evolution of C_4 photosynthesis). Plant Physiol. 111, 1251–1261.

Mawphlang, O.I.L., and Kharshiing, E.V. (**2017**). Photoreceptor mediated plant growth responses: implications for photoreceptor engineering toward improved performance in crops. Front. Plant Sci. 8, 1181.

Mcelrone, A., Choat, B., Gambetta, G., and Brodersen, C. (**2013**). Water uptake and transport in vascular plants. Nat. Educ. Knowl. 4, 6.

McKown, A.D., and Dengler, N.G. (**2007**). Key innovations in the evolution of Kranz anatomy and C_4 vein pattern in *Flaveria* (*Asteraceae*). Am. J. Bot. 94, 382–399.

McKown, A.D., and Dengler, N.G. (**2009**). Shifts in leaf vein density through accelerated vein formation in C_4 *Flaveria* (*Asteraceae*). Ann. Bot. 104, 1085–1098.

McMillen, G.G., and McClendon, J.H. (**1983**). dependence of photosynthetic rates on leaf density thickness in deciduous woody plants grown in sun and shade. Plant Physiol. 72, 674–678.

Mehrtens, F., Kranz, H., Bednarek, P., and Weisshaar, B. (**2005**). The *Arabidopsis* transcription factor MYB12 is a flavonol-specific regulator of phenylpropanoid biosynthesis. Plant Physiol. 138, 1083–1096.

Mizukami, Y., and Fischer, R.L. (**2000**). Plant organ size control: AINTEGUMENTA regulates growth and cell numbers during organogenesis. Proc. Natl. Acad. Sc.i USA 97, 942–947.

Moore, M., Vogel, M., and Dietz, K. (**2014**). The acclimation response to high light is initiated within seconds as indicated by upregulation of AP2/ERF transcription factor network in *Arabidopsis thaliana*. Plant Signal Behav. 9, 976479.

Moore, P.D. (**1982**). Evolution of photosynthetic pathways in flowering plants. Nature 295, 647–648.

Muhaidat, R., Sage, R.F., and Dengler, N.G. (**2007**). Diversity of Kranz anatomy and biochemistry in C_4 eudicots. Am. J. Bot. 94, 362–381.

Mühlenbock, P., Szechynska-Hebda, M., Plaszczyca, M., Baudo, M., Mateo, A., Mullineaux, P.M., Parker, J.E., Karpinska, B., and Karpinski, S. (**2008**). Chloroplast signaling and LESION SIMULATING DISEASE1 regulate crosstalk between light acclimation and immunity in *Arabidopsis*. Plant Cell 20, 2339–2356.

Müller, P., Li, X.-P., and Niyogi, K.K. (**2001**). Non-Photochemical Quenching. a response to excess light energy. Plant Physiol. 125, 1558–1566.

5 References

Mullis, K.B., and Faloona, F.A. (**1987**). Specific synthesis of DNA in vitro via a polymerase-catalyzed chain reaction. Meth. Enzymol. 155, 335–350.

Nelson, T., and Dengler, N. (**1997**). Leaf vascular pattern formation. The Plant Cell 9, 1121–1135.

Niinemets, Ü., (**2002**). Research review. Components of leaf dry mass per area – thickness and density – alter leaf photosynthetic capacity in reverse directions in woody plants. New Phytol. 144, 35–47.

Nikovics, K., Blein, T., Peaucelle, A., Ishida, T., Morin, H., Aida, M., and Laufs, P. (**2006**). The balance between the MIR164A and CUC2 genes controls leaf margin serration in *Arabidopsis*. Plant Cell 18, 2929–2945.

Niyogi, K.K. (**1999**). PHOTOPROTECTION REVISITED: Genetic and Molecular Approaches. Annu. Rev. Plant Physiol. Plant Mol. Biol. 50, 333–359.

Nobel Park S. (**1991**). Achievable productivities of certain CAM plants: basis for high values compared with C_3 and C_4 plants. New Phytol. 119, 183–205.

Nole-Wilson, S., Tranby, T.L., and Krizek, B.A. (**2005**). AINTEGUMENTA-like (AIL) genes are expressed in young tissues and may specify meristematic or division-competent states. Plant Mol. Biol. 57, 613–628.

Nomura, M., Katayama, K., Nishimura, A., Ishida, Y., Ohta, S., Komari, T., Miyao-Tokutomi, M., Tajima, S., and Matsuoka, M. (**2000**). The promoter of rbcS in a C_3 plant (rice) directs organ-specific, light-dependent expression in a C_4 plant (maize), but does not confer bundle sheath cell-specific expression. Plant Mol. Biol. 44, 99–106.

Oaks, A. (**1994**). Efficiency of Nitrogen Utilization in C_3 and C_4 Cereals. Plant Physiol. 106, 407–414.

Ohnishi, J., and Kanai, R. (**1983**). Differentiation of Photorespiratory Activity between Mesophyll and Bundle Sheath Cells of C4 Plants I. Glycine Oxidation by Mitochondria. Plant Cell Physiol. 24, 1411–1420.

Ohnishi, J., Yamazaki, M., and Kanai, R. (**1985**). Differentiation of Photorespiratory Activity between Mesophyll and Bundle Sheath Cells of C4 Plants II. Peroxisomes of Panicum miliaceum L. Plant Cell Physiol. 26, 797–803.

Oliver, D.J., Neuburger, M., Bourguignon, J., and Douce, R. (**1990**). Interaction between the Component Enzymes of the Glycine Decarboxylase Multienzyme Complex. Plant Physiol. 94, 833–839.

Patel, M., and Berry, J.O. (**2008**). Rubisco gene expression in C_4 plants. J. Exp. Bot. 59, 1625–1634.

Peer, W.A., and Murphy, A.S. (**2007**). Flavonoids and auxin transport: modulators or regulators? Trends Plant Sci. 12, 556–563.

Pérez-Pérez, J.M., Candela, H., Robles, P., López-Torrejón, G., del Pozo, J.C., and Micol, J.L. (**2010**). A role for AUXIN RESISTANT3 in the coordination of leaf growth. Plant Cell Physiol. 51, 1661–1673.

Pérez-Pérez, J.M., Serrano-Cartagena, J., and Micol, J.L. (**2002**). Genetic analysis of natural variations in the architecture of *Arabidopsis thaliana* vegetative leaves. Genetics 162, 893–915.

Perilli, S., Moubayidin, L., and Sabatini, S. (**2010**). The molecular basis of cytokinin function. Curr. Opin. Plant Biol. 13, 21–26.

5 References

Perrot-Rechenmann, C. (2010). Cellular Responses to Auxin: Division versus Expansion. Cold Spring Harb. Perspect. Biol. 2, 1-15.

Pillitteri, L.J., and Dong, J. (2013). Stomatal Development in *Arabidopsis*. TAB 11, e0162.

Pospíšil, P. (**2016**). Production of Reactive Oxygen Species by Photosystem II as a Response to Light and Temperature Stress. Front Plant Sci 7, 1950.

Powell, A.M. (**1978**). Systematics of *Flaveria* (Flaveriinae--*Asteraceae*). Ann. Mo. Bot. Gard. 65, 590–636.

Qi, J., Wang, Y., Yu, T., Cunha, A., Wu, B., Vernoux, T., Meyerowitz, E., and Jiao, Y. (**2014**). Auxin depletion from leaf primordia contributes to organ patterning. PNAS 111, 18769–18774.

Raghavendra, A.S., and Sage, R.F., eds. (**2010**). C_4 Photosynthesis and related CO_2 concentrating mechanisms (Dordrecht: Springer).

Reinhardt, D., Mandel, T., and Kuhlemeier, C. (**2000**). Auxin regulates the initiation and radial position of plant lateral organs. Plant Cell 12, 507–518.

Reinhardt, D., Pesce, E.-R., Stieger, P., Mandel, T., Baltensperger, K., Bennett, M., Traas, J., Friml, J., and Kuhlemeier, C. (**2003**). Regulation of phyllotaxis by polar auxin transport. Nature 426, 255–260.

Reintanz, B., Lehnen, M., Reichelt, M., Gershenzon, J., Kowalczyk, M., Sandberg, G., Godde, M., Uhl, R., and Palme, K. (**2001**). bus, a Bushy *Arabidopsis* CYP79F1 knockout mutant with abolished synthesis of short-chain aliphatic glucosinolates. Plant Cell 13, 351–367.

Ren, H., and Gray, W.M. (**2015**). SAUR Proteins as Effectors of Hormonal and Environmental Signals in Plant Growth. Mol Plant 8, 1153–1164.

Rishmawi, L., Bühler, J., Jaegle, B., Hülskamp, M., and Koornneef, M. (**2017**). Quantitative trait loci controlling leaf venation in *Arabidopsis*: Leaf venation QTL in *Arabidopsis*. Plant, Cell & Environment 40, 1429–1441.

Roeder, A.H.K., Chickarmane, V., Cunha, A., Obara, B., Manjunath, B.S., and Meyerowitz, E.M. (**2010**). variability in the control of cell division underlies sepal epidermal patterning in *Arabidopsis thaliana*. PLOS Biology 8, e1000367.

Rosche, E., Chitty, J., Westhoff, P., and Taylor, W.C. (**1998**). Analysis of promoter activity for the gene encoding pyruvate orthophosphate dikinase in stably transformed C_4 *Flaveria* Species. Plant Physiol. 117, 821–829.

Rose, J.K.C., Braam, J., Fry, S.C., and Nishitani, K. (**2002**). The XTH family of enzymes involved in xyloglucan endotransglucosylation and endohydrolysis: current perspectives and a new unifying nomenclature. Plant Cell Physiol. 43, 1421–1435.

Rossel, J.B., Wilson, I.W., and Pogson, B.J. (**2002**). Global changes in gene expression in response to high light in *Arabidopsis*. Plant Physiol. 130, 1109–1120.

Rossel, J.B., Wilson, P.B., Hussain, D., Woo, N.S., Gordon, M.J., Mewett, O.P., Howell, K.A., Whelan, J., Kazan, K., and Pogson, B.J. (**2007**). systemic and intracellular responses to photooxidative stress in *Arabidopsis*. The Plant Cell 19, 4091–4110.

Roth-Nebelsick, A., Uhl, D., Mosbrugger, V., and Kerp, H. (**2001**). Evolution and Function of Leaf Venation Architecture: A Review. Ann. Bot. 87, 553–566.

5 References

Sack L., and Scoffoni C. (**2013**). Leaf venation: structure, function, development, evolution, ecology and applications in the past, present and future. New Phytol. 198, 983–1000.

Sage Rowan F. (**2003**). The evolution of C4 photosynthesis. New Phytol. 161, 341–370.

Sage, R.F., Khoshravesh, R., and Sage, T.L. (**2014**). From proto-Kranz to C_4 Kranz: building the bridge to C_4 photosynthesis. J. Exp. Bot. 65, 3341–3356.

Sage, R.F., Sage, T.L., and Kocacinar, F. (**2012**). Photorespiration and the Evolution of C_4 Photosynthesis. Annu. Rev. Plant Biol. 63, 19–47.

Sage, T.L., Busch, F.A., Johnson, D.C., Friesen, P.C., Stinson, C.R., Stata, M., Sultmanis, S., Rahman, B.A., Rawsthorne, S., and Sage, R.F. (**2013**). Initial Events during the Evolution of C_4 Photosynthesis in C_3 Species of *Flaveria*. Plant Physiol. 163, 1266–1276.

Saito, K., Yonekura-Sakakibara, K., Nakabayashi, R., Higashi, Y., Yamazaki, M., Tohge, T., and Fernie, A.R. (**2013**). The flavonoid biosynthetic pathway in *Arabidopsis*: structural and genetic diversity. Plant Physiol. Biochem. 72, 21–34.

Saito, S., Hirai, N., Matsumoto, C., Ohigashi, H., Ohta, D., Sakata, K., and Mizutani, M. (**2004**). *Arabidopsis* CYP707As encode (+)-abscisic acid 8'-hydroxylase, a key enzyme in the oxidative catabolism of abscisic acid. Plant Physiol. 134, 1439–1449.

Scarpella, E., Barkoulas, M., and Tsiantis, M. (**2010**). control of leaf and vein development by auxin. Cold Spring Harb. Perspect. Biol. 2(1) Scarpella E, Barkoulas M, Tsiantis M. Control of Leaf and Vein Development by Auxin. Cold Spring Harbor Perspectives in Biology. 2010;2(1):a001511.

Schaller, G.E., Street, I.H., and Kieber, J.J. (**2014**). Cytokinin and the cell cycle. Curr. Opin. Plant Biol. 21, 7–15.

Schindelin, J., Arganda-Carreras, I., Frise, E., Kaynig, V., Longair, M., Pietzsch, T., Preibisch, S., Rueden, C., Saalfeld, S., Schmid, B., (**2012**). Fiji: an open-source platform for biological-image analysis. Nat. Methods 9, 676–682.

Schulze, S., Mallmann, J., Burscheidt, J., Koczor, M., Streubel, M., Bauwe, H., Gowik, U., and Westhoff, P. (**2013**). Evolution of C_4 photosynthesis in the genus *Flaveria*: establishment of a photorespiratory CO_2 pump. Plant Cell 25, 2522–2535.

Schulze, S., Westhoff, P., and Gowik, U. (**2016**). Glycine decarboxylase in C_3, C_4 and C_3-C_4 intermediate species. Curr. Opin. Plant Biol. 31, 29–35.

Shani, Z., Dekel, M., Roiz, L., Horowitz, M., Kolosovski, N., Lapidot, S., Alkan, S., Koltai, H., Tsabary, G., Goren, R., (**2006**). Expression of endo-1,4-β-glucanase in *Arabidopsis thaliana* is associated with plant growth, xylem development and cell wall thickening. Plant Cell Rep. 25, 1067–1074.

Sharrock, R.A., and Quail, P.H. (**1989**). Novel phytochrome sequences in *Arabidopsis thaliana*: structure, evolution, and differential expression of a plant regulatory photoreceptor family. Genes Dev. 3, 1745–1757.

Sheehy, J.E., Hardy, B., and Mitchell, P.L., eds. (**2000**). Redesigning rice photosynthesis to increase yield (Los Baños: Philippines International Rice Research Institute).

Sheen, J. (**1999**). C_4 gene expression. Annu. Rev. Plant. Physiol. Plant. Mol. Biol. 32.

Sherp, A.M., Westfall, C.S., Alvarez, S., and Jez, J.M. (**2018**). *Arabidopsis thaliana* GH3.15 acyl acid amido synthetase has a highly specific substrate preference for the auxin precursor indole-3-butyric acid. J. Biol. Chem. 293, 4277–4288.

5 References

Shu, G., Pontieri, V., Dengler, N.G., and Mets, L.J. (**1999**). Light Induction of Cell Type Differentiation and Cell-Type-Specific Gene Expression in Cotyledons of a C_4 Plant, *Flaveria trinervia*. Plant Physiol. 121, 731–741.

Sommer, M., Bräutigam, A., and Weber, A.P.M. (**2012**). The dicotyledonous NAD malic enzyme C_4 plant Cleome gynandra displays age-dependent plasticity of C_4 decarboxylation biochemistry. Plant Biology 14, 621–629.

Somssich, M., Je, B.I., Simon, R., and Jackson, D. (**2016**). CLAVATA-WUSCHEL signaling in the shoot meristem. Development 143, 3238–3248.

Steeves, T.A., and Sussex, I.M. (1989). Patterns in Plant Development (Cambridge: Cambridge University Press).

Steynen, Q.J., and Schultz, E.A. (**2003**). The FORKED genes are essential for distal vein meeting in *Arabidopsis*. Development 130, 4695–4708.

Stockhaus, J., Poetsch, W., Steinmüller, K., and Westhoff, P. (**1994**). Evolution of the C4 phosphoenolpyruvate carboxylase promoter of the C4 dicot *Flaveria trinervia*: an expression analysis in the C_3 plant tobacco. Mol. Gen. Genet. *245*, 286–293.

Sun, T. (**2010**). Gibberellin signal transduction in stem elongation & leaf growth. In Plant hormones: Biosynthesis, signal transduction, action!, P.J. Davies, ed. (Dordrecht: Springer), 308–328.

Suzuki, I., Cretin, C., Omata, T., and Sugiyama, T. (**1994**). transcriptional and posttranscriptional regulation of nitrogen-responding expression of phosphoenolpyruvate carboxylase gene in Maize. Plant Physiol 105, 1223–1229.

Swarup, R., and Péret, B. (**2012**). AUX/LAX family of auxin influx carriers—an overview. Front Plant Sci 3, 1–11.

Swindell, W.R., Huebner, M., and Weber, A.P. (**2007**). Transcriptional profiling of *Arabidopsis* heat shock proteins and transcription factors reveals extensive overlap between heat and non-heat stress response pathways. BMC Genomics *8*, 125.

Szechyńska-Hebda, M., and Karpiński, S. (**2013**). Light intensity-dependent retrograde signalling in higher plants. J. Plant Physiol. 170, 1501–1516.

Sztatelman, O., Waloszek, A., Banaś, A.K., and Gabryś, H. (**2010**). Photoprotective function of chloroplast avoidance movement: in vivo chlorophyll fluorescence study. J. Plant Physiol. 167, 709–716.

Takemiya, A., Inoue, S., Doi, M., Kinoshita, T., and Shimazaki, K. (**2005**). Phototropins Promote Plant Growth in Response to Blue Light in Low Light Environments. Plant Cell 17, 1120–1127.

Terashima, I., Hanba, Y.T., Tholen, D., and Niinemets, Ü. (2011). Leaf functional anatomy in relation to photosynthesis. Plant Physiol. 155, 108–116.

To, J.P.C., Haberer, G., Ferreira, F.J., Deruère, J., Mason, M.G., Schaller, G.E., Alonso, J.M., Ecker, J.R., and Kieber, J.J. (**2004**). Type-A *Arabidopsis* response regulators are partially redundant negative regulators of cytokinin signaling. Plant Cell 16, 658–671.

Traas, J., and Monéger, F. (2010). Systems biology of organ initiation at the shoot apex. Plant Physiol. 152, 420–427.

Tsiantis, M., Brown, M.I.N., Skibinski, G., and Langdale, J.A. (**1999**). Disruption of Auxin Transport Is Associated with Aberrant Leaf Development in Maize. Plant Physiol. 121, 1163–1168.

5 References

Tsuge, T., Tsukaya, H., and Uchimiya, H. (**1996**). Two independent and polarized processes of cell elongation regulate leaf blade expansion in *Arabidopsis thaliana* (L.) Heynh. Development 122, 1589–1600.

Tsukaya, H., Kozuka, T., and Kim, G.-T. (**2002**). Genetic control of petiole length in *Arabidopsis thaliana*. Plant Cell Physiol. 43, 1221–1228.

Tsukaya, H., Tsuge, T., and Uchimiya, H. (**1994**). The cotyledon: A superior system for studies of leaf development. Planta 195, 309–312.

Tuinstra, M.R., Ejeta, G., and Goldsbrough, P.B. (**1997**). Heterogeneous inbred family (HIF) analysis: a method for developing near-isogenic lines that differ at quantitative trait loci. Theor. Appl. Genet. 95, 1005–1011.

Vialet-Chabrand, S., Matthews, J.S.A., Simkin, A.J., Raines, C.A., and Lawson, T. (**2017**). Importance of fluctuations in light on plant photosynthetic acclimation. Plant Physiol. 173, 2163–2179.

Visscher, P.M., Wray, N.R., Zhang, Q., Sklar, P., McCarthy, M.I., Brown, M.A., and Yang, J. (**2017**). 10 Years of GWAS Discovery: Biology, Function, and Translation. Am. J. Hum. Gen. 101, 5–22.

von Caemmerer, S., and Furbank, R.T. (**2003**). The C_4 pathway: an efficient CO_2 pump. Photosyn. Res. 77, 191–207.

von Caemmerer, S., Quick, W.P., and Furbank, R.T. (**2012**). The development of C_4 Rice: Current progress and future challenges. Science 336, 1671–1672.

Voznesenskaya, E.V., Franceschi, V.R., Kiirats, O., Freitag, H., and Edwards, G.E. (**2001**). Kranz anatomy is not essential for terrestrial C_4 plant photosynthesis. Nature 414, 543–546.

Wagle, P., Nikolić, M., and Frommolt, P. (**2015**). QuickNGS elevates Next-Generation Sequencing data analysis to a new level of automation. BMC Genomics 16, 487.

Wagner, T.A., and Kohorn, B.D. (**2001**). Wall-associated kinases are expressed throughout plant development and are required for cell expansion. Plant Cell 13, 303–318.

Wang, J.L., Long, J.J., Hotchkiss, T., and Berry, J.O. (**1993**). C4 Photosynthetic Gene Expression in Light- and Dark-Grown Amaranth Cotyledons. Plant Physiol. 102, 1085–1093.

Wang, Y.H. (**2008**). How effective is T-DNA insertional mutagenesis in *Arabidopsis*? J. Biochem. Tech. 1, 11-20.

Wargent, J.J., Moore, J.P., Roland Ennos, A., and Paul, N.D. (**2009**). Ultraviolet radiation as a limiting factor in leaf expansion and development. Photochem. Photobiol. 85, 279–286.

Weigel, D. (**2012**). Natural Variation in *Arabidopsis*: from molecular genetics to ecological genomics. Plant Physiol. 158, 2–22.

Werner, T., Motyka, V., Laucou, V., Smets, R., Onckelen, H.V., and Schmülling, T. (**2003**). Cytokinin-deficient transgenic *Arabidopsis* plants show multiple developmental alterations indicating opposite functions of cytokinins in the regulation of shoot and root meristem activity. The Plant Cell 15, 2532–2550.

Westfall, C.S., Sherp, A.M., Zubieta, C., Alvarez, S., Schraft, E., Marcellin, R., Ramirez, L., and Jez, J.M. (**2016**). *Arabidopsis thaliana* GH3.5 acyl acid amido synthetase mediates metabolic crosstalk in auxin and salicylic acid homeostasis. Proc. Natl. Acad. Sci. USA 113, 13917–13922.

5 References

Weston, E., Thorogood, K., Vinti, G., and Lopez-Juez, E. (**2000**). Light quantity controls leaf-cell and chloroplast development in *Arabidopsis thaliana* wild type and blue-light-perception mutants. Planta 211, 807–815.

Wiludda, C., Schulze, S., Gowik, U., Engelmann, S., Koczor, M., Streubel, M., Bauwe, H., and Westhoff, P. (**2012**). Regulation of the photorespiratory GLDPA gene in C_4 *Flaveria*: an intricate interplay of transcriptional and posttranscriptional processes. Plant Cell 24, 137–151.

Yang, Y., Hammes, U.Z., Taylor, C.G., Schachtman, D.P., and Nielsen, E. (**2006**). High-affinity auxin transport by the AUX1 influx carrier protein. Curr. Biol. 16, 1123–1127.

Yazdanpanah, F., Hanson, J., Hilhorst, H.W.M., and Bentsink, L. (**2017**). Differentially expressed genes during the imbibition of dormant and after-ripened seeds – a reverse genetics approach. BMC Plant Biol. 17, 151.

Yoo, C.Y., Hasegawa, P.M., and Mickelbart, M.V. (**2011**). Regulation of stomatal density by the GTL1 transcription factor for improving water use efficiency. Plant Signal. Behav. 6, 1069–1071.

You, J., and Chan, Z. (**2015**). ROS regulation during abiotic stress responses in crop plants. Front Plant Sci 6,1092.

Zhang, R., Wang, B., Ouyang, J., Li, J., and Wang, Y. (**2008**). *Arabidopsis* indole synthase, a homolog of tryptophan synthase alpha, is an enzyme involved in the Trp-independent indole-containing metabolite biosynthesis. J. Integr. Plant Biol. 50, 1070–1077.

Zhang, Y., Du, L., Xu, R., Cui, R., Hao, J., , C., and Li, Y. (**2015**). Transcription Factors SOD7/NGAL2 and DPA4/NGAL3 act redundantly to regulate seed size by directly repressing KLU expression in *Arabidopsis thaliana*. Plant Cell 27, 620–632.

Zheng, N., Schulman, B.A., Song, L., Miller, J.J., Jeffrey, P.D., Wang, P., Chu, C., Koepp, D.M., Elledge, S.J., Pagano, M., (**2002**). Structure of the Cul1-Rbx1-Skp1-F boxSkp2 SCF ubiquitin ligase complex. Nature 416, 703–709.

6 Supplements

Supplemental Table 1 Candidate genes for QTL-VD.
Displayed are Gene-ID, common name, GO-Term, annotated function and T-DNA mutant phenotype. Mutations in between the parental accessions are indicated by: S: premature stop codon. M: single missense mutation, MM: multiple missense mutations D: amino acid deletion. Genes without additional letter did not show mutations in the genomic sequence but are in the candidate gene list according to their annotated function. Further analysis of these genes (for example promoter analysis) is required.

Gene ID	Name	GO-Term	Function	T-DNA line	Gene ID	Name	GO-Term	Function	T-DNA line
AT4G01820 /MM	ATP-BINDING CASSETTE B3	-	-	N658664 No difference	AT4G00830 / MM	LHP1-INTERACTING FACTOR 2	Response to hormone	Involved in plant innate immune response	-
AT4G01830 / MM	ATP-BINDING CASSETTE B5	-	-	-	AT4G00880 / M	SMALL AUXIN UPREGULATED RNA 31	Response to auxin		-
AT4G02450/ M	P23-1	Regulation of auxin polar transport	-	-	AT4G01060 / MM	CAPRICE-LIKE PYB83	Response to hormone	Involved in epidermal cell differentiation and in endoreduplication	-
AT4G02610 /MM		Auxin biosynthesis process	Aldolase-type TIM barrel family protein	N526326	AT4G01280 / D, M	REVEILLE 5	Response to hormone	Minor role in clock regulation	N834379
AT4G01710	CROOKED	Actin cytoskeleton organization	Encodes a actin polymerization factor. Involved in cell expansion of trichome	-	AT4G01540 / MM	*Arabidopsis* NAC DOMAIN CONTAINING PROTEIN 68	Leaf morphogenesis	regulates cell division	-
AT4G02380 / M	AtLEA5	Response to hormone	-	-	AT4G02330 / MM	PME41	Cell wall modification	pectin methylesterase that is sensitive to chilling	-

								stress and brassinosteroid regulation	
AT4G02520	ATGSTF2	Auxin-activated signalling pathway	glutathione transferase	-	AT4G02570 / MM	CULLIN 1	Auxin-activated signalling pathway	Cullin that is a component of SCF ubiquitin ligase complexes involved in mediating responses to auxin and jasmonic acid	*axr6-2* (Hobbie *et al.*, 2012)
AT4G03080 / MM	BRI1 SUPPRESSOR 1	brassinosteroid mediated signalling pathway	-	-	AT4G02780 / MM	ABC33	gibberellic acid mediated signalling pathway,	Catalyses the conversion of geranylgeranyl pyrophosphate (GGPP) to copalyl pyrophosphate (CPP) of gibberellin biosynthesis	-
AT4G00220 / MM	JAGGED LATERAL ORGANS	Xylem development	-	N669218 No difference	AT4G00730 / MM	ANTHOCYANINLESS 2	Plant type cell wall modification	Involved in the accumulation of anthocyanin and in root development	-
AT4G00450 / MM	MEDIATOR 12	Regulation of development		-	AT4G00850 / MM	GIF3	Cell proliferation	Transcription co-activators	-

AT4G00480 / MM	MYC1	Trichome patterning		-	AT4G01500 / MM	NGATHA4	Leaf development	AP2/B3-like transcriptional factor family protein	-
AT4G01630 / MM	EXPANSIN A17	involved in multidimensional cell growth		-	AT4G02030 / MM	VACUOLAR PROTEIN SORTING 51	leaf vascular tissue pattern formation	-	-
AT4G01800 / MM	ALBINO OR GLASSY YELLOW 1	Regulation of photosynthesis	ATPase subunit of the chloroplast Sec translocation machinery	-	AT4G02350 / MM	EXOCYST COMPLEX COMPONENT SEC15B	Auxin polar transport	-	-
AT4G01930 / MM	Cysteine/ Histidine-rich C1 domain family protein	Intracellular signal transduction	unknown	-	AT4G02440 / M	EMPFINDLICHER IM DUNKELROTEN LICHT 1	Leaf development	F-box protein that functions as a negative regulator in phytochrome A (phyA)-specific light signalling	-
AT4G01180 / MM	XH/XS domain-containing protein	Gene silencing by RNA	-	-	AT4G02460 / D, M	POSTMEIOTIC SEGREGATION 1	DNA recombination	The protein appears to play a role in DNA mismatch repair and in the suppression of somatic homologous recombination.	-
AT4G01730 /MM	DHHC-type zinc finger family protein	Cytoplasmic vesicle membrane	Unknown	WiscDsLox507B01	AT4G02560 / MM	LUMINIDEPENDENS	Cell differentiation	Encodes a nuclear localized protein with	-

								similarity to transcriptional regulators	
AT4G02990 / MM	BELAYA SMERT	Developmental process	a plastid-localized protein homologous to mitochondrial transcription termination factors (mTERF) found in anima	-	AT4G02590 / M	UNFERTILIZED EMBRYO SAC 12	multicellular organism development	bHLH protein	-

Supplemental Table 2 *Arabidopsis* Accessions and stock numbers.

Accession	*Arabidopsis* Stock #	Reference
Aa-0	CS6600	Courtesy of M. Hülskamp
Aitba	CS76347	Courtesy of M. Hülskamp
Alst	CS22550	Courtesy of M. Hülskamp
Altenb-2	CS76353	Courtesy of M. Hülskamp
An	N944	Courtesy by M. Koornneef
Apast	CS76368	Courtesy of M. Hülskamp
Bd-0	CS962	Courtesy of M. Hülskamp
Benk-1	CS22530	Courtesy of M. Hülskamp
Bozen-1	CS76357	Courtesy of M. Hülskamp
C24	CS906	Courtesy by M. Koornneef
Chi-0	CS1072	Courtesy of M. Hülskamp
Col-0	CS907	Courtesy by M. Koornneef
Cvi	N8580	Courtesy by M. Koornneef
Eri	CS22548	Courtesy by M. Koornneef
KI-5	CS6761	Courtesy of M. Hülskamp
Kidr-1	CS76376	Courtesy of M. Hülskamp
Kly-2	CS9631	Courtesy of M. Hülskamp
Lan-0	CS6768	Courtesy of M. Hülskamp
Lm-2	CS6784	Courtesy of M. Hülskamp
Koch-1	CS76396	Courtesy of M. Hülskamp
Koz2	CS76383	Courtesy of M. Hülskamp
Kly-4	CS76384	Courtesy of M. Hülskamp
Kyo-1	JW10231	Courtesy by M. Koornneef
Lago-1	CS76367	Courtesy of M. Hülskamp
Ler	N20	Courtesy by M. Koornneef
Litva	CS925	Courtesy of M. Hülskamp

Lp2-2	CS22594	Courtesy of M. Hülskamp
Ms-0	CS22655	Courtesy of M. Hülskamp
Mz-0	CS22636	Courtesy of M. Hülskamp
Nw-0	CS6811	Courtesy of M. Hülskamp
Ob-0	CS6816	Courtesy of M. Hülskamp
Pna17	CS28647	Courtesy of M. Hülskamp
Pog-0	CS6842	Courtesy of M. Hülskamp
Pt-0	CS6843	Courtesy of M. Hülskamp
Ra-0	CS22632	Courtesy of M. Hülskamp
Ren-1	CS76586	Courtesy of M. Hülskamp
Rhen-1	CS22536	Courtesy of M. Hülskamp
Rmx-A02	CS22568	Courtesy of M. Hülskamp
Sg-1	CS6858	Courtesy of M. Hülskamp
Sha	CS929	Courtesy by M. Koornneef
Shakhdara	CS76382	Courtesy of M. Hülskamp
Shigu-2	CS76374	Courtesy of M. Hülskamp
Si-0	CS1524	Courtesy of M. Hülskamp
Sorbo	CS22653	Courtesy of M. Hülskamp
Su-1	CS77877	Courtesy of M. Hülskamp
Tha-1	CS22537	Courtesy of M. Hülskamp
Tol-0	CS8020	Courtesy of M. Hülskamp
Tu-Scha	CS76401	Courtesy of M. Hülskamp
Vezzano-2	CS76349	Courtesy of M. Hülskamp
Wei-1	CS22622	Courtesy of M. Hülskamp
Wt-5	CS22637	Courtesy of M. Hülskamp

6 Supplements

Supplemental Table 3 Cluster-analysis Bin identities and gene number.
The Identities of the Bins including Bin Code and Bin names are shown, as well as gene number found in each bin.

Cluster 1			Cluster 5			Cluster 8		
Bin Code	**Bin Name**	**# genes**	**Bin Code**	**Bin Name**	**# genes**	**Bin Code**	**Bin Name**	**# genes**
17	hormone metabolism	1	1	PS	20	2	major CHO metabolism	4
26	misc	1	2	major CHO metabolism	3	3	minor CHO metabolism	1
27	RNA	1	3	minor CHO metabolism	6	4	glycolysis	1
33	development	1	7	OPP	1	8	TCA	1
35	not assigned	3	8	TCA	2	9	ATP synthesis	2
	total number of genes	**7**	9	ATP synthesis	1	10	cell wall	3
Cluster 2			10	cell wall	27	11	lipid metabolism	4
Bin Code	**Bin Name**	**# genes**	11	lipid metabolism	13	12	N-metabolism	2
10	cell wall	1	12	N-metabolism	2	13	amino acid metabolism	4
16	secondary metabolism	2	13	amino acid metabolism	5	15	metal handling	3
27	RNA	1	15	metal handling	5	16	secondary metabolism	17
	total number of genes	**4**	16	secondary metabolism	19	17	hormone metabolism	16
Cluster 3			17	hormone metabolism	33	18	Co-factor and vitamine metabolism	1
Bin Code	**Bin Name**	**# genes**	19	tetrapyrrole synthesis	5	20	stress	23
1	PS	1	20	stress	21	21	redox	4
2	major CHO metabolism	4	21	redox	9	26	misc	44
6	gluconeogenese	1	23	nucleotide metabolism	4	27	RNA	28
7	OPP	1	26	misc	61	28	DNA	3
9	ATP synthesis	1	27	RNA	60	29	protein	24
10	cell wall	11	28	DNA	17	30	signalling	15
11	lipid metabolism	6	29	protein	62	31	cell	2
12	N-metabolism	1	30	signalling	27	32	micro RNA	1
13	amino acid metabolism	5	31	cell	18	33	development	9
14	S-assimilation	1	32	micro RNA	10	34	transport	16
15	metal handling	3	33	development	18	35	not assigned	82
16	secondary metabolism	10	34	transport	22		total number of genes	**310**
17	hormone metabolism	6	35	not assigned	182	**Cluster 9**		
19	tetrapyrrole synthesis	1		total number of genes	**653**	**Bin Code**	**Bin Name**	**# genes**
20	stress	19	**Cluster 6**			1	PS	2
21	redox	2	**Bin Code**	**Bin Name**	**# genes**	2	major CHO metabolism	13
23	nucleotide metabolism	4	1	PS	81	3	minor CHO metabolism	11
26	misc	26	2	major CHO metabolism	13	4	glycolysis	3
27	RNA	32	3	minor CHO metabolism	11	5	fermentation	1
28	DNA	8	4	glycolysis	8	7	OPP	6
29	protein	26	7	OPP	5	8	TCA	5
30	signalling	33	8	TCA	7	9	ATP synthesis	8
31	cell	9	9	ATP synthesis	5	10	cell wall	38
32	micro RNA	1	10	cell wall	78	11	lipid metabolism	27
33	development	16	11	lipid metabolism	48	15	metal handling	10
34	transport	18	12	N-metabolism	1	16	secondary metabolism	53
35	not assigned	72	13	amino acid metabolism	17	17	hormone metabolism	58
	total number of genes	**318**	15	metal handling	7	18	Co-factor and vitamine metabolism	4
Cluster 4			16	secondary metabolism	36	20	stress	103
Bin Code	**Bin Name**	**# genes**	17	hormone metabolism	63	21	redox	22
1	PS	1	18	Co-factor and vitamine metabolism	5	22	polyamine metabolism	2
2	major CHO metabolism	1	19	tetrapyrrole synthesis	17	23	nucleotide metabolism	16
3	minor CHO metabolism	1	20	stress	92	24	Biodegradation of Xenobiotics	3
6	gluconeogenese	1	21	redox	15	25	C1-metabolism	2
7	OPP	1	22	polyamine metabolism	1	26	misc	131
10	cell wall	11	23	nucleotide metabolism	13	27	RNA	227
11	lipid metabolism	4	24	Biodegradation of Xenobiotics	2	28	DNA	47
13	amino acid metabolism	2	25	C1-metabolism	2	29	protein	215
15	metal handling	1	26	misc	130	30	signalling	109
16	secondary metabolism	1	27	RNA	225	31	cell	36
17	hormone metabolism	12	28	DNA	72	32	micro RNA	12
19	tetrapyrrole synthesis	1	29	protein	210	33	development	72
20	stress	8	30	signalling	122	34	transport	118
21	redox	9	31	cell	108	35	not assigned	620
26	misc	13	32	micro RNA	16		total number of genes	**1974**
27	RNA	11	33	development	62	**Cluster 10**		
28	DNA	5	34	transport	89	**Bin Code**	**Bin Name**	**# genes**
29	protein	7	35	not assigned	713	2	major CHO metabolism	1
30	signalling	4		total number of genes	**2274**	3	minor CHO metabolism	1
31	cell	1	**Cluster 7**			8	TCA	1
32	micro RNA	3	**Bin Code**	**Bin Name**	**# genes**	10	cell wall	1
33	development	2	1	PS	1	11	lipid metabolism	3
34	transport	4	13	amino acid metabolism	2	12	N-metabolism	1
35	not assigned	30	16	secondary metabolism	4	13	amino acid metabolism	6
	total number of genes	**134**	21	redox	1	14	S-assimilation	2
			23	nucleotide metabolism	1	15	metal handling	1
			27	RNA	2	16	secondary metabolism	15
			30	signalling	1	17	hormone metabolism	7
			32	micro RNA	1	20	stress	1
			34	transport	2	21	redox	2
			35	not assigned	2	26	misc	21
				total number of genes	**17**	27	RNA	5
						29	protein	8
						30	signalling	4
						32	micro RNA	1
						33	development	3
						34	transport	3
						35	not assigned	24
							total number of genes	**111**

6 Supplements

Supplemental Table 4 Leaf development genes according to literature.
Displayed are fold changes of differentially expressed genes in high-light. S1: stage 1, S2: stage 2, S3: stage 3. Blue colours indicate up-regulated genes, yellow shades indicate down-regulated genes. <2 indicate fold change levels lower than 2

Leaf development genes					Leaf development genes					Leaf development genes				
Protein name	ID	S1	S2	S3	**Protein name**	ID	S1	S2	S3	**Protein name**	ID	S1	S2	S3
REV	AT5G60690	<2	<2	<2	ABP1	AT4G02980	<2	<2	<2	CYCD3;1	AT4G34160	<2	<2	-3.27
AN	AT1G01510	<2	<2	<2	GID1A	AT3G05120	<2	<2	<2	CDKB1	AT3G54180	<2	<2	<2
SYD	AT2G46020	<2	<2	<2	CDKD	AT1G66750	<2	<2	<2	KP1	AT3G44730	<2	<2	-3.43
ROT3	AT4G36380	<2	<2	<2	CDKF	AT4G28980	<2	<2	<2	DEL1	AT3G48160	<2	<2	-2.6
ROT4	AT2G36985	<2	<2	<2	CYCH	AT5G27620	<2	<2	<2	SIM	AT5G04470	<2	<2	<2
PHAN	AT2G37630	<2	<2	<2	E2Fb	AT5G22220	<2	<2	<2	SMR1	AT3G10525	<2	<2	<2
PAC	AT2G48120	<2	<2	<2	E2Fc	AT1G47870	<2	<2	<2	SMR2	AT1G08180	<2	<2	3.25
TCP5	AT5G60970	<2	<2	<2	Dpa	AT5G02470	<2	<2	<2	KRP	AT2G23430	<2	<2	<2
TCP10	AT2G31070	<2	<2	<2	DPb	AT5G03415	<2	<2	<2	ANT	AT4G37750	<2	<2	-2.72
TCP13	AT3G02150	<2	<2	<2	CDC6	AT2G29680	<2	<2	-31.26	ORS1	AT3G29035	<2	<2	<2
TCP17	AT5G08070	<2	<2	<2	CDT1	AT1G52827	<2	<2	<2	GRF1	AT2G22840	<2	<2	<2
TCP24	AT1G30210	<2	<2	<2	MCM3	AT5G46280	<2	<2	<2	GRF2	AT1G78300	<2	<2	<2
PHV	AT1G30490	<2	<2	<2	ORC1	AT4G14700	<2	<2	<2	miR396A	AT2G10606	<2	<2	<2
NGA1	AT2G46870	<2	<2	-2.51	ORC3	AT5G16690	<2	<2	<2	miR396B	AT5G35407	<2	<2	<2
NGA2	AT3G61970	<2	<2	<2	RNR1	AT2G21790	<2	<2	<2	GIF1	AT5G28640	<2	<2	-4.75
NGA3	AT1G01030	<2	<2	<2	PCNA1	AT1G07370	<2	<2	<2	TCP1	AT1G67260	<2	3.22	4.59
NGA4	AT4G01500	<2	<2	<2	SAMBA	AT1G32310	<2	<2	<2	TCP2	AT4G18390	<2	<2	<2
PIN1	AT1G73590	<2	<2	3.89	MYB3R	AT2G16720	<2	<2	<2	TCP3	AT1G53230	<2	<2	2.12
LOP1	AT5G55540	<2	<2	-3.12	MAS	AT2G36850	<2	<2	<2	TCP4	AT3G15030	<2	<2	<2
TMO7	AT1G74500	<2	<2	<2	NPSN11	AT2G35190	<2	<2	-4.32	TCP12	AT1G68800	<2	<2	-5.43
SEP	At4g34190	<2	<2	<2	CDC20	AT4G33270	<2	<2	-3.01	TCP14	AT3G47620	<2	<2	-2.58
WRKY	AT1G13960	<2	<2	<2	NACK1	AT1G18370	<2	<2	-3.32	BB	AT3G63530	<2	<2	<2
WRKY61	AT1G18860	<2	<2	7.74	CCS52	AT4G11920	<2	<2	<2	MED25	AT4G34040	<2	<2	<2
WRKY71	AT1G29860	<2	<2	5.85	APC10	AT2G18290	<2	<2	-2.13	CYP78A5	AT1G13710	<2	<2	<2
WRKY40	AT1G80840	<2	<2	3.15	HBT	AT2G20000	<2	<2	<2	CYP90A1	AT5G05690	<2	<2	-6.36
WUS	AT2G17950	<2	<2	<2	AXR3	AT1G04250	2.15	<2	<2	AHA	AT1G17260	<2	<2	<2
CLV1	AT1G75820	<2	<2	-2.24	FZR2	AT4G22910	<2	<2	<2	XTH33	AT1G10550	<2	<2	<2
CVL2	AT1G65380	<2	<2	<2	FZR3	AT5G13840	<2	<2	<2	YUC1	AT4G32540	<2	<2	<2
CVL3	AT2G27250	<2	<2	<2	OSD1	AT3G57860	<2	<2	<2	YUC2	AT4G13260	<2	<2	-4.08
miR394	AT1G20375	<2	<2	<2	PPD1	AT4G14713	<2	<2	<2	CMT1	AT1G80740	<2	<2	<2
LCR	AT1G27340	<2	<2	<2	PPD2	AT4G14720	<2	<2	<2	RPT2a	AT4G29040	<2	<2	<2
TOR	AT1G50030	<2	<2	<2	JAG	AT1G68480	<2	<2	<2	KRP2	AT3G50630	<2	<2	<2
RAPTOR1	AT3G08850	<2	<2	<2	NUB	AT1G13400	<2	<2	<2	CUC2	AT5G53950	<2	<2	<2
LST8	AT3G18140	<2	<2	<2	AG	AT4G18960	<2	2.9	2.52	miR164	AT5G01747	<2	<2	-3.42

CSLG3	AT4G23990	<2	3.52	25.18	BOP1	AT3G57130	<2	<2	<2	SOD7	AT3G11580	<2	<2	2.54
EBP1	AT3G51800	<2	<2	<2	BOP2	AT2G41370	<2	<2	<2					
CDKA	AT3G48750	<2	<2	<2	TRY	AT5G53200	<2	3.09	<2					
CYCA	AT1G15570	<2	<2	-2.97	CPC	AT2G46410	<2	<2	<2					
CYCB	AT1G16330	<2	<2	-2.43	MYBL2	AT1G71030	<2	-2.07	-2.39					
CYCD	AT2G22490	<2	<2	<2	ARGOS	AT3G59900	<2	<2	<2					

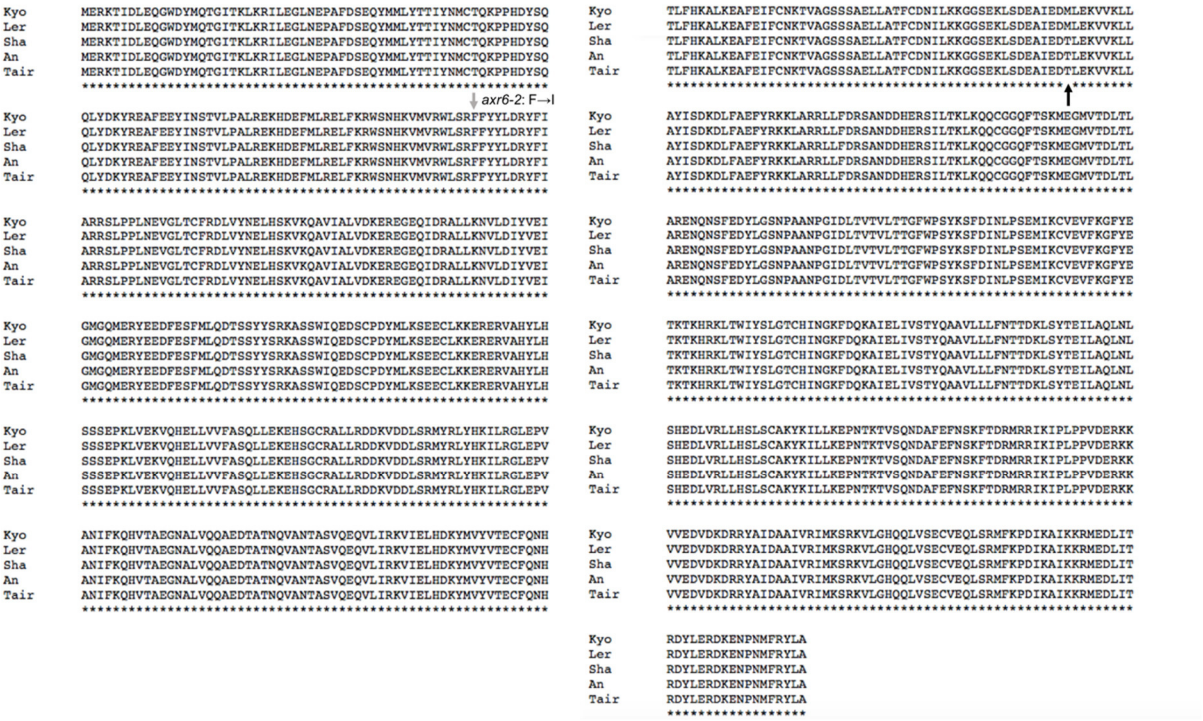

Supplemental Figure 1 Alignment of CUL1 CDS of 4 AMPRIL parental accession.
Alignment of coding sequences of Kyo, Ler, Sha and An with TAIR consensus sequence. Asterisks indicate no aberration between sequences. Light grey arrowhead indicates axr6-2 mutation site. Black arrowhead indicates the sequence difference between the four accessions.

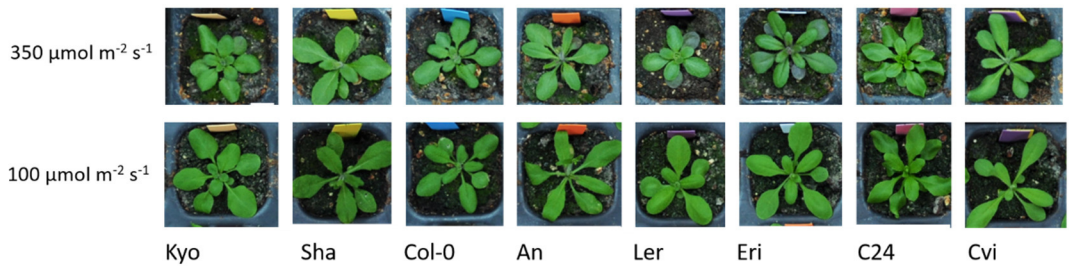

Supplemental Figure 2 Rosettes of high-light-grown AMPRIL parental accessions.
Rosette phenotype of 21 days-old AMPRIL parental accessions grown at 350 µmol m^{-2} s^{-1} and 100 µmol m^{-2} s^{-1}.

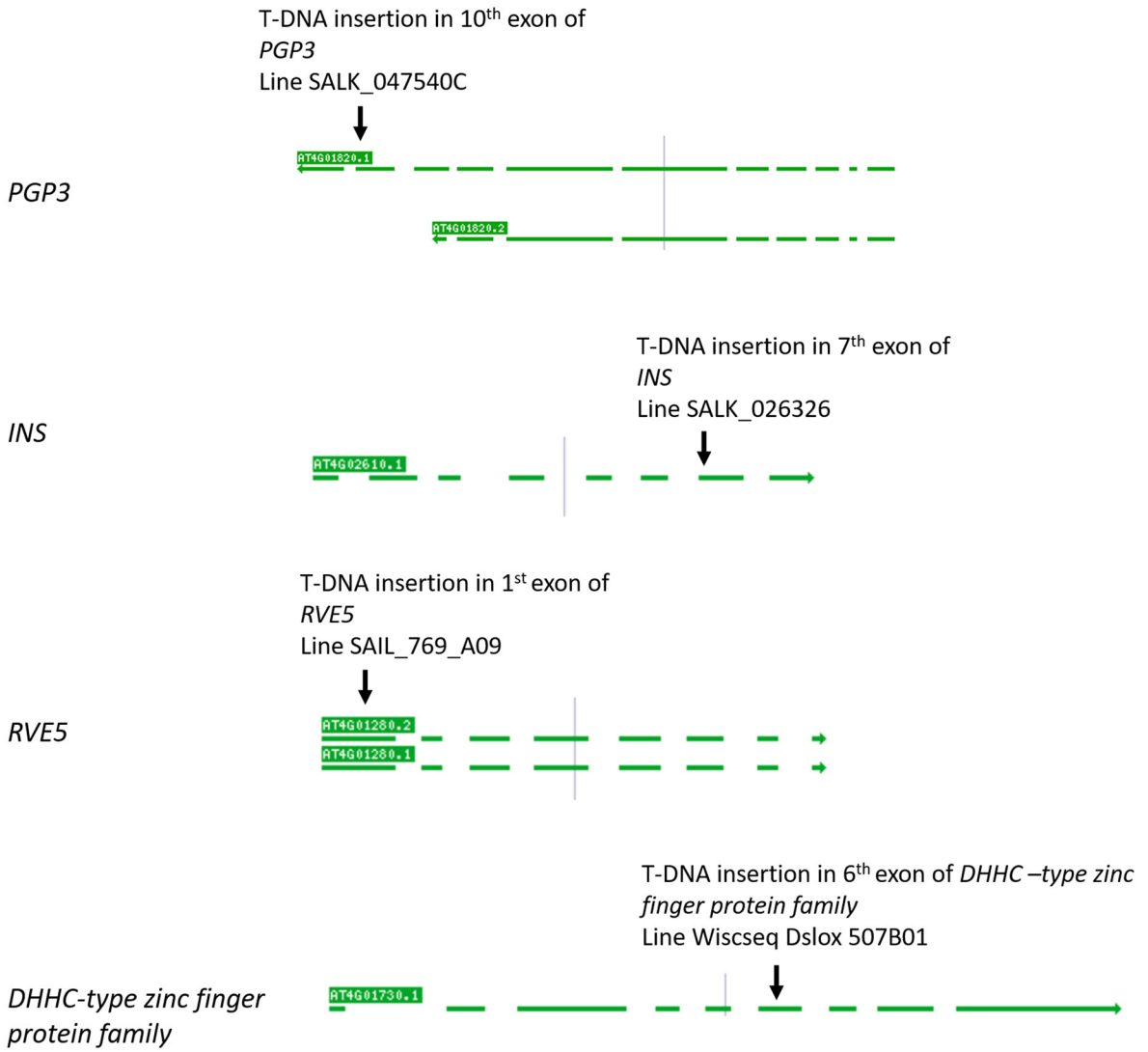

Supplemental Figure 3 T-DNA insertion sites in the T-DNA mutants.
Exons are shown in green. Splicing variants are also shown and consecutively numbered. Arrows indicate the T-DNA insertion sites.

FG18/GF07_I

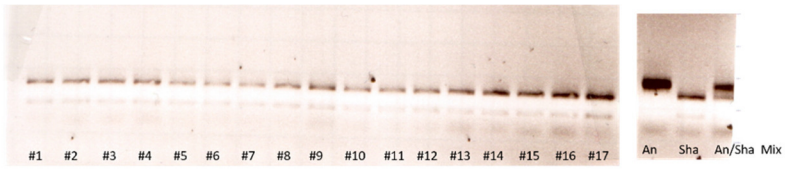

Gentoype/ Individuum	#1	#2	#3	#4	#5	#6	#7	#8	#9	#10	#11	#12	#13	#14	#15	#16	#17
An																	
Sha	X	X	X	X	X	X	X	X	X	X	X	X	X	X	X	X	X
heterozygous																	

FG18/GF07_II

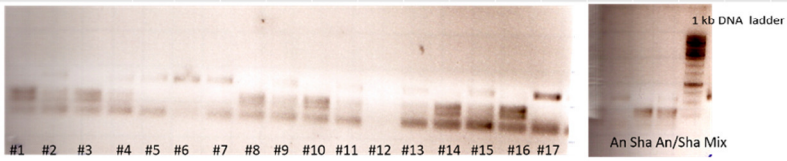

Gentoype/ Individuum	#1	#2	#3	#4	#5	#6	#7	#8	#9	#10	#11	#12	#13	#14	#15	#16	#17
An					X	X	X					?					X
Sha	X		X					X		X				X		X	
heterozygous		X		X					X		X		X		X		

FG18/GF07_III

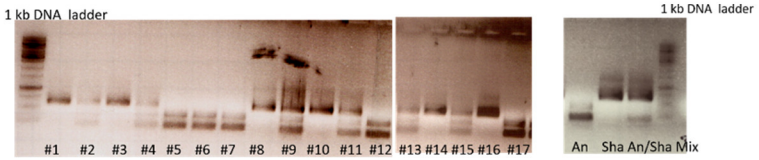

Gentoype/ Individuum	# 1	#2	#3	#4	#5	#6	#7	#8	#9	#10	#11	#12	#13	#14	#15	#16	#17
An					X	X	X					X					X
Sha	X		X					X		X				X		X	
heterozygous		X		X					X		X		X		X		

FG18/GF07_IIV

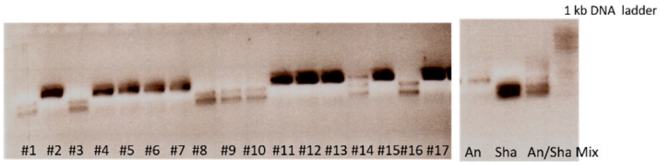

Gentoype/ Individuum	#1	#2	#3	#4	#5	#6	#7	#8	#9	#10	#11	#12	#13	#14	#15	#16	#17
An		X		X	X	X	X				X	X	X		X		X
Sha	X		X					X	X	X						X	
heterozygous														X			

Supplemental Figure 4 Agarose gels for genotyping of QTL-VD in FG18 individuals.
Exemplary agarose gels of overnight digests of PCR products for genotyping of FG18 plants. (enzymes used for digests are listed in table 15). #1-#17: F7 individuals of line FG18. Also, PCR products with genomic DNA of parental accessions An and Sha were used as controls. An/Sha mix: mix of genomic DNA of An and Sha as template for PCR. Tables indicate corresponding genotypes. From this analysis, individual plants were phenotyped that show homozygous genotype for each parental allele. For marker FG18/GF07_1, all individuals showed Sha genotype. For line FG18, plants homozygous Sha for the marker FG18/GF07_1 but otherwise homozygous for An were regarded as homozygous An. For the other assessed lines, this did not occur. Individuals with an ? were genotyped again (not shown).

7 Acknowledgements

First and foremost, I want to thank Prof. Dr. Ute Höcker for being an excellent supervisor during the time of my PhD. For her continuous feedback, inspiration and fruitful discussions I am deeply thankful. I also want to thank the members of my thesis advisory committee Prof. Dr. Martin Hülskamp and Prof. Dr. Peter Westhoff for helpful feedback during the yearly meetings. I am grateful to Prof. Dr. Hülskamp for being the second examiner of my thesis and to Prof. Dr. Karin Schnetz for being head of my examination committee.

I want to thank all past and present members of the Höcker group for their support, discussions and for being great colleagues. Special thanks go to Martin, Leonie, Stephen, Song, Xu, Natalia and Lisa for welcoming me into the group. Apple Breaks and Thirsty Thursdays are events I really miss with you guys.
Leo, who worked on the *Flaveria* project with me was a huge help. I also want to thank the student helps Lisa, Ilmars and Julia for helping me with phenotyping and greenhouse work. The staff of the greenhouse supported me a lot with special care-taking of the plants to make the QTL-experiments successful and I am truly grateful for their effort. I would also like to thank the members of CEPLAS for their feedback on my project during the young research seminars. Silke and Agatha, thank you for the great peer-to-peer meetings during the writing process.
For their helpful feedback and fruitful discussions on this manuscript I duly acknowledge Steph, Jathish, Martin and Bernard.

Finally, I want to thank my family Renate, Laura, Tom, Sonja, Clara, Arne and Maia for always encouraging me to follow my goals and for inspiring me every day.
I am deeply thankful for the support, affection, trust and love I got from Ulf and Linda during the last years.

8 Erklärung zur Dissertation

8 Erklärung zur Dissertation

Ich versichere, dass ich die von mir vorgelegte Dissertation selbstständig angefertigt, die benutzten Quellen und Hilfsmittel vollständig angegeben und die Stellen der Arbeit – einschließlich Tabellen, Karten und Abbildungen –, die anderen Werken im Wortlaut oder dem Sinn nach entnommen sind, in jedem Einzelfall als Entlehnung kenntlich gemacht habe; dass diese Dissertation noch keiner anderen Fakultät oder Universität zur Prüfung vorgelegen hat; dass sie – abgesehen von unten angegebenen Teilpublikationen – noch nicht veröffentlicht worden ist sowie dass ich eine solche Veröffentlichung vor Abschluss des Promotionsverfahrens nicht vornehmen werde.
Die von mir vorgelegte Dissertation ist von Prof. Dr. Ute Höcker betreut worden.

Name	Beitrag	Referenz
Leonard Gol	Erstellen von *Flaveria* Konfokal-Bildern	Praktikumsbericht